# Supporting Information

# Al-alkyl Borate (AAB) Salts Cocatalysts for Olefin Polymerization: Exploration of N-donor Ligand Variations

*Gaia Urciuoli,[a,b,c] Francesco Zaccaria,[a,c,]* Cristiano Zuccaccia,[b,c,]* Roberta Cipullo,[a,c,]* Peter H. M. Budzelaar,[a] Leonardo Tensi,[d] Antonio Vittoria,[a] Christian Ehm,[a,c] Alceo Macchioni,[b,c] Vincenzo Busico[a,c]*

[a] Department of Chemical Sciences, Federico II University of Naples, via Cinthia, 80126 Napoli, Italy;
[b] Department of Chemistry, Biology and Biotechnology, University of Perugia, via Elce di Sotto 8, 06123 Perugia, Italy;
[c] DPI, P.O. Box 902, 5600 AX Eindhoven, the Netherlands;
[d] Department of Pharmaceutical Sciences, University of Perugia, Via A. Fabretti 48, 06123 Perugia, Italy.

## Table of Contents

# 1. Additional details on the synthesis and characterization of Al_L, AlHAl_L and relevant byproducts

## 1.1 Characterization details for Al_L and AlHAl_L

***Al_DMA-Ph.*** $^{1}$H NMR (400 MHz, benzene-$d_6$): 7.34 (d, 4H, $^{3}J$ = 7.4 Hz, H3), 7.28 (d, 4H, $^{3}J$ = 8.6 Hz, H2), 7.23 (dd, 4H, $^{3}J$ = 7.4 Hz, H4), 7.16 (m, 2H, H5), 6.63 (d, 4H, $^{3}J$ = 8.6 Hz, H1), 2.02 (s, 12H, N-$CH_3$), 1.56 (m, 2H, Al-$CH_2CH(CH_3)_2$), 0.97 (d, 12H, $^{3}J$ = 6.4 Hz, Al-$CH_2CH(CH_3)_2$), 0.07 (d, 4H, $^{3}J$ = 6.8 Hz, Al-$CH_2CH(CH_3)_2$) ppm. $^{13}$C NMR (100 MHz, benzene-$d_6$): 143.6 (aromatic N-C), 141.6 (aromatic C), 138.4 (aromatic C), 129.2 (C4), 128.6 (C5), 128.0 (C2), 126.6 (C3), 120.7 (C1), 46.9 (N-$CH_3$), 27.8 (Al-$CH_2CH(CH_3)_2$), 25.8 (Al-$CH_2CH(CH_3)_2$), 20.6 (Al-$CH_2CH(CH_3)_2$) ppm.

***AlHAl_DMA-Ph.*** $^{1}$H NMR (400 MHz, benzene-$d_6$): 7.41 (d, 4H, $^{3}J$ = 7.6 Hz, H3), 7.39 (d, 4H, $^{3}J$ = 8.8 Hz, H2), 7.25 (dd, 4H, $^{3}J$ = 7.6 Hz, H4), 7.17 (m, 2H, H5), 6.86 (d, 4H, $^{3}J$ = 8.8 Hz, H1), 2.89 (bs, 1H, Al-*H*-Al), 2.43 (s, 12H, N-$CH_3$), 1.62 (m, 4H, Al-$CH_2CH(CH_3)_2$), 0.89 (d, 12H, $^{3}J$ = 6.6 Hz, Al-$CH_2CH(CH_3)_2$), 0.84 (d, 12H, $^{3}J$ = 6.6 Hz, Al-$CH_2CH(CH_3)_2$), 0.09 (d, 8H, $^{3}J$ = 7.0 Hz, Al-$CH_2CH(CH_3)_2$) ppm. $^{13}$C NMR (100 MHz, benzene-$d_6$): 143.2 (aromatic N-C), 141.7 (aromatic C), 138.4 (aromatic C), 129.2 (C4), 128.6 (C2), 128.6 (C5), 126.9 (C3), 120.4 (C1), 46.9 (N-$CH_3$), 27.7 (Al-$CH_2CH(CH_3)_2$), 27.6 (Al-$CH_2CH(CH_3)_2$), 25.6 (Al-$CH_2CH(CH_3)_2$), 21.8 (Al-$CH_2CH(CH_3)_2$) ppm.

***Al_DMA-Cl.*** $^{1}$H NMR (400 MHz, chlorobenzene-$d_5$): 7.06 (d, 4H, $^{3}J$ = 8.8 Hz, aromatic *m*-H), 6.60 (d, 4H, $^{3}J$ = 8.8 Hz, aromatic *o*-H), 2.27 (s, 12H, N-$CH_3$), 1.62 (m, 2H, Al-$CH_2CH(CH_3)_2$), 0.94 (d, 12H, $^{3}J$ = 6.4 Hz, Al-$CH_2CH(CH_3)_2$), 0.14 (d, 4H, $^{3}J$ = 6.8 Hz, Al-$CH_2CH(CH_3)_2$) ppm. $^{13}$C NMR (100 MHz, chlorobenzene-$d_5$): 143.4 (aromatic N-C), 135.1 (aromatic *p*-C), 130.2 (aromatic *m*-C), 121.7 (aromatic *o*-C), 47.5 (N-$CH_3$), 27.9 (Al-$CH_2CH(CH_3)_2$), 26.1 (Al-$CH_2CH(CH_3)_2$), 20.8 (Al-$CH_2CH(CH_3)_2$) ppm.

***AlHAl_DMA-Cl.*** $^{1}$H NMR (400 MHz, chlorobenzene-$d_5$): 7.18 (d, 4H, $^{3}J$ = 9.0 Hz, aromatic *m*-H), 6.87 (d, 4H, $^{3}J$ = 9.0 Hz, aromatic *o*-H), 2.86 (bs, 1H, Al-*H*-Al), 2.62 (s, 12H, N-$CH_3$), 1.59 (m, 4H, Al-$CH_2CH(CH_3)_2$), 0.86 (d, 12H, $^{3}J$ = 6.4 Hz, Al-$CH_2CH(CH_3)_2$), 0.83 (d, 12H, $^{3}J$ = 6.4 Hz, Al-$CH_2CH(CH_3)_2$), 0.07 (d, 4H, $^{3}J$ = 7.0 Hz, Al-$CH_2CH(CH_3)_2$) ppm. $^{13}$C NMR (100 MHz, chlorobenzene-$d_5$): 143.2 (aromatic N-C), 134.9 (aromatic *p*-C), 130.5 (aromatic *m*-C), 121.6 (aromatic *o*-C), 47.3 (N-$CH_3$), 27.8 (Al-$CH_2CH(CH_3)_2$), 25.7 (Al-$CH_2CH(CH_3)_2$), 21.9 (Al-$CH_2CH(CH_3)_2$) ppm.

***Al_DMCA.*** $^{1}$H NMR (400 MHz, chlorobenzene-$d_5$): 2.53 (t, 2H, $^{3}J$ = 11.0 Hz, H1), 2.09 (s, 12H, N-$CH_3$), 1.67 (m, 2H, Al-$CH_2CH(CH_3)_2$), 1.66 (m, 4H, H3), 1.65 (m, 4H, H2), 1.47 (bd, 2H, $^{2}J$ = 12.7 Hz, H4), 0.98 (m, 4H, H3), 0.98 (m, 4H, H2), 0.96 (d, 12H, $^{3}J$ = 6.4 Hz, Al-$CH_2CH(CH_3)_2$), 0.88 (m, 2H, H4), 0.00 (d, 4H, $^{3}J$ = 6.4 Hz, Al-

C$H_2$CH(C$H_3$)$_2$) ppm. $^{13}$C NMR (100 MHz, chlorobenzene-$d_5$): 67.4 (C1), 41.4 (N-C$H_3$), 28.1 (Al-C$H_2$CH(*C*$H_3$)$_2$), 27.0 (H2), 25.8 (Al-C$H_2$*C*H(C$H_3$)$_2$), 25.5 (H3), 25.0 (H4), 22.4 (Al-*C*$H_2$CH(C$H_3$)$_2$) ppm.

***AlHAl_DMCA.*** $^1$H NMR (400 MHz, chlorobenzene-$d_5$): 2.87 (s, 1H, Al-*H*-Al), 2.56 (t, 2H, $^3J$ = 11.2 Hz, H1), 2.18 (s, 12H, N-C$H_3$), 1.80 (m, 4H, Al-C$H_2$C*H*(C$H_3$)$_2$), 1.69 (bm, 4H, H3), 1.65 (bm, 4H, H2), 1.48 (bd, 2H, $^2J$ = 13.0 Hz, H4), 1.06 (m, 4H, H3), 1.04 (m, 4H, H2), 1.01 (d, 12H, $^3J$ = 6.4 Hz, Al-CH$_2$CH(C*H*$_3$)$_2$), 1.00 (d, 12H, $^3J$ = 6.4 Hz, Al-CH$_2$CH(C*H*$_3$)$_2$), 0.90 (m, 2H, H4), 0.20 (dd, 4H, $^3J$ = 7.0 Hz, $^2J$ = 14.7 Hz, Al-C*H*$_2$CH(CH$_3$)$_2$), 0.18 (dd, 4H, $^3J$ = 7.0 Hz, $^3J$ = 14.7 Hz, Al-C*H*$_2$CH(CH$_3$)$_2$) ppm. $^{13}$C NMR (100 MHz, chlorobenzene-$d_5$): 66.0 (C1), 41.3 (N-C$H_3$), 27.9 (Al-CH$_2$CH(*C*H$_3$)$_2$), 27.8 (Al-CH$_2$CH(*C*H$_3$)$_2$), 27.0 (C2), 25.7 (Al-CH$_2$*C*H(CH$_3$)$_2$), 25.1 (C3), 24.8 (C4), 22.1 (Al-*C*H$_2$CH(CH$_3$)$_2$) ppm.

***Al_DMHA.*** $^1$H NMR (400 MHz, benzene-$d_6$): 2.35 (t, 4H, $^3J$ = 8.4 Hz, H1), 1.85 (s, 12H, N-C$H_3$), 1.59 (m, 2H, Al-CH$_2$C*H*(CH$_3$)$_2$), 1.4-1.2 (m, 48H, H3-H14)), 1.31 (m, 4H, H15), 1.13 (m, 4H, H2), 0.97 (d, 12H, $^3J$ = 6.4 Hz, Al-CH$_2$CH(C*H*$_3$)$_2$), 0.93 (t, 6H, $^3J$ = 7.0 Hz, H16), -0.13 (d, 4H, $^3J$ = 6.9 Hz, Al-C*H*$_2$CH(CH$_3$)$_2$) ppm. $^{13}$C NMR (100 MHz, benzene-$d_6$): 58.5 (C1), 43.3 (N-C$H_3$), 32-29 (C3-C14)), 27.7 (Al-CH$_2$CH(*C*H$_3$)$_2$), 25.8 (Al-CH$_2$*C*H(CH$_3$)$_2$), 22.8 (C15), 19.9 (C2), 19.3 (Al-C*H*$_2$CH(CH$_3$)$_2$), 13.9 (C16) ppm.

***AlHAl_DMHA***.$^1$H NMR (400 MHz, benzene-$d_6$): 2.63 (bs, 1H, Al-*H*-Al), 2.36 (t, 4H, $^3J$ = 8.4 Hz, H1), 1.99 (s, 12H, N-C$H_3$), 1.80 (m, 4H, Al-CH$_2$C*H*(CH$_3$)$_2$), 1.4 - 1.2 (m, 48H, H3-H14), 1.32 (m, 4H, H15), 1.24 (m, 4H, H2), 0.97 (d, 24H, $^3J$ = 6.5 Hz, Al-CH$_2$CH(C*H*$_3$)$_2$), 0.93 (t, 6H, $^3J$ = 6.8 Hz, H16), 0.17 (dd, 4H, $^3J$ = 7.0 Hz, $^2J$ = 14.6 Hz, Al-C*H*$_2$CH(CH$_3$)$_2$), 0.12 (dd, 4H, $^3J$ = 7.0 Hz, $^2J$ = 14.6 Hz, Al-C*H*$_2$CH(CH$_3$)$_2$) ppm. $^{13}$C NMR (100 MHz, benzene-$d_6$): 59.1 (C1), 43.9 (N-C$H_3$), 32-29 (C3-C14), 27.6 (Al-CH$_2$CH(*C*H$_3$)$_2$), 25.7 (Al-CH$_2$*C*H(CH$_3$)$_2$), 22.8 (C15), 22.0 (C2), 21.3 (Al-*C*H$_2$CH(CH$_3$)$_2$), 13.9 (C16) ppm.

***Al_Py-2,6-Me.*** $^1$H NMR (400 MHz, benzene-$d_6$): 6.96 (t, 2H, $^3J$ = 7.8 Hz, aromatic *p*-H), 6.39 (d, 4H, $^3J$ = 7.8 Hz, aromatic *m*-H), 1.85 (s, 12H, Ar-C$H_3$) 1.25 (m, 2H, Al-CH$_2$C*H*(CH$_3$)$_2$), 0.78 (d, 12H, $^3J$ = 6.6 Hz, Al-CH$_2$CH(C*H*$_3$)$_2$), 0.26 (d, 4H, $^3J$ = 6.4 Hz, Al-C*H*$_2$CH(CH$_3$)$_2$) ppm. $^{13}$C NMR (100 MHz, benzene-$d_6$): 157.4 (aromatic *o*-C), 142.5 (aromatic *p*-C), 125.9 (aromatic *m*-C), 29.0 (Al-*C*H$_2$CH(CH$_3$)$_2$), 27.4 (Al-CH$_2$CH(*C*H$_3$)$_2$), 25.6 (Al-CH$_2$*C*H(CH$_3$)$_2$), 23.0 (Ar-C$H_3$) ppm.

***Al_Py-3,5-Me.*** $^1$H NMR (400 MHz, benzene-$d_6$): 7.70 (bs, 4H, aromatic *o*-H), 6.74 (bs, 2H, aromatic *p*-H), 1.81 (m, 2H, Al-CH$_2$C*H*(CH$_3$)$_2$), 1.68 (s, 12H, Ar-C$H_3$), 0.93 (d, 12H, $^3J$ = 6.6 Hz, Al-CH$_2$CH(C*H*$_3$)$_2$), 0.46 (d, 4H, $^3J$ = 7.2 Hz, Al-C*H*$_2$CH(CH$_3$)$_2$) ppm. $^{13}$C NMR (100 MHz, benzene-$d_6$): 144.9 (aromatic *m*-C), 143.2 (aromatic *o*-C), 137.5 (aromatic *p*-C), 27.6 (Al-CH$_2$CH(*C*H$_3$)$_2$), 25.7 (Al-CH$_2$*C*H(CH$_3$)$_2$), 19.4 (Al-*C*H$_2$CH(CH$_3$)$_2$), 17.1 (Ar-C$H_3$) ppm.

***Al_Py-3,5-F.*** $^1$H NMR (400 MHz, benzene-$d_6$): 7.46 (d, 4H, $^4J$ = 1.8 Hz, aromatic *o*-H), 6.30 (tt, 2H, $^3J_{HF}$ = 7.8 Hz, $^4J_{HH}$ = 1.8 Hz, aromatic *p*-H), 1.60 (m, 2H, Al-CH$_2$C*H*(CH$_3$)$_2$), 0.78 (d, 12H, $^3J$ = 6.6 Hz, Al-CH$_2$CH(C*H*$_3$)$_2$), 0.09 (d,

4H, $^{3}J$ = 7.3 Hz, Al-C$H_2$CH($CH_3$)$_2$) ppm. $^{13}$C NMR (100 MHz, benzene-$d_6$): 160.6 ($^{1}J_{CF}$ = 265 Hz, aromatic *m*-C), 132.0 ($^{2}J_{CF}$ = 24.2 Hz, aromatic *o*-C), 119.5 ($^{2}J_{CF}$ = 23.4 Hz, aromatic *p*-C), 27.4 (Al-$CH_2$CH($CH_3$)$_2$), 25.2 (Al-$CH_2$CH($CH_3$)$_2$), 18.5 (Al-$CH_2$CH($CH_3$)$_2$) ppm. $^{19}$F NMR (400 MHz, benzene-$d_6$): -110.4 (aromatic *m*-F) ppm.

***Al_Py-4-NMe$_2$.*** $^{1}$H NMR (400 MHz, benzene-$d_6$): 7.46 (d, 4H, aromatic *m*-H), 5.82 (d, 4H, aromatic *o*-H), 2.11 (s, 12H, N-$CH_3$), 1.95 (m, 2H, Al-$CH_2$C*H*($CH_3$)$_2$), 1.07 (d, 12H, $^{3}J$ = 6.6 Hz, Al-$CH_2$CH(C$H_3$)$_2$), 0.46 (d, 4H, $^{3}J$ = 7.0 Hz, Al-C$H_2$CH($CH_3$)$_2$) ppm. $^{13}$C NMR (100 MHz, benzene-$d_6$): 155.4 (aromatic *p*-C), 144.5 (aromatic *m*-C), 106.9 (aromatic *o*-C), 37.8 (N-$CH_3$), 27.9 (Al-$CH_2$CH(*C*$H_3$)$_2$), 26.0 (Al-$CH_2$*C*H($CH_3$)$_2$), 19.8 (Al-*C*$H_2$CH($CH_3$)$_2$) ppm.

***Al_QUI.*** $^{1}$H NMR (400 MHz, benzene-$d_6$): 8.38 (d, 2H, $^{3}J$ = 5.0 Hz, H1), 7.65 (m, 4H, H3 and H7), 7.21 (d, 2H, $^{3}J$ = 8.2 Hz, H4), 7.04 (dd, 2H, $^{3}J$ = 7.2 Hz, H6), 6.97 (m, 2H, H5), 6.81 (dd, 2H, $^{3}J$ = 8.2 Hz, $^{3}J$ = 5.0 Hz, H2), 1.45 (m, 2H, Al-$CH_2$C*H*($CH_3$)$_2$), 0.81 (d, 12H, $^{3}J$ = 6.6 Hz, Al-$CH_2$CH(C$H_3$)$_2$), 0.64 (d, 4H, $^{3}J$ = 7.0 Hz, Al-C$H_2$CH($CH_3$)$_2$) ppm. $^{13}$C NMR (100 MHz, benzene-$d_6$): 149.7 (C1), 145.0 (aromatic N-C) 144.9 (C3), 142.7 (aromatic C), 133.3 (C6), 130.1 (C4), 129.0 (C5), 121.5 (C7), 121.2 (C2), 27.5 (Al-$CH_2$CH(*C*$H_3$)$_2$), 25.7 (Al-$CH_2$*C*H($CH_3$)$_2$), 23.5 (Al-*C*$H_2$CH($CH_3$)$_2$) ppm.

## 1.2 NMR spectra of Al_L and AlHAl_L

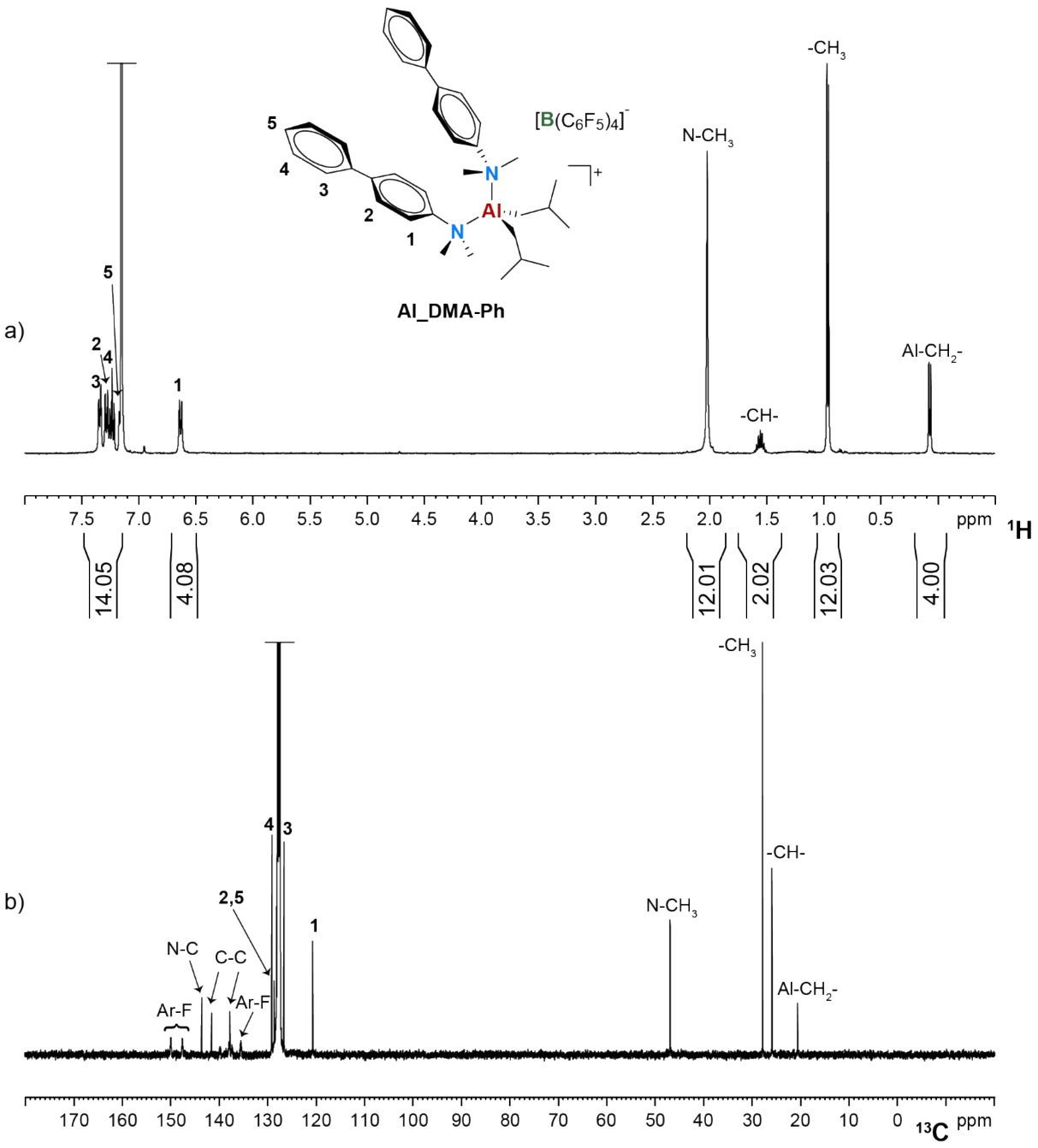


**Figure S1.** a) $^{1}$H and b) $^{13}$C NMR spectra (benzene-$d_6$, 298K) of **Al_DMA-Ph**.

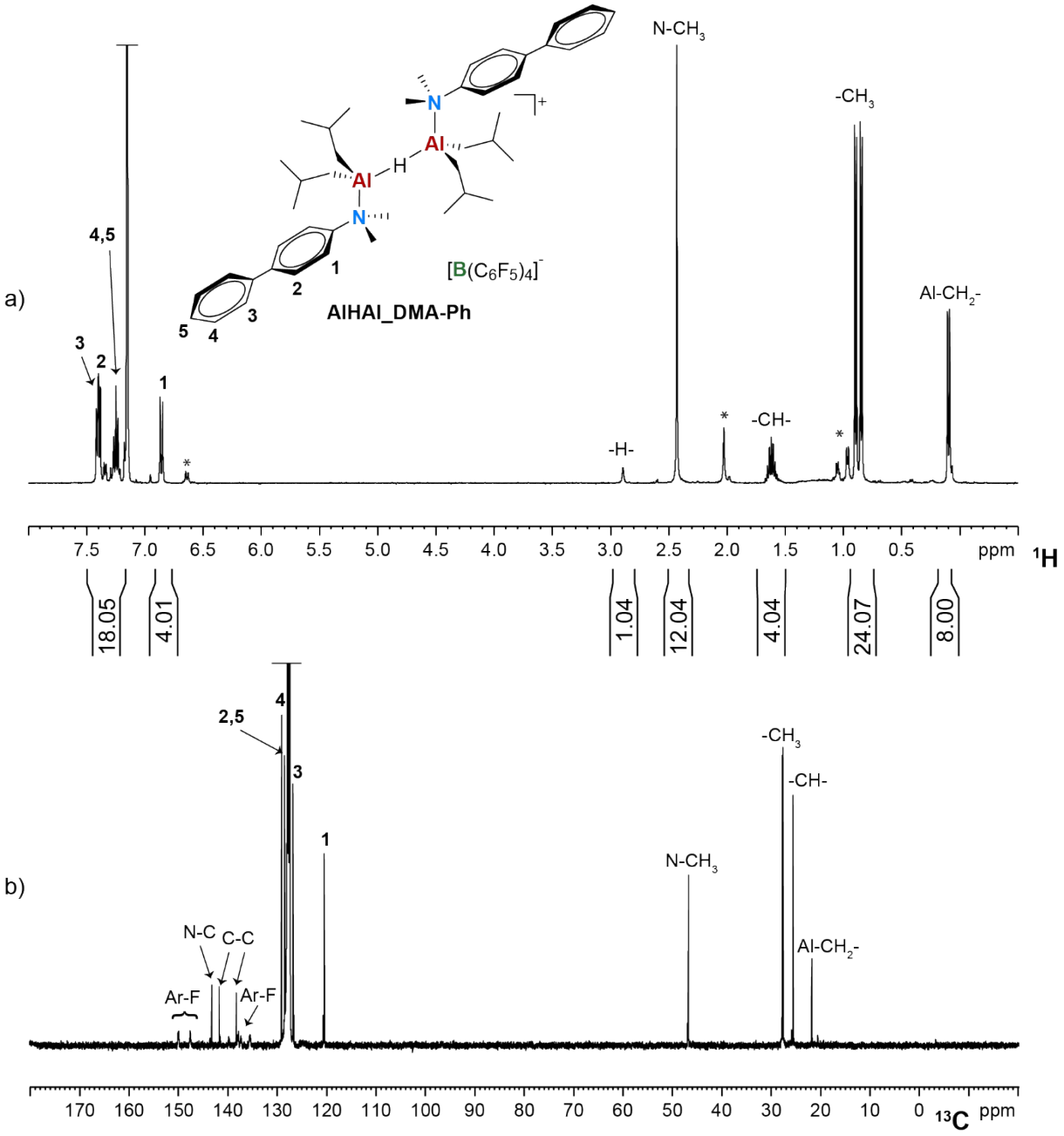


**Figure S2.** a) $^{1}$H and b) $^{13}$C NMR spectra (benzene-$d_6$, 298K) of **AlHAl_DMA-Ph**. * = residual **Al_DMA-Ph**.

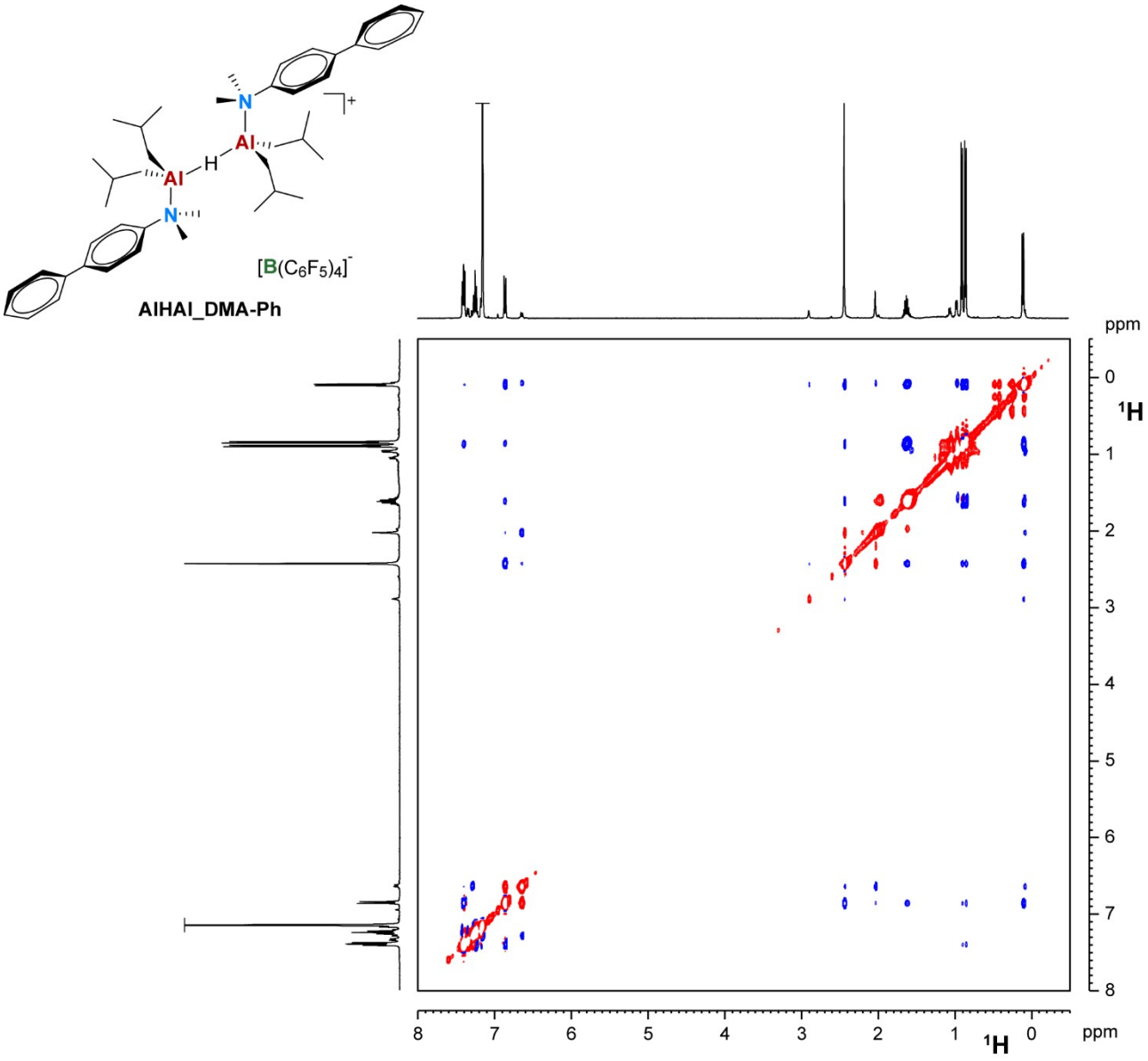


**Figure S3.** $^{1}$H NOESY NMR spectrum (benzene-$d_6$, 298K) of **AlHAl_DMA-Ph**.

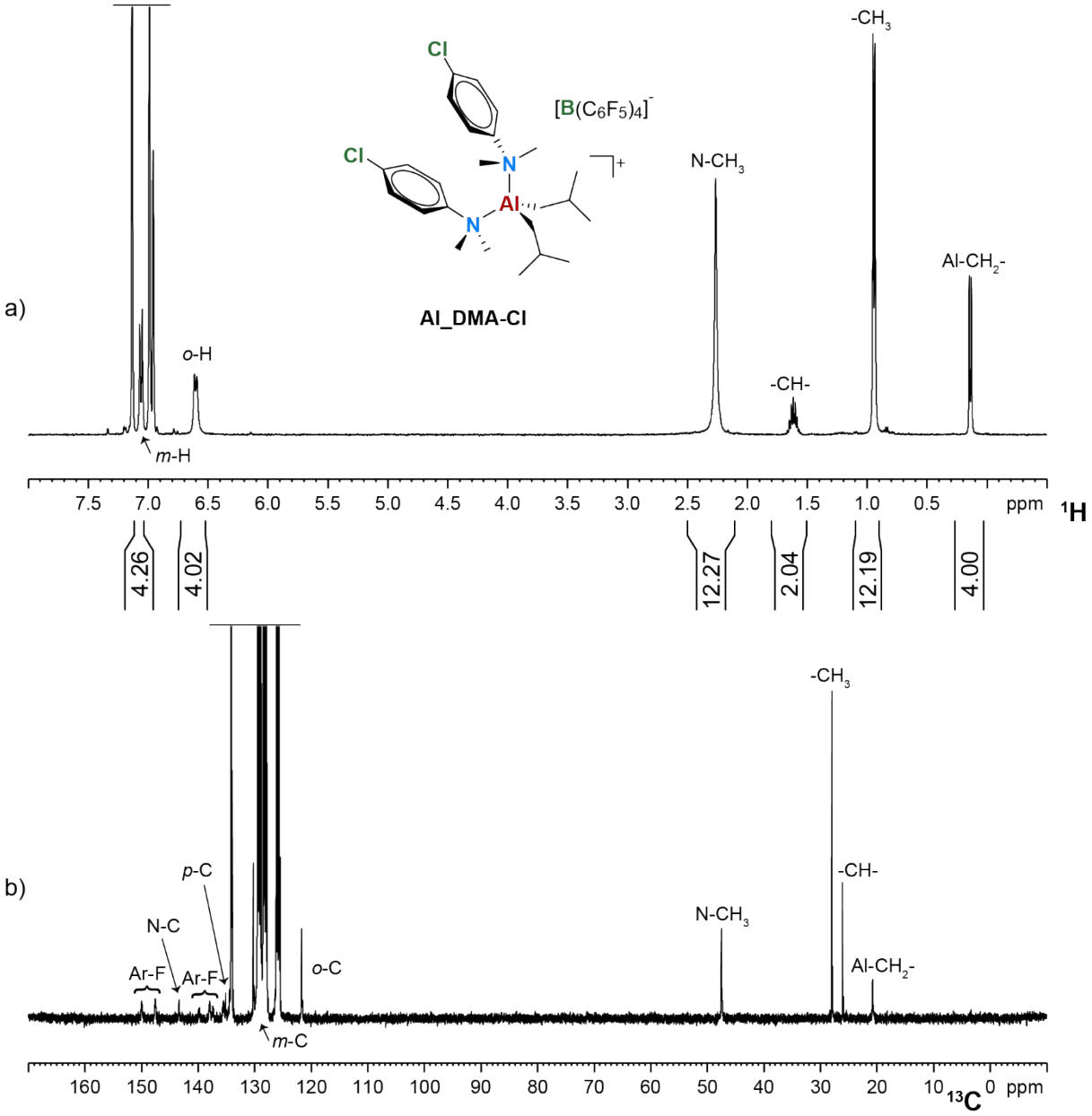


**Figure S4.** a) $^{1}$H and b) $^{13}$C NMR spectra (chlorobenzene-$d_5$, 298K) of **Al_DMA-Cl**.

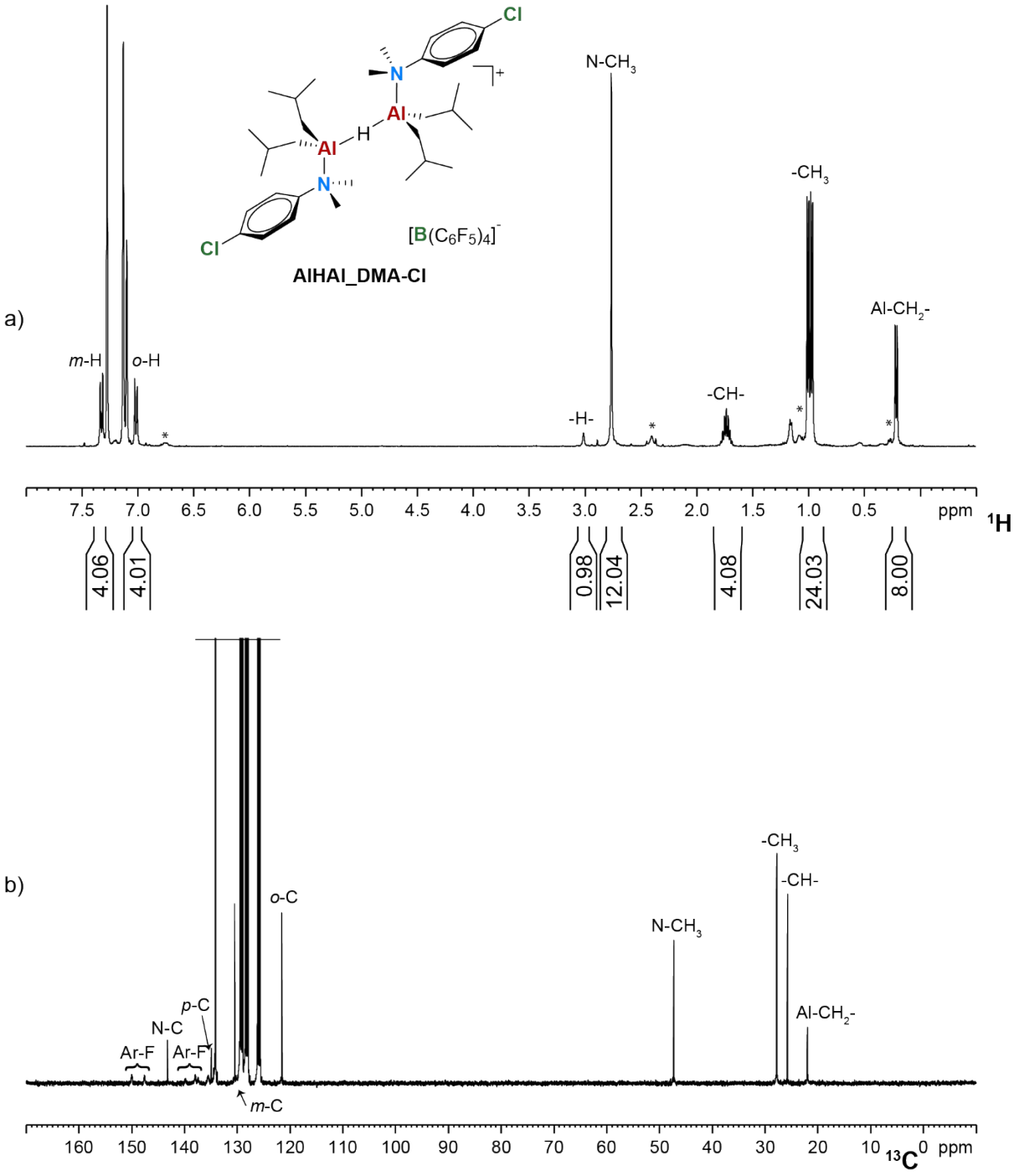


**Figure S5.** a) $^{1}$H and b) $^{13}$C NMR spectra (chlorobenzene-$d_5$, 298K) of **AlHAl_DMA-Cl**. * = residual **Al_DMA-Cl**.

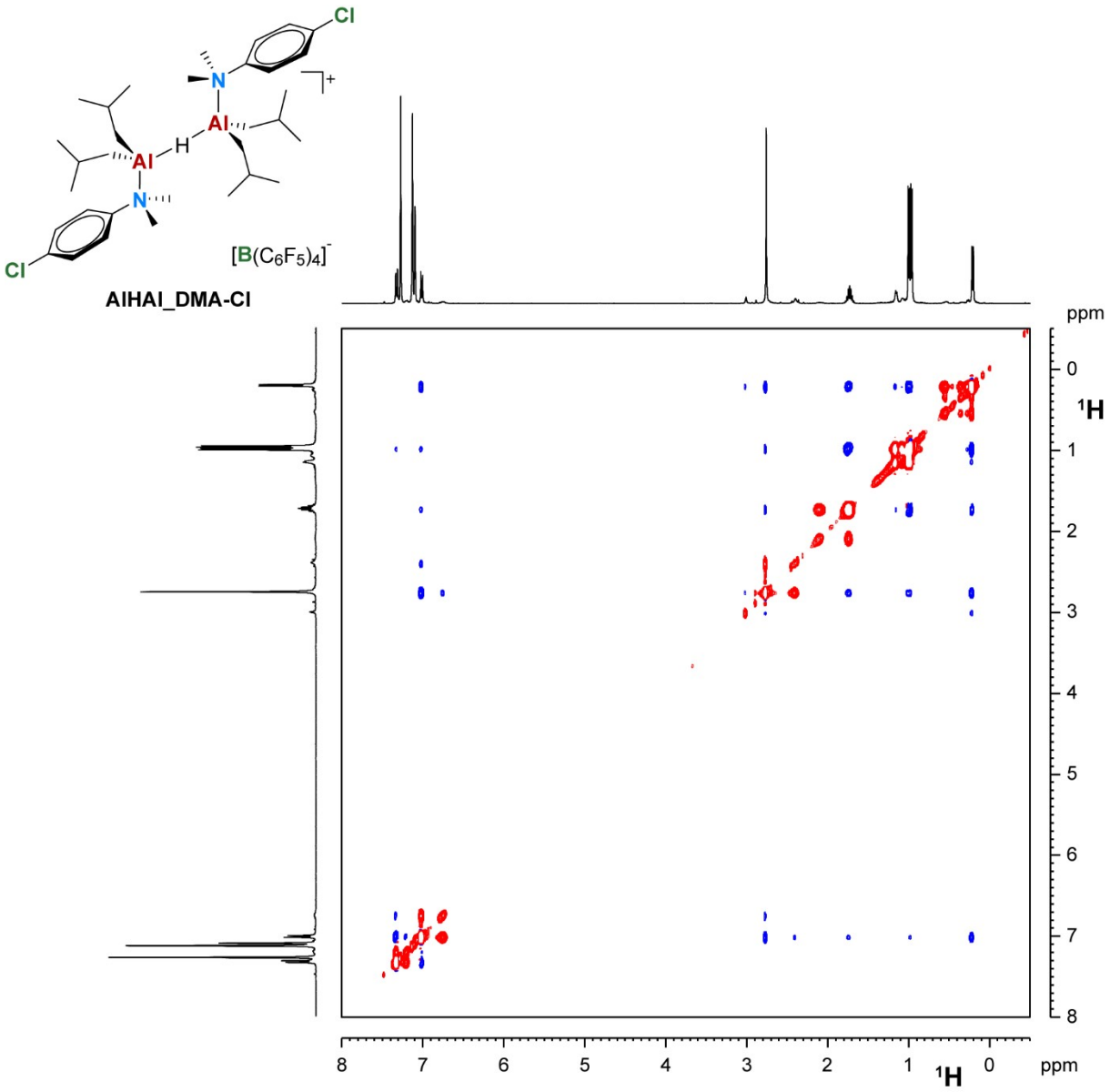


**Figure S6.** $^{1}$H NOESY NMR spectrum (chlorobenzene-$d_5$, 298K) of **AlHAl_DMA-Cl**.

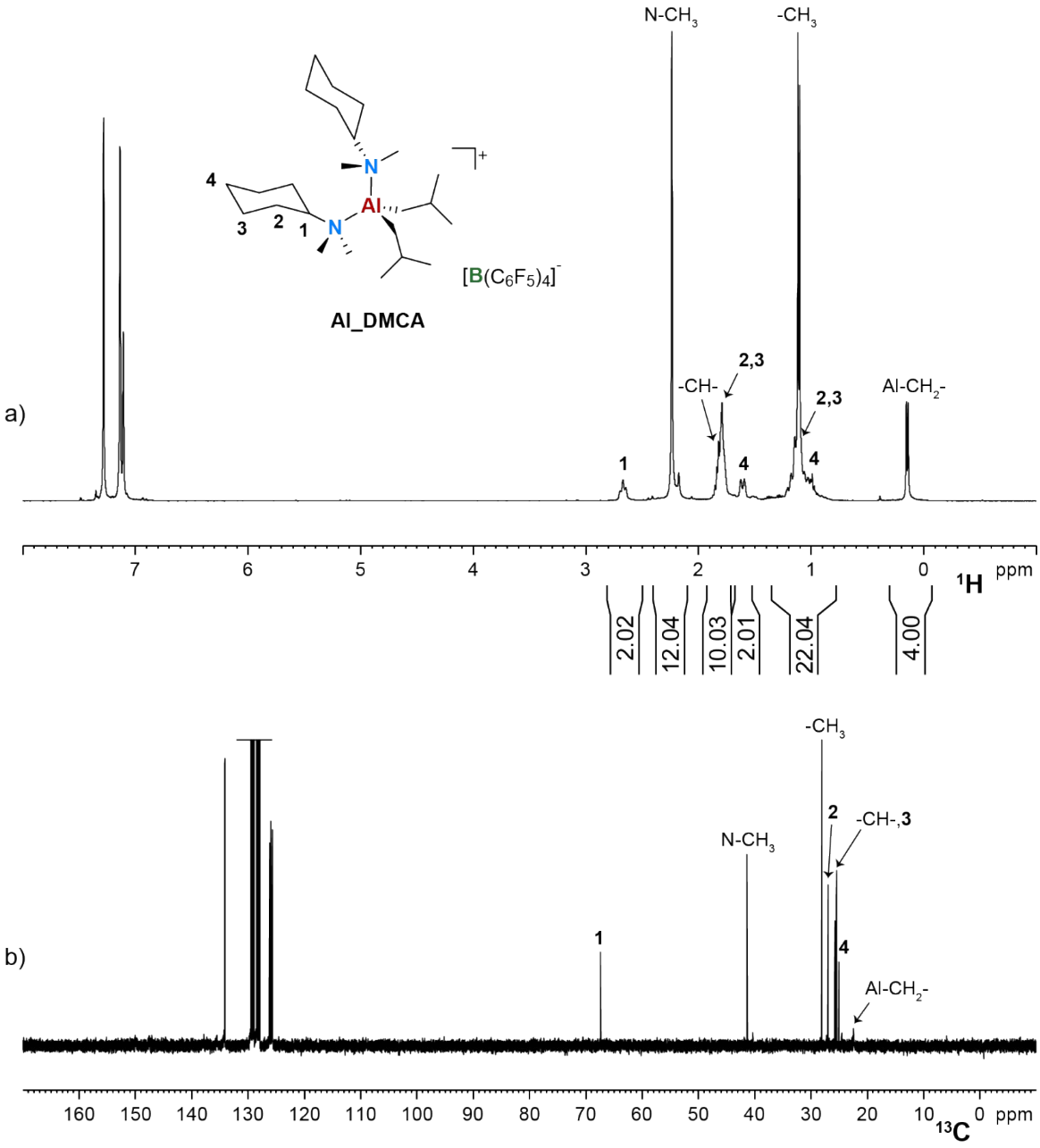


**Figure S7.** a) $^{1}$H and b) $^{13}$C NMR spectra (chlorobenzene-$d_5$, 298K) of **Al_DMCA**.

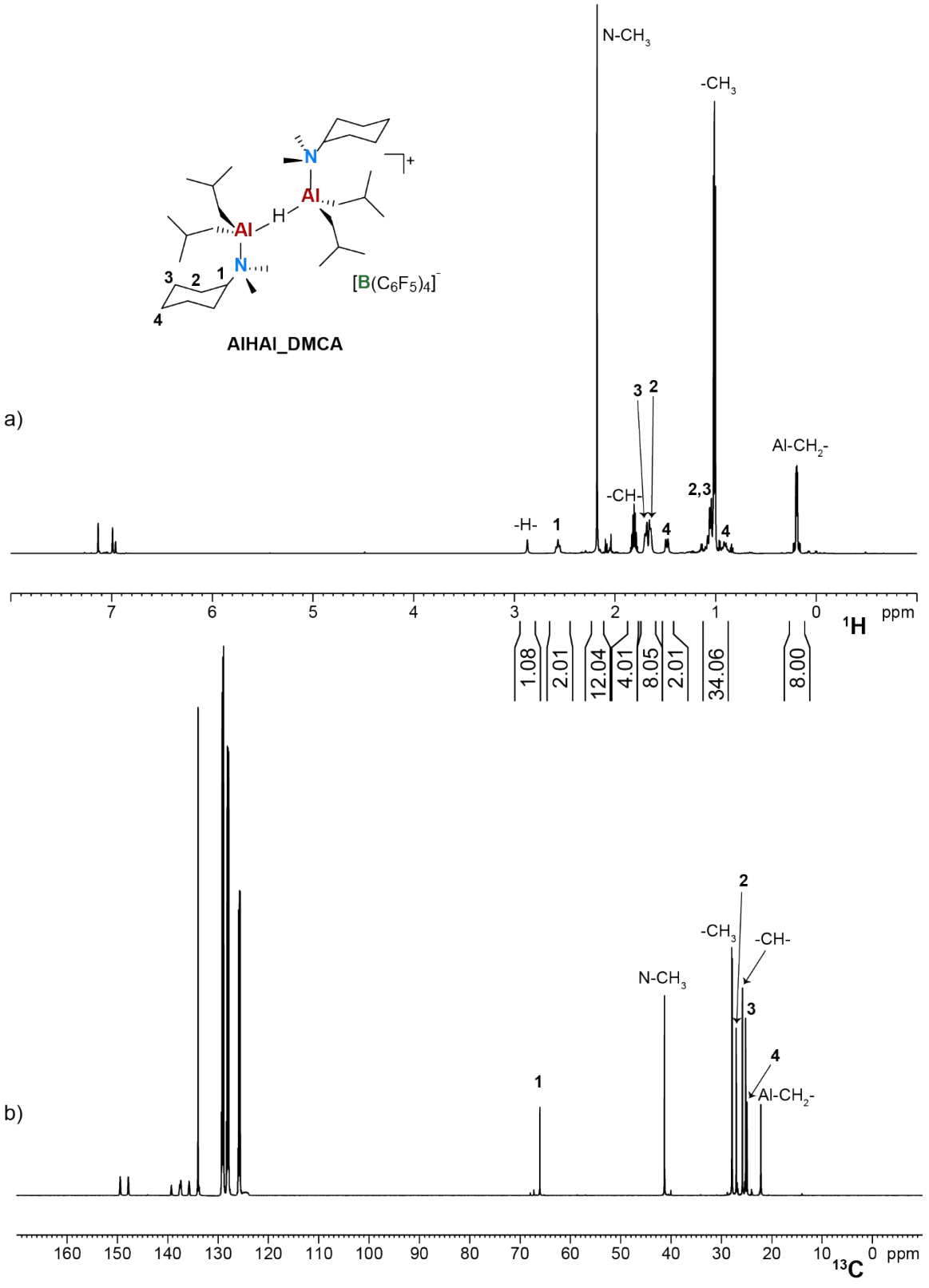


**Figure S8.** a) $^{1}$H and b) $^{13}$C NMR spectra (chlorobenzene-$d_5$, 298K) of **AlHAl_DMCA**.

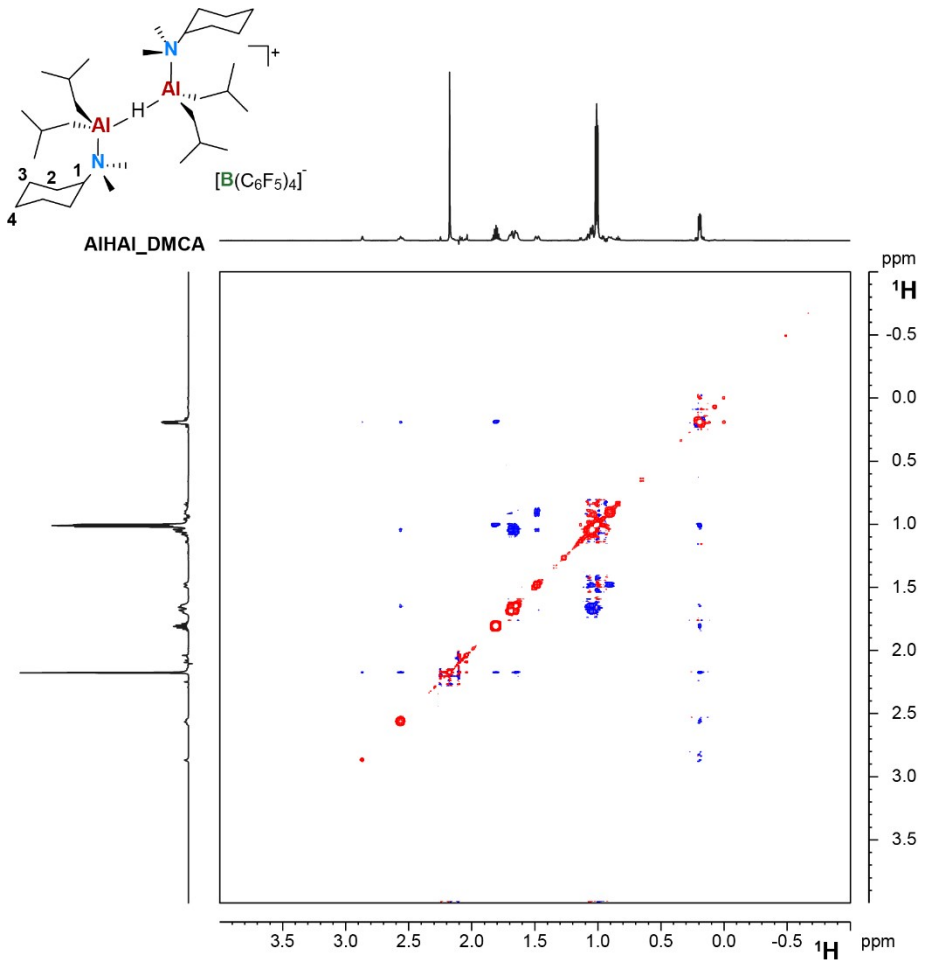


**Figure S9.** $^{1}$H NOESY NMR spectrum (chlorobenzene-$d_6$, 298K) of **AlHAl_DMCA**.

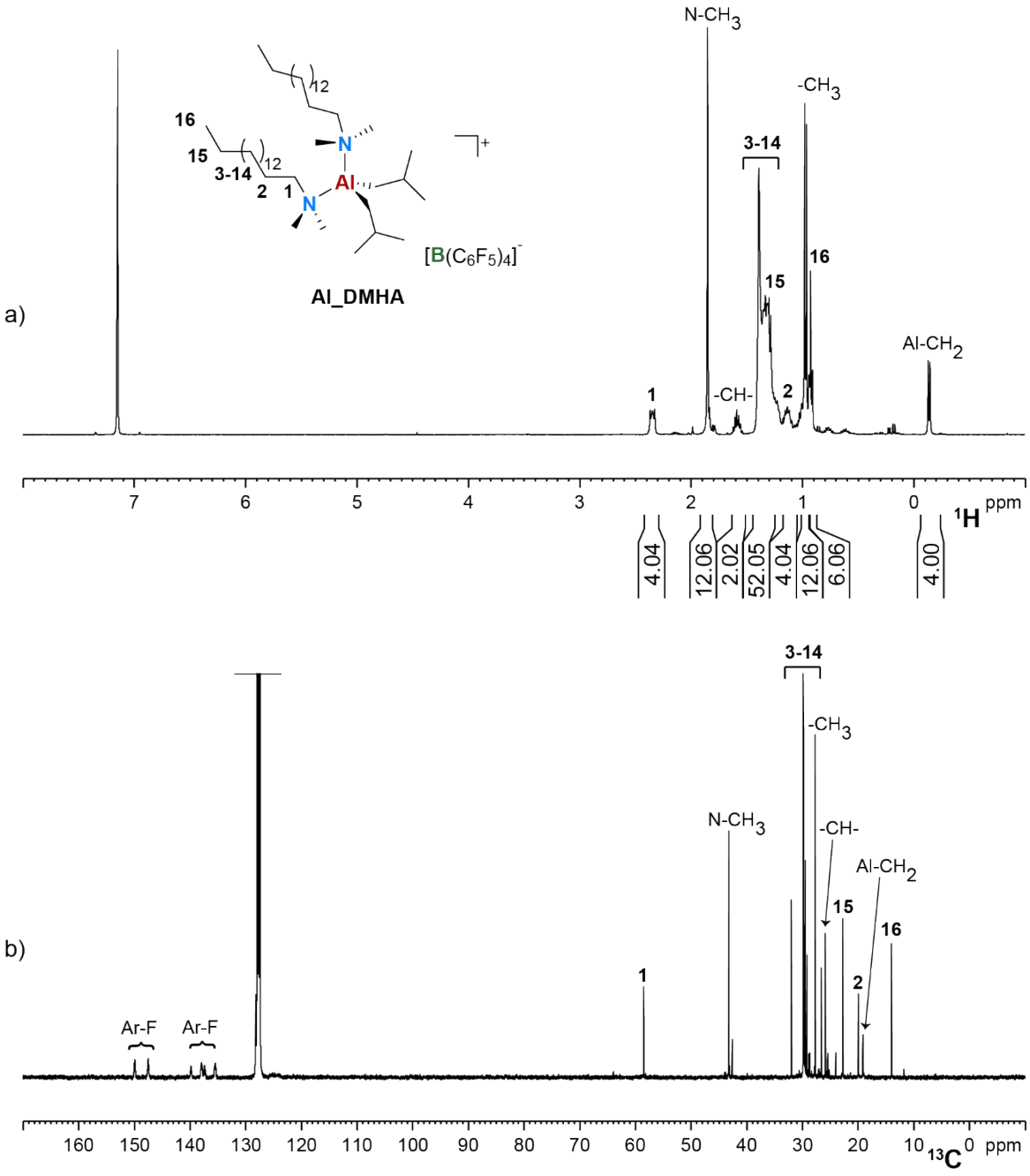


**Figure S10.** a) $^{1}H$ and b) $^{13}C$ NMR spectra (benzene-$d_6$, 298K) of **Al_DMHA**.

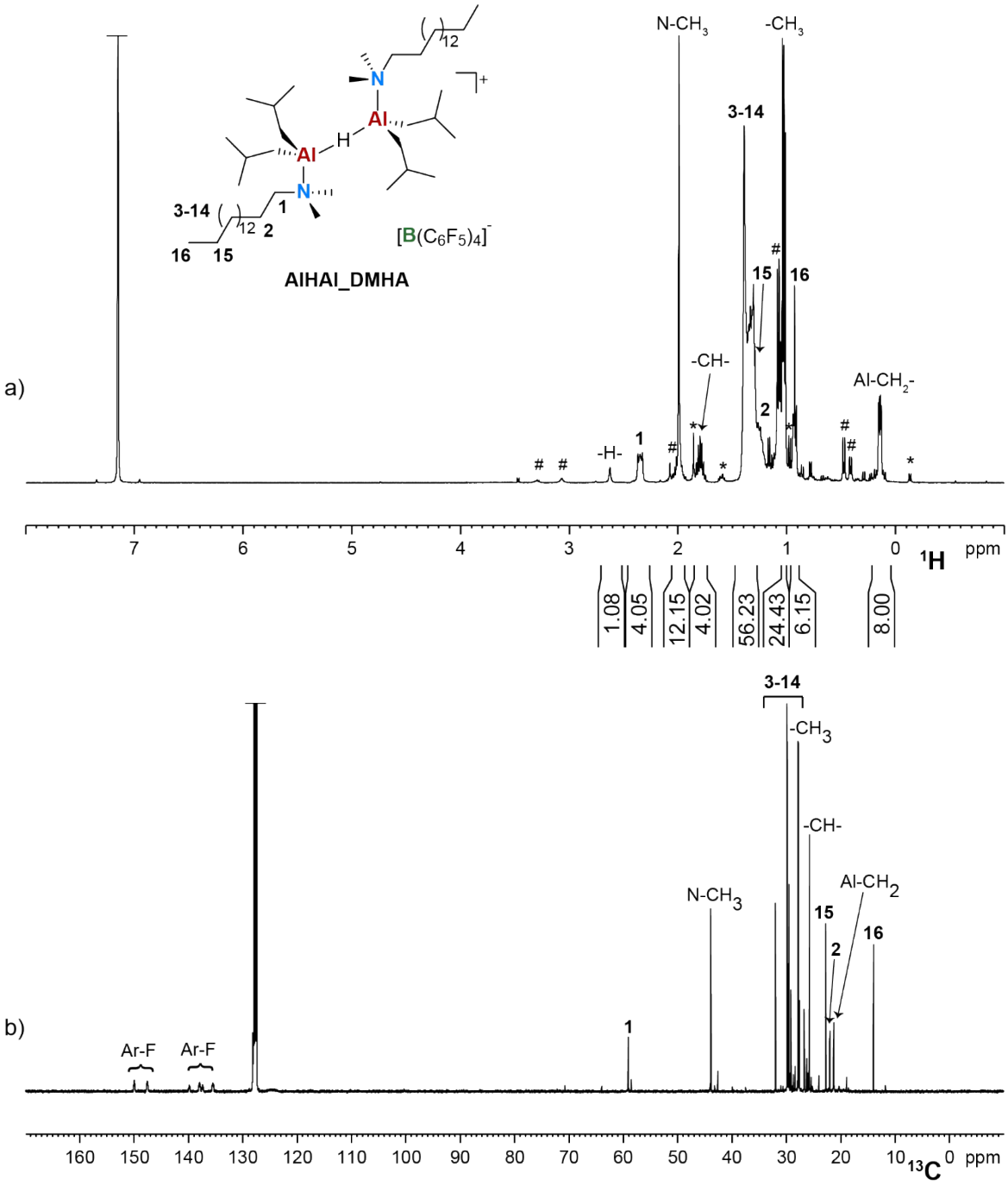


**Figure S11.** a) $^{1}$H and b) $^{13}$C NMR spectra (benzene-$d_6$, 298K) of **AlHAl_DMHA**. * = residual **Al_DMHA**; # = residual DIBAL-H.

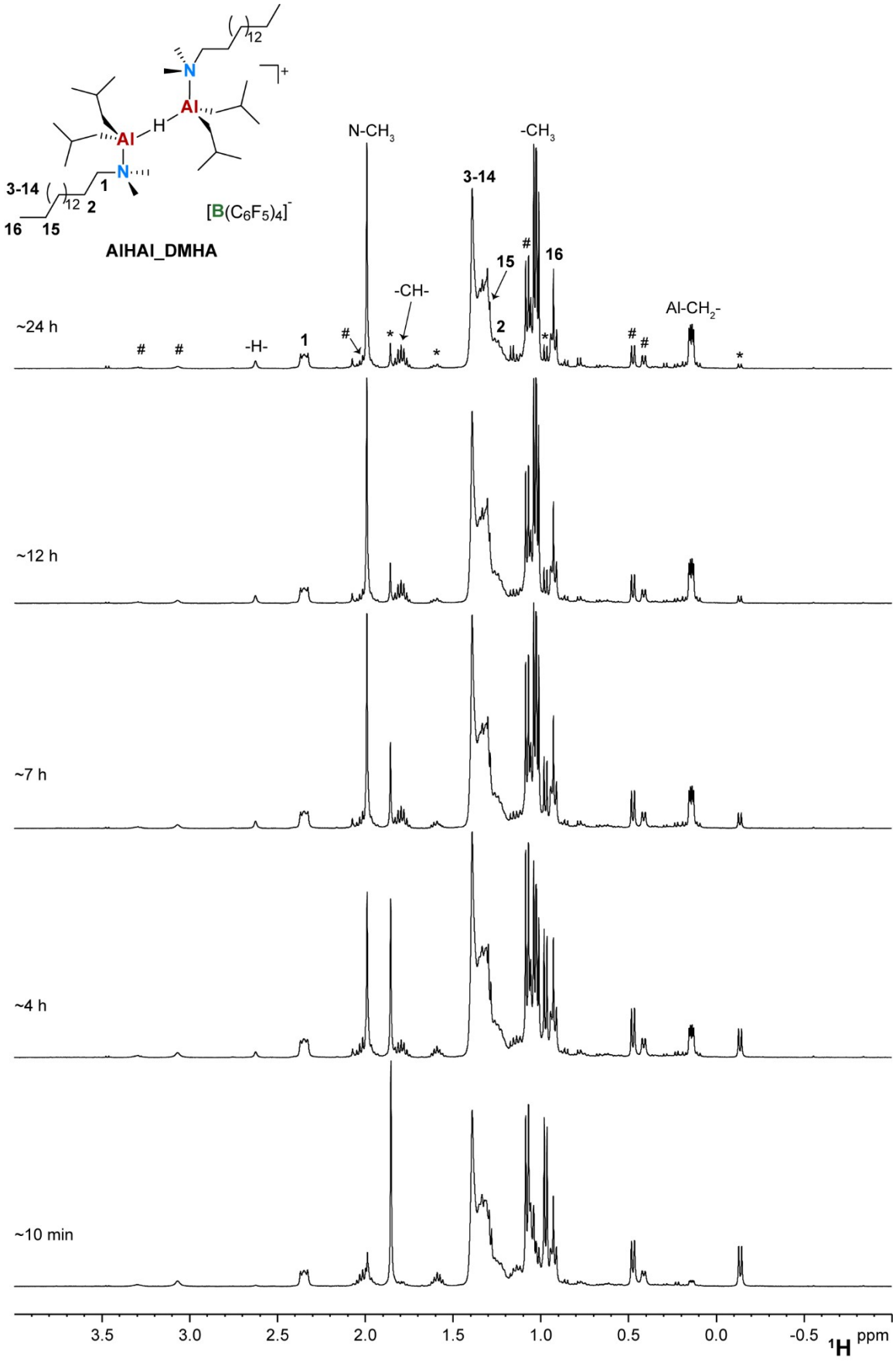


**Figure S12.** Comparison of $^{1}$H NMR spectra (benzene-$d_6$, 298K) of **AlHAl_DMHA** at increasing reaction time. * = residual **Al_DMHA**; # = residual DIBAL-H.

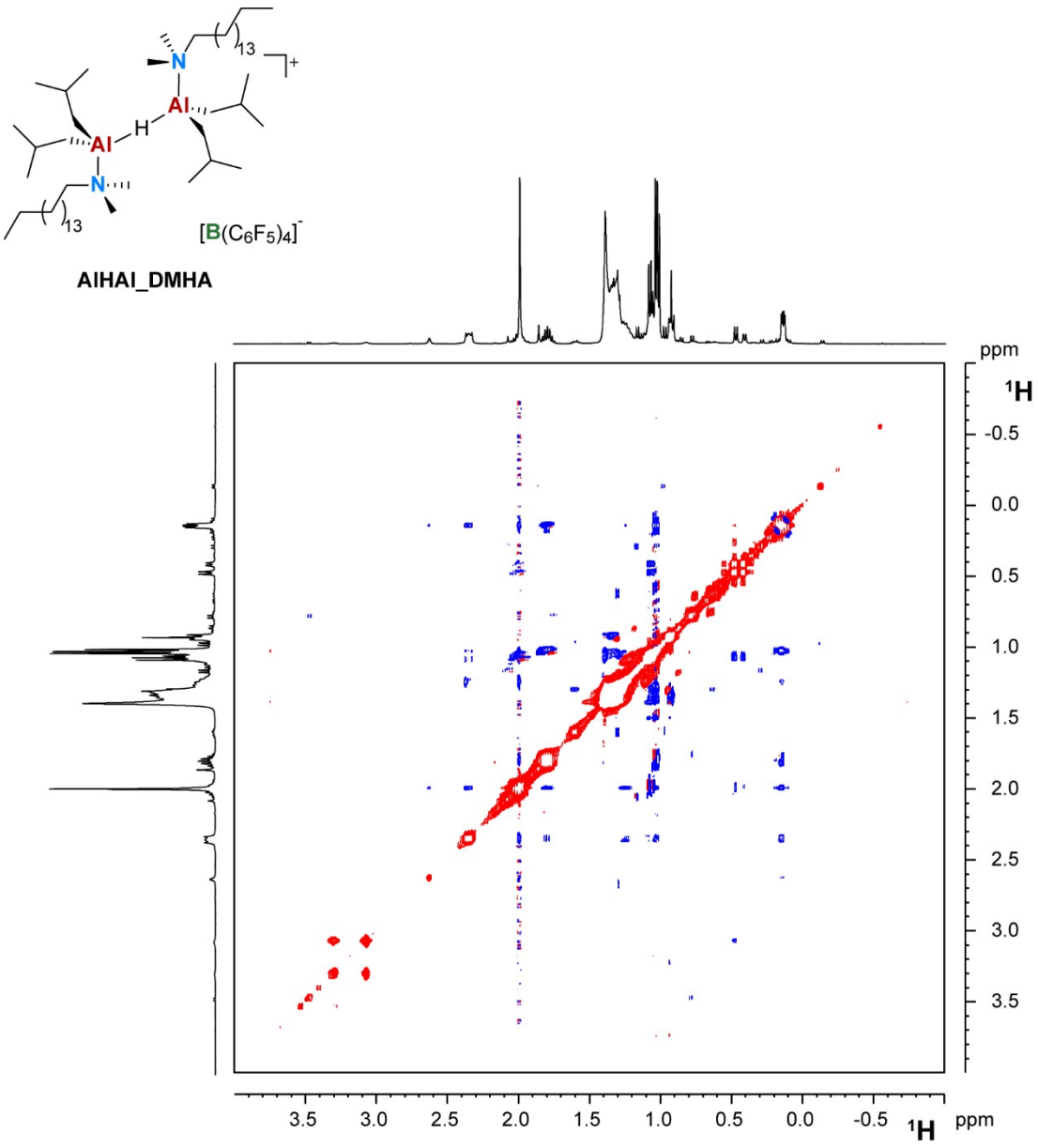


**Figure S13.** $^{1}$H NOESY spectrum (benzene-$d_6$, 298K) of **AlHAl_DMHA**.

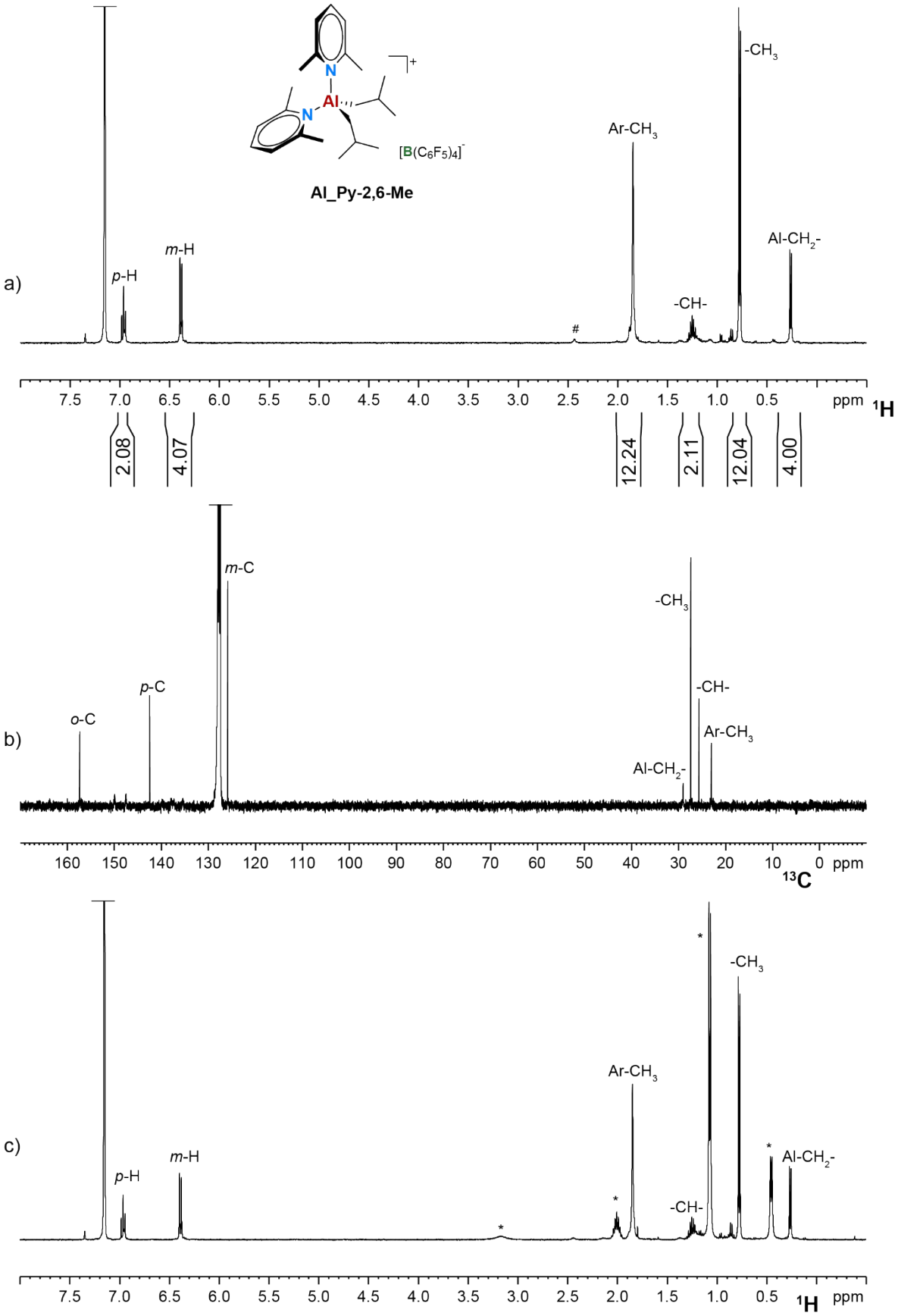


**Figure S14.** a) $^{1}$H and b) $^{13}$C NMR spectra (benzene-$d_6$, 298K) of **Al_Py-2,6-Me**, and c) $^{1}$H NMR spectrum of a **Al_Py-2,6-Me**/DiBAL-H mixture resulting in no detectable amounts of **AlHAl_Py-2,6-Me**. * = DIBALH; # = pyridinium borate.

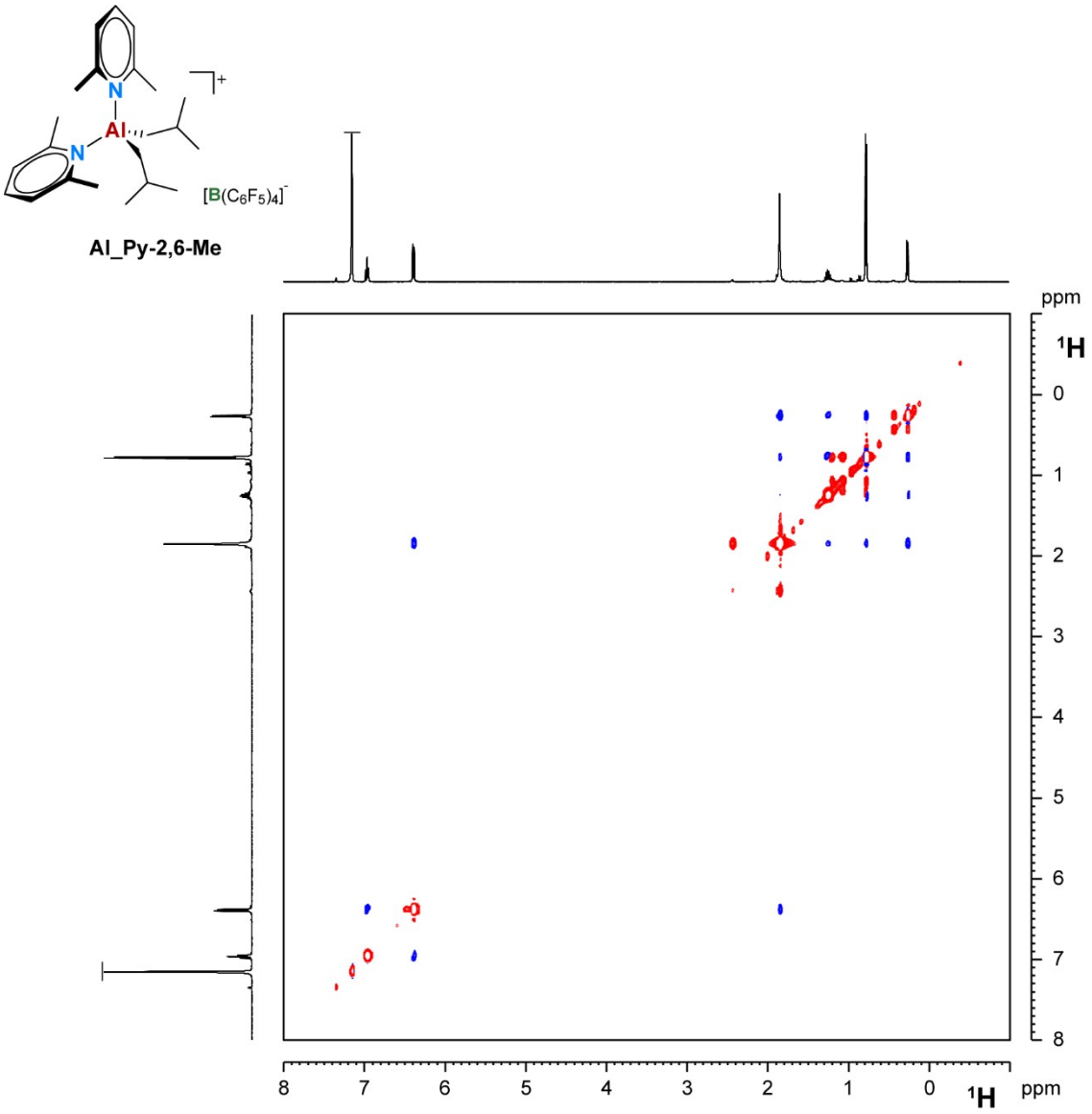


**Figure S15.** $^{1}$H NOESY NMR spectrum (benzene-$d_6$, 298K) of **Al_Py-2,6-Me**.

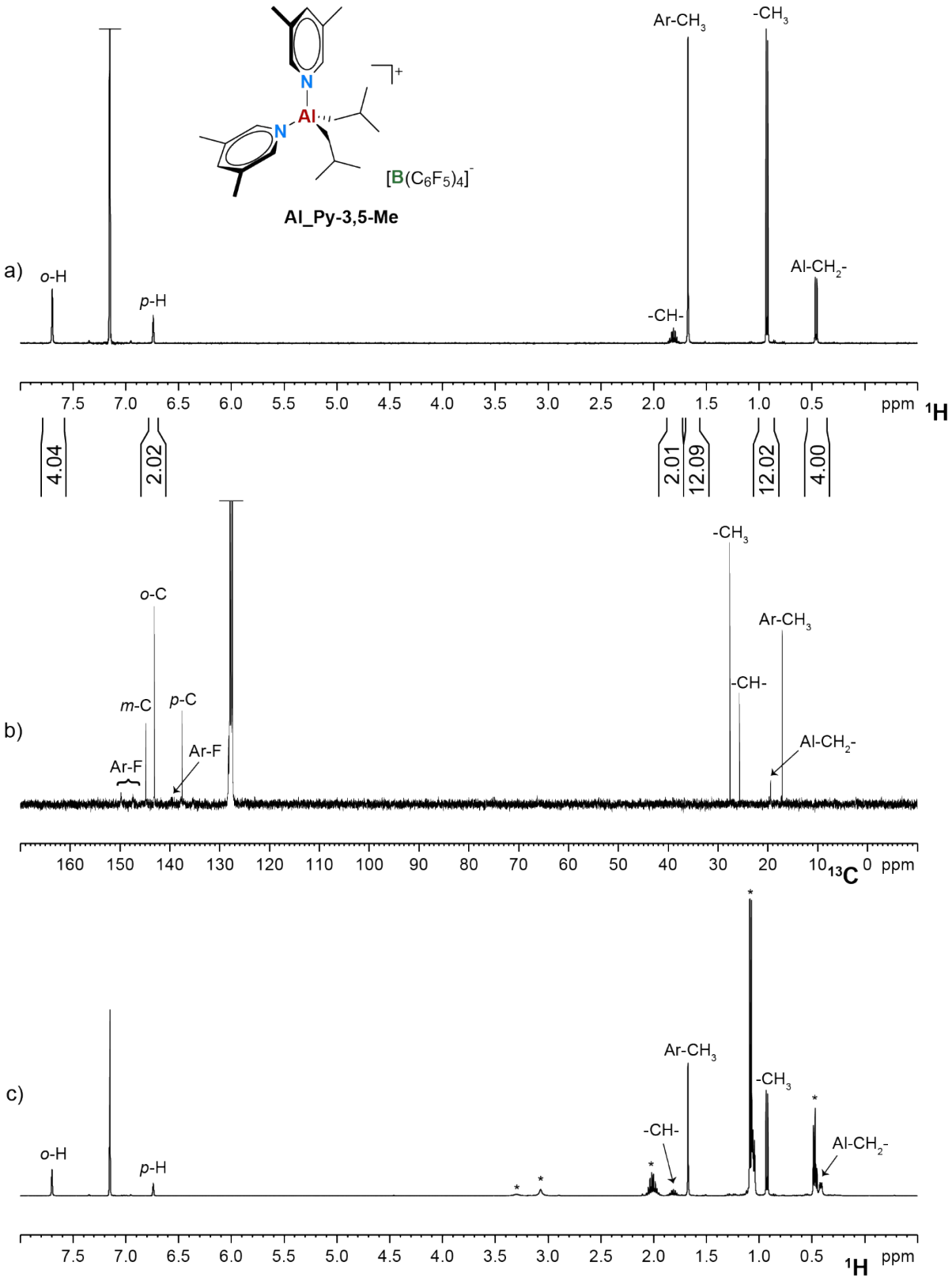


**Figure S16.** a) $^{1}$H and b) $^{13}$C NMR spectra (benzene-$d_6$, 298K) of **Al_Py-3,5-Me**, and c) $^{1}$H NMR spectrum of a **Al_Py-3,5-Me**/DiBAL-H mixture resulting in no detectable amounts of **AlHAl_Py-3,5-Me**. * = DIBALH.

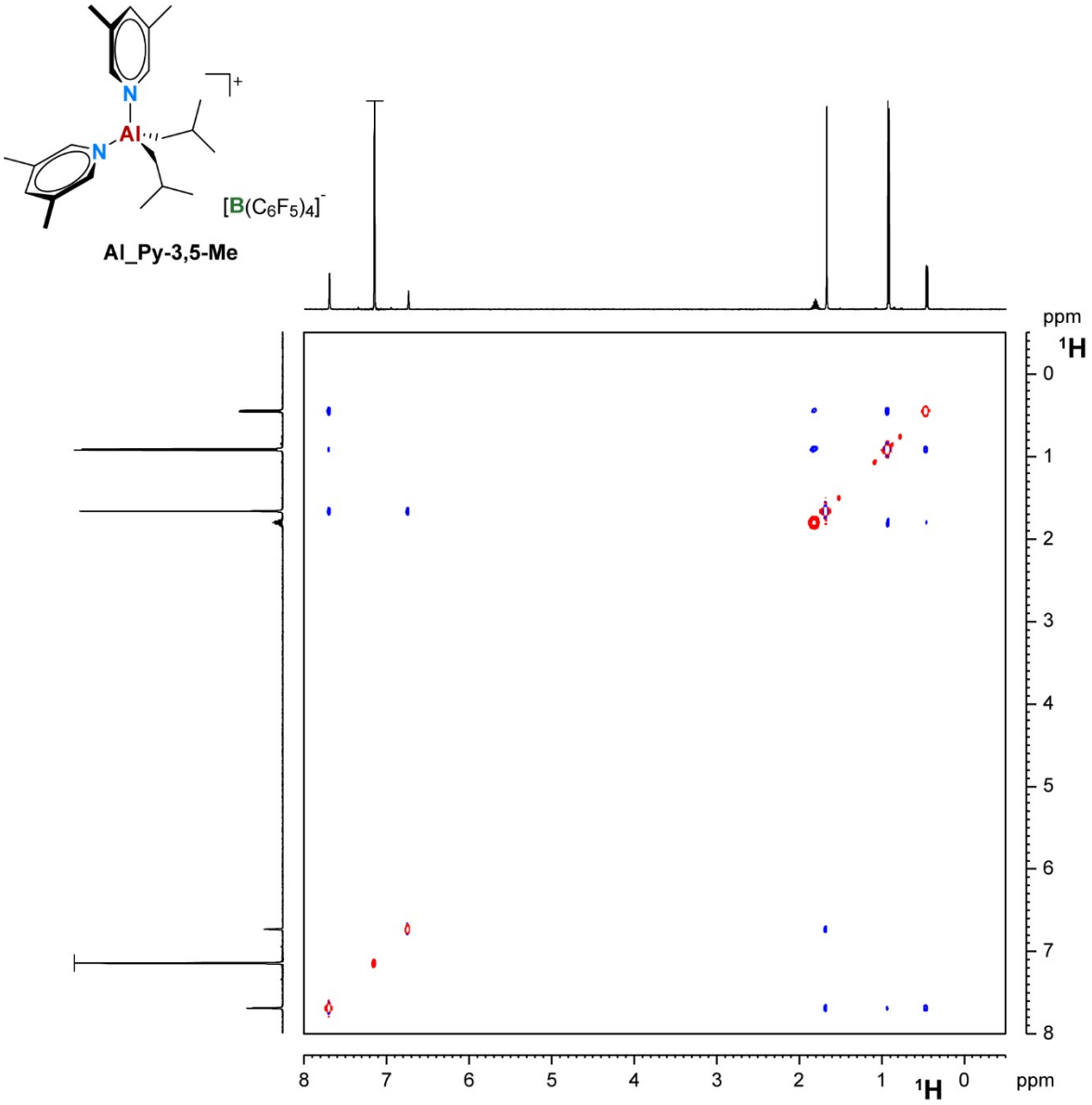


**Figure S17.** $^{1}$H NOESY NMR spectrum (benzene-$d_6$, 298K) of **Al_Py-3,5-Me**.

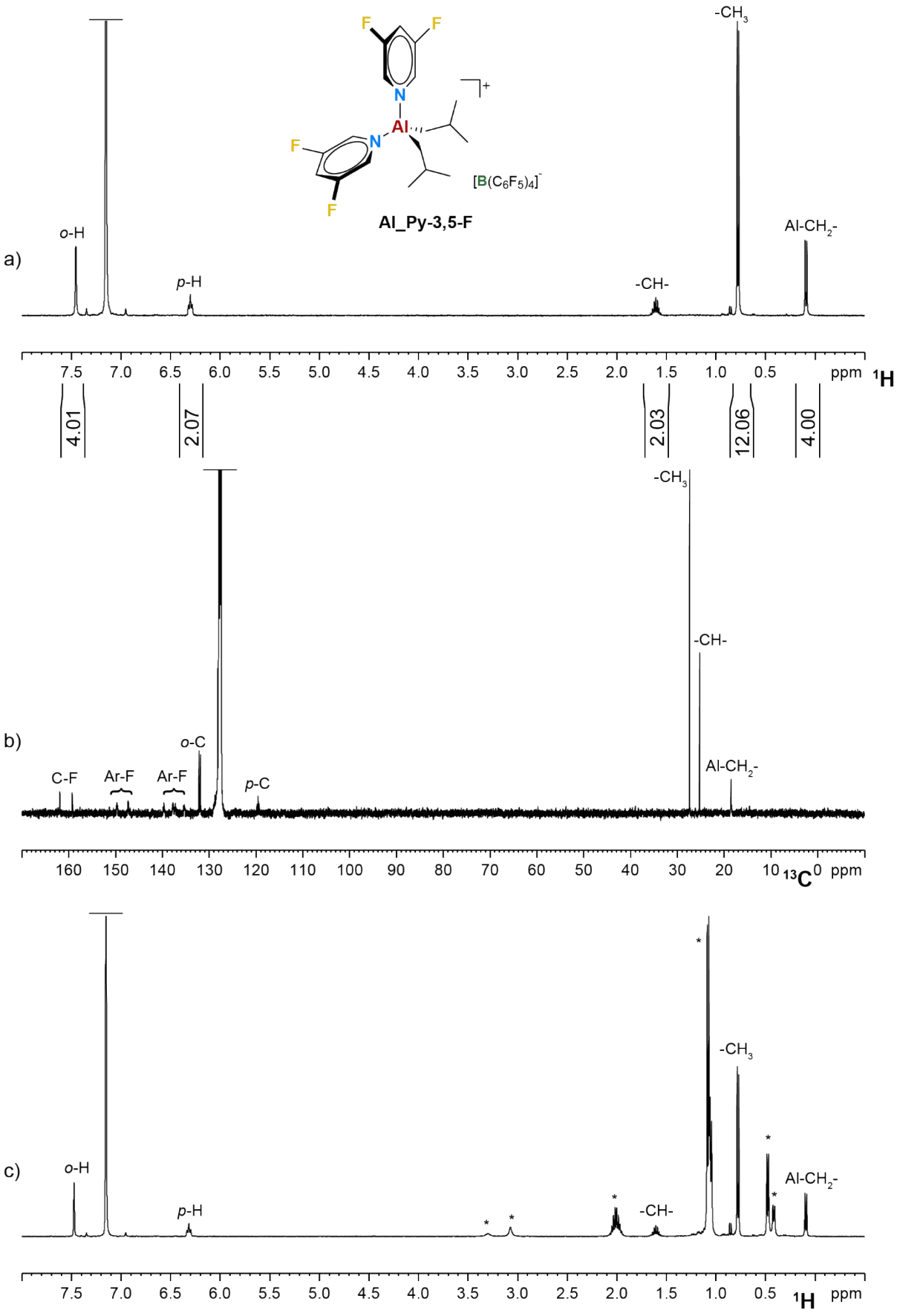


**Figure S18.** a) $^{1}$H and b) $^{13}$C NMR spectra (benzene-$d_6$, 298K) of **Al_Py-3,5-F**, and c) $^{1}$H NMR spectrum of a **Al_Py-3,5-F**/DiBAL-H mixture resulting in no detectable amounts of **AlHAl_Py-3,5-F**. * = DIBALH.

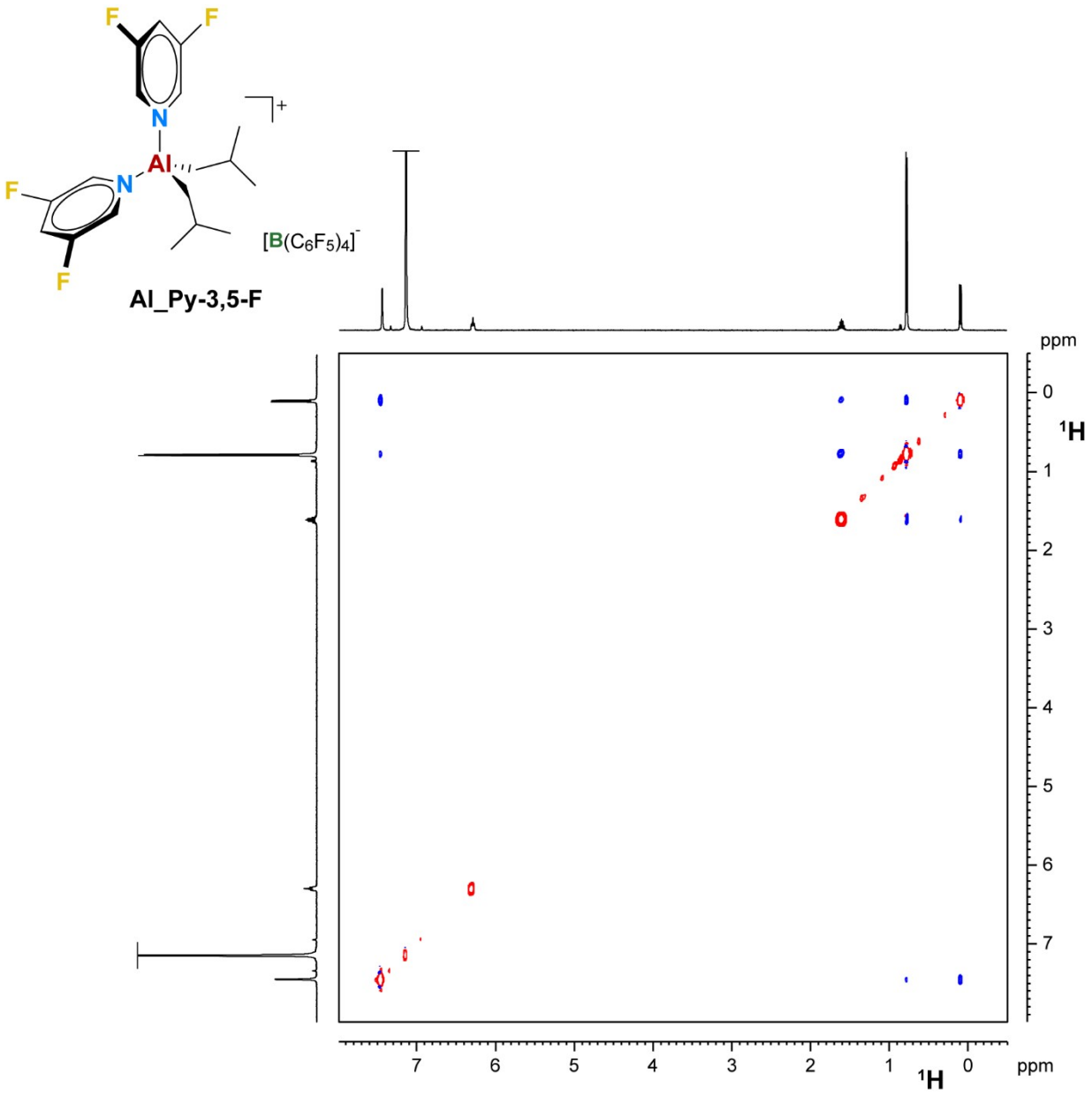


**Figure S19.** $^{1}$H NOESY NMR spectrum (benzene-$d_6$, 298K) of **Al_Py-3,5-F**.

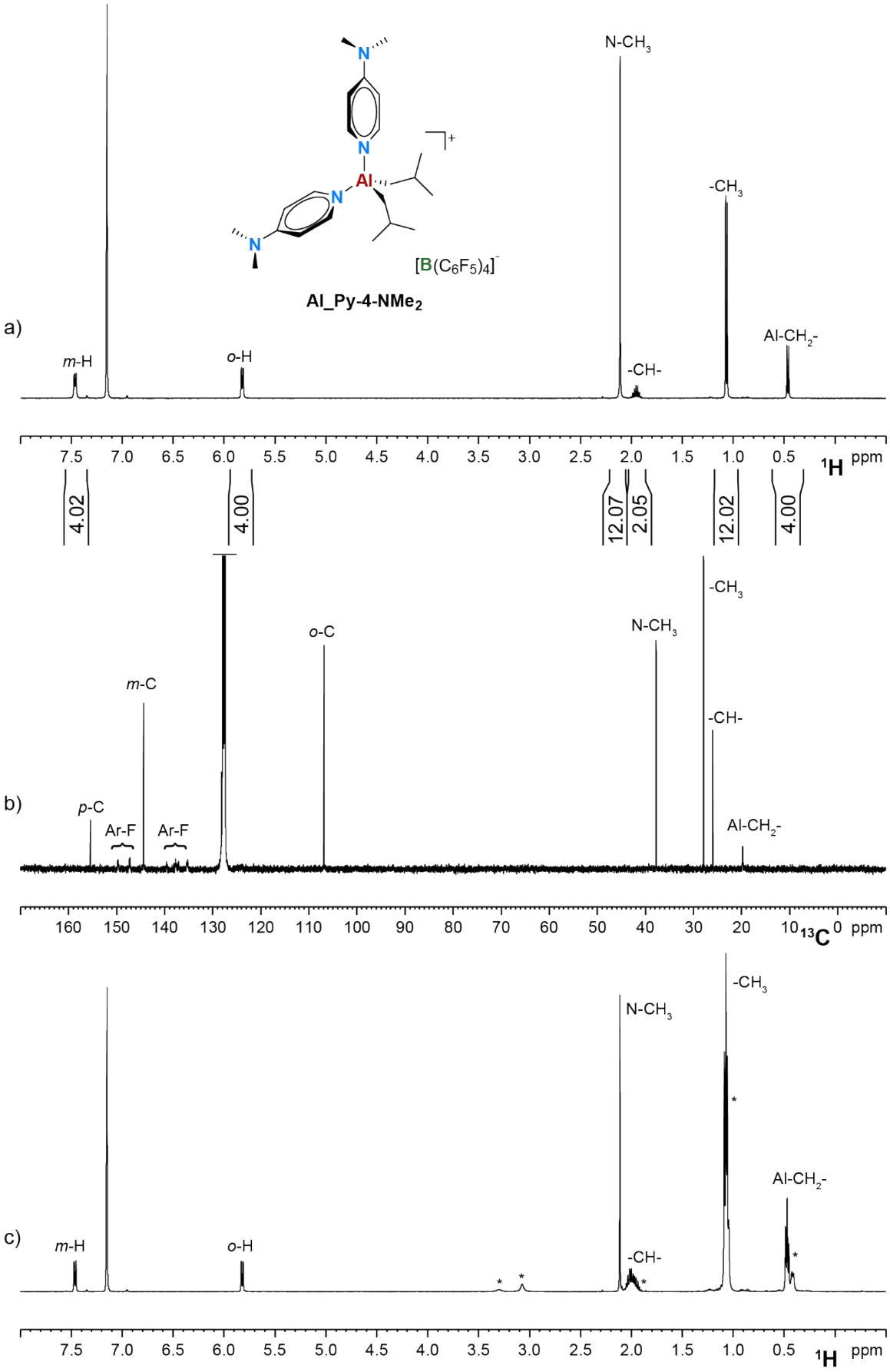


**Figure S20.** a) $^{1}$H and b) $^{13}$C NMR spectra (benzene-$d_6$, 298K) of **Al_Py-4-NMe$_2$**, and c) $^{1}$H NMR spectrum of a **Al_Py-4-NMe$_2$**/DiBAL-H mixture resulting in no detectable amounts of **AlHAl_Py-4-NMe$_2$**. * = DIBALH.

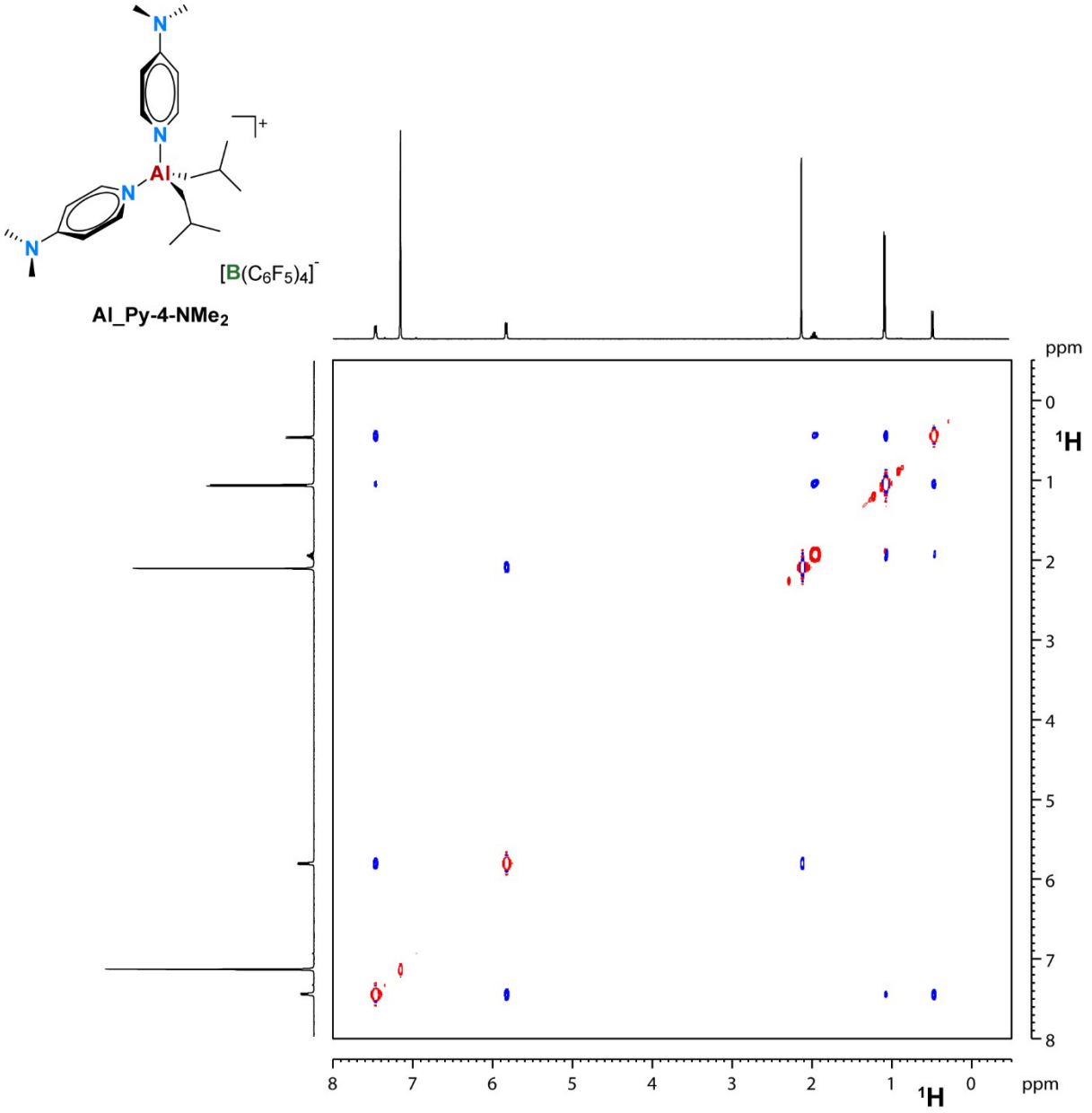


**Figure S21.** $^{1}$H NOESY NMR spectrum (benzene-$d_6$, 298K) of **Al_Py-4-NMe$_2$**.

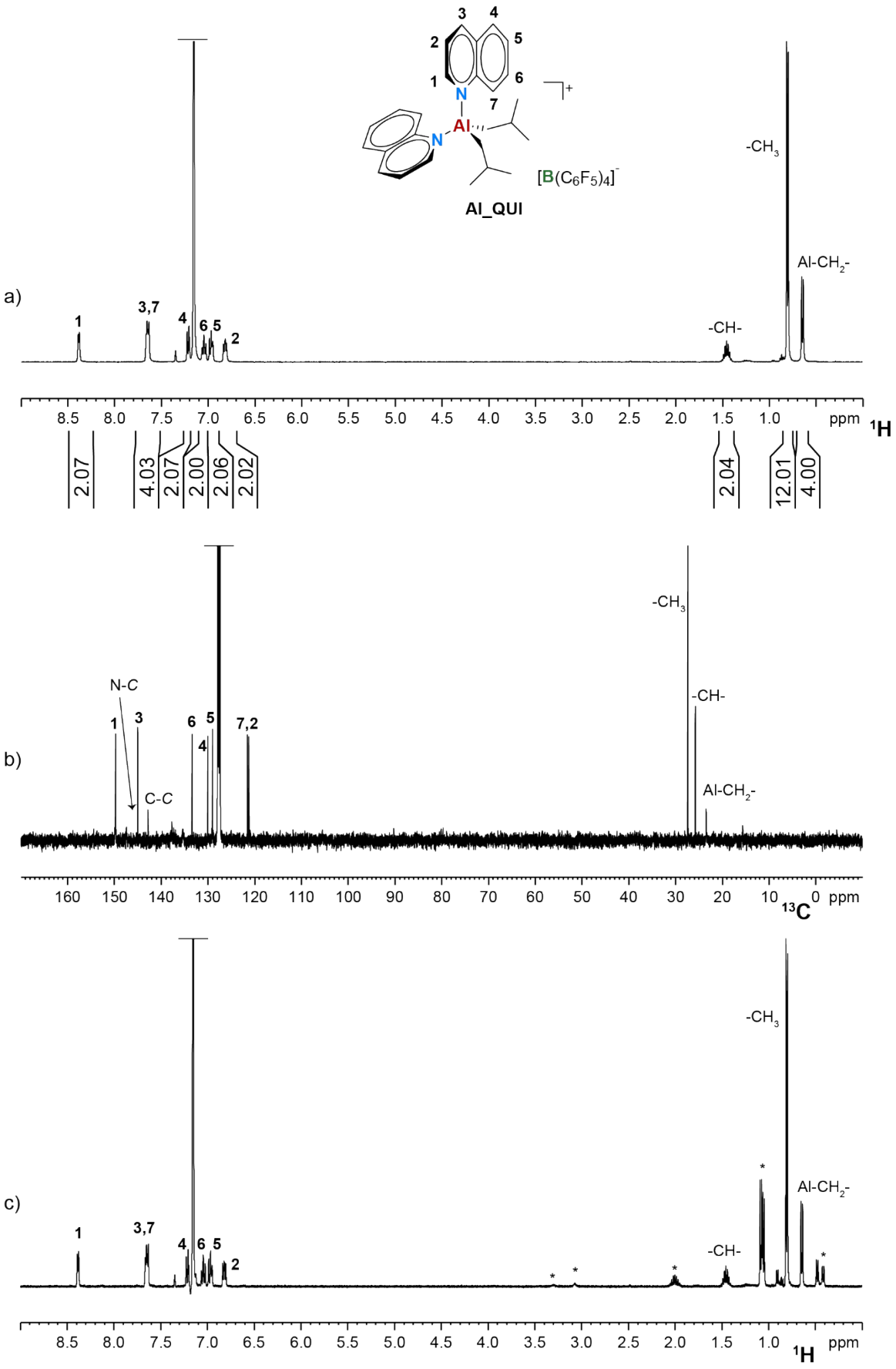


**Figure S22.** a) $^{1}$H and b) $^{13}$C NMR spectra (benzene-$d_6$, 298K) of **Al_QUI**, and c) $^{1}$H NMR spectrum of a **Al_QUI**/DiBAL-H mixture resulting in no detectable amounts of **AlHAl_QUI**. * = DIBALH.

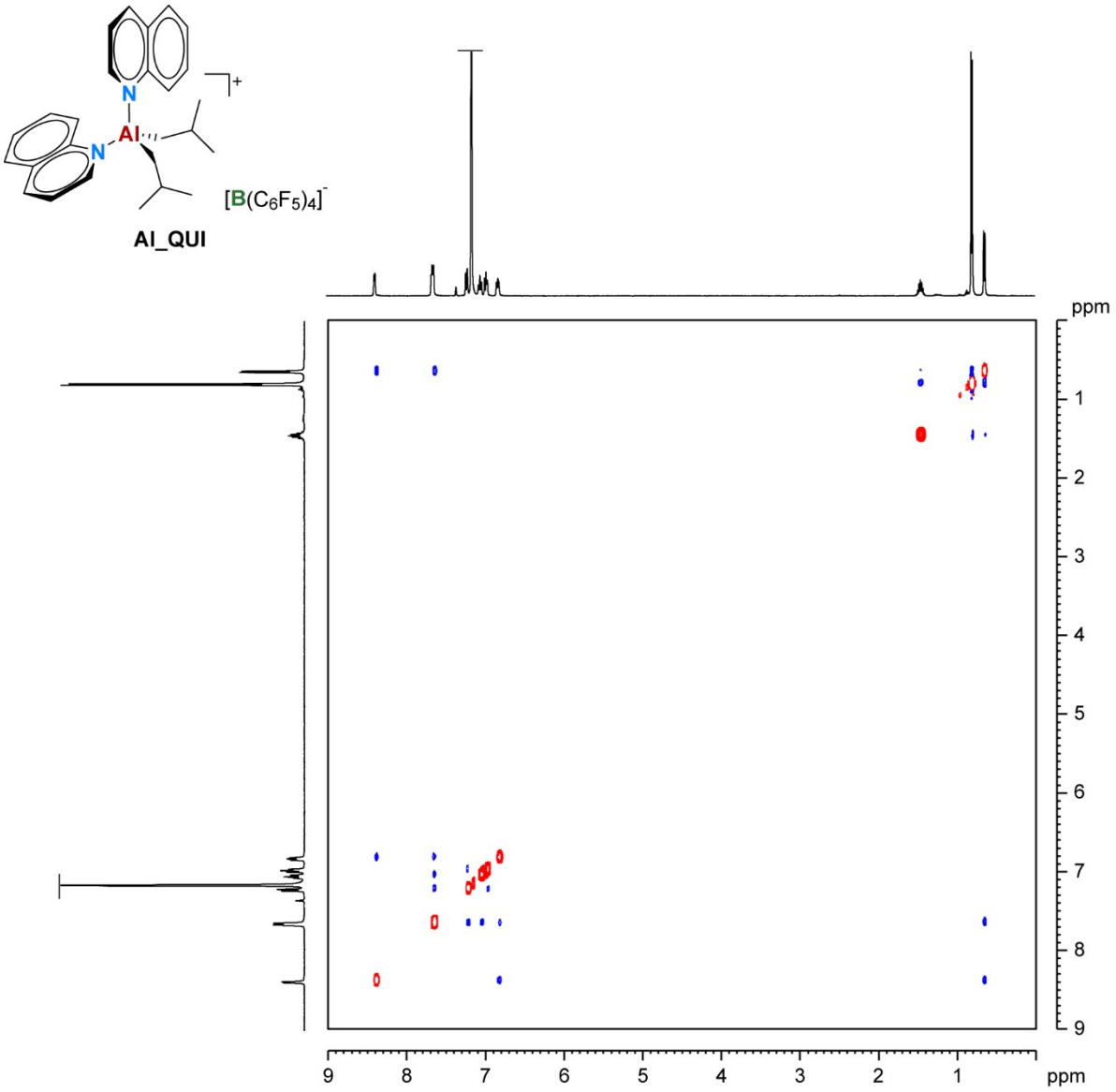


**Figure S23.** $^{1}$H NOESY NMR spectrum (benzene-$d_6$, 298K) of **Al_QUI**.

## 1.3 Additional information on the observed side reactions

### 1.3.1 Synthesis and reactivity of Al_Cyclo1

***Al_Cyclo1.*** Solid TTB (166 mg, 0.18 mmol) was added in small aliquots to a preformed and stirred solution of TIBAL (45 µL, 0.18 mmol) and **DMA-2-Me** (52 µL, 0.36 mmol) in toluene (1 mL). The resulting mixture was vigorously stirred for 72 h at room temperature. Upon stopping the stirring, a colorless oil precipitated. Pentane (6 mL) was added to facilitate precipitation of ionic byproducts. The supernatant was then removed, and the oil further extracted with pentane (2 x 6 mL). All the pentane fractions were then combined and dried under vacuum to obtain a white solid containing **Al_cyclo1** (61% yield) and $Ph_3CH$ byproduct. Alternative synthetic procedure using **DMA-2-Me**, BuLi and DIBAL-Cl have been reported in literature (see Figure S27).[1,2]

$^1$H NMR (400 MHz, benzene-$d_6$): 7.29 (bd, 1H, $^3J$ = 7.4 Hz, H1), 6.97 (ddd, 1H, $^3J$ = 7.4 Hz, $^3J$ = 7.4 Hz, $^4J$ = 1.2 Hz, H3), 6.86 (ddd, 1H, $^3J$ = 7.4 Hz, $^3J$ = 7.8 Hz, $^4J$ = 1.2 Hz, H2), 6.56 (bd, 1H, $^3J$ = 7.8 Hz, H4), 2.09 (s, 6H, N-$CH_3$), 1.98 (m, 2H, Al-$CH_2CH(CH_3)_2$), 1.52 (bs, 2H, Ar-$CH_2$-Al), 1.16 (d, 6H, $^3J$ = 6.4 Hz, Al-$CH_2CH(CH_3)_2$), 1.15 (d, 6H, $^3J$ = 6.4 Hz, Al-$CH_2CH(CH_3)_2$), 0.19 (dd, 2H, $^2J$ = 13.8 Hz, $^3J$ = 7.2 Hz, Al-$CH_2CH(CH_3)_2$), 0.06 (dd, 2H, $^2J$ = 13.8 Hz, $^3J$ = 6.8 Hz, Al-$CH_2CH(CH_3)_2$) ppm. $^{13}$C NMR (100 MHz, benzene-$d_6$): 148.7 (C-N), 142.3 (*C*-$CH_2$-), 132.3 (C1), 127.2 (C3), 124.3 (C2), 117.2 (C4), 46.0 (N-$CH_3$), 28.3 (Al-$CH_2CH(CH_3)_2$), 26.6 (Al-$CH_2CH(CH_3)_2$), 21.0 (Al-$CH_2CH(CH_3)_2$) ppm.

*In another solvent.* $^1$H NMR (400 MHz, chlorobenzene-$d_5$): 7.25 (bd, 1H, $^3J$ = 7.6 Hz, H1), 6.99 (m, 1H, H3), 6.92 (m, 1H, H2), 6.81 (bd, 1H, $^3J$ = 7.4 Hz, H4), 2.37 (s, 6H, N-$CH_3$), 1.86 (m, 2H, Al-$CH_2CH(CH_3)_2$), 1.41 (bs, 2H, Ar-$CH_2$-Al), 1.02 (d, 6H, $^3J$ = 7.4 Hz, Al-$CH_2CH(CH_3)_2$), 1.01 (d, 6H, $^3J$ = 7.4 Hz, Al-$CH_2CH(CH_3)_2$), 0.08 (dd, 2H, $^2J$ = 13.8 Hz, $^3J$ = 7.2 Hz, Al-$CH_2CH(CH_3)_2$), -0.04 (dd, 2H, $^2J$ = 13.8 Hz, $^3J$ = 7.0 Hz, Al-$CH_2CH(CH_3)_2$) ppm.

***Al_Cyclo1_DMA-2-Me.*** Solid TTB (30 mg, 32 µmol) was added in small aliquots to a preformed and stirred solution of **DMA-2-Me** (5 µL, 35 µmol) and **Al_cyclo1** (9.6 mg, 35 µmol) in toluene (1 mL). The resulting mixture was vigorously stirred for a few minutes at room temperature. Upon stopping the stirring, a colorless oil precipitated. Pentane (3 mL) was added to facilitate precipitation of ionic products. The supernatant was then removed, and the oil further washed with pentane (3 mL) and benzene-$d_6$ (150 µL). After the last washing, the residue was dried under vacuum to obtain **Al_Cyclo1_DMA-2-Me** as a white solid (22 mg, 69% yield).

$^1$H NMR (400 MHz, chlorobenzene-$d_5$): 7.04 (m, 1H, H11), 7.04 (m, 1H, H9), 7.02 (m, 1H, H2), 6.99 (m, 2H, H3 and C-H10), 6.94 (m, 1H, H4), 6.78 (d, 1H, $^3J$ = 7.8 Hz, H1), 6.75 (d, 1H, $^3J$ = 7.8 Hz, H12), 2.48 (bs, 3H, N-$CH_3$ (6)), 2.42 (bs, 3H, N-$CH_3$ (7)), 2.37 (bs, 3H, N-$CH_3$ (14)), 2.23 (bs, 3H, N-$CH_3$ (13)), 2.14 (s, 3H, Ar-$CH_3$ (5)), 1.40 (d, 1H, $^2J$ = 17.0 Hz, Ar-$CH_2$(8)-Al), 1.25 (m, 1H, Al-$CH_2CH(CH_3)_2$), 1.20 (d, 1H, $^2J$ = 17.0 Hz, Ar-$CH_2$(8)-Al), 0.73 (d, 3H, $^3J$ = 6.4 Hz, Al-$CH_2CH(CH_3)_2$), 0.69 (d, 3H, $^3J$ = 6.6 Hz, Al-$CH_2CH(CH_3)_2$), -0.02 (dd, 1H, $^2J$ = 14.8 Hz, $^3J$ =

5.6 Hz, Al-C$H_2$CH$(CH_3)_2$), -0.19 (dd, 1H, $^2J$ = 14.8 Hz, $^3J$ = 5.6 Hz, Al-C$H_2$CH$(CH_3)_2$) ppm. $^{13}$C NMR (100 MHz, chlorobenzene-$d_5$): 145.8 (aromatic N-C), 143.7 (aromatic N-C), 135.9 (aromatic *C*-$CH_2$-Al), 135.6 (C4), 132.3 (C9), 130.3 (aromatic *C*-$CH_3$), 129.3 (C2 and C11), 128.6 (C3), 128.0 (C10), 120.7 (C1), 116.9 (C12), 48.0 (C14), 47.6 (C7), 47.2 (C6), 46.3 (C13), 27.5 (Al-$CH_2$CH(*C*$H_3)_2$), 26.9 (Al-$CH_2$CH(*C*$H_3)_2$), 25.9 (Al-$CH_2$*C*H$(CH_3)_2$), 22.3 (C5), 18.6 (Al-*C*$H_2$CH$(CH_3)_2$), 12.0 (Ar-$CH_2$-Al) ppm.

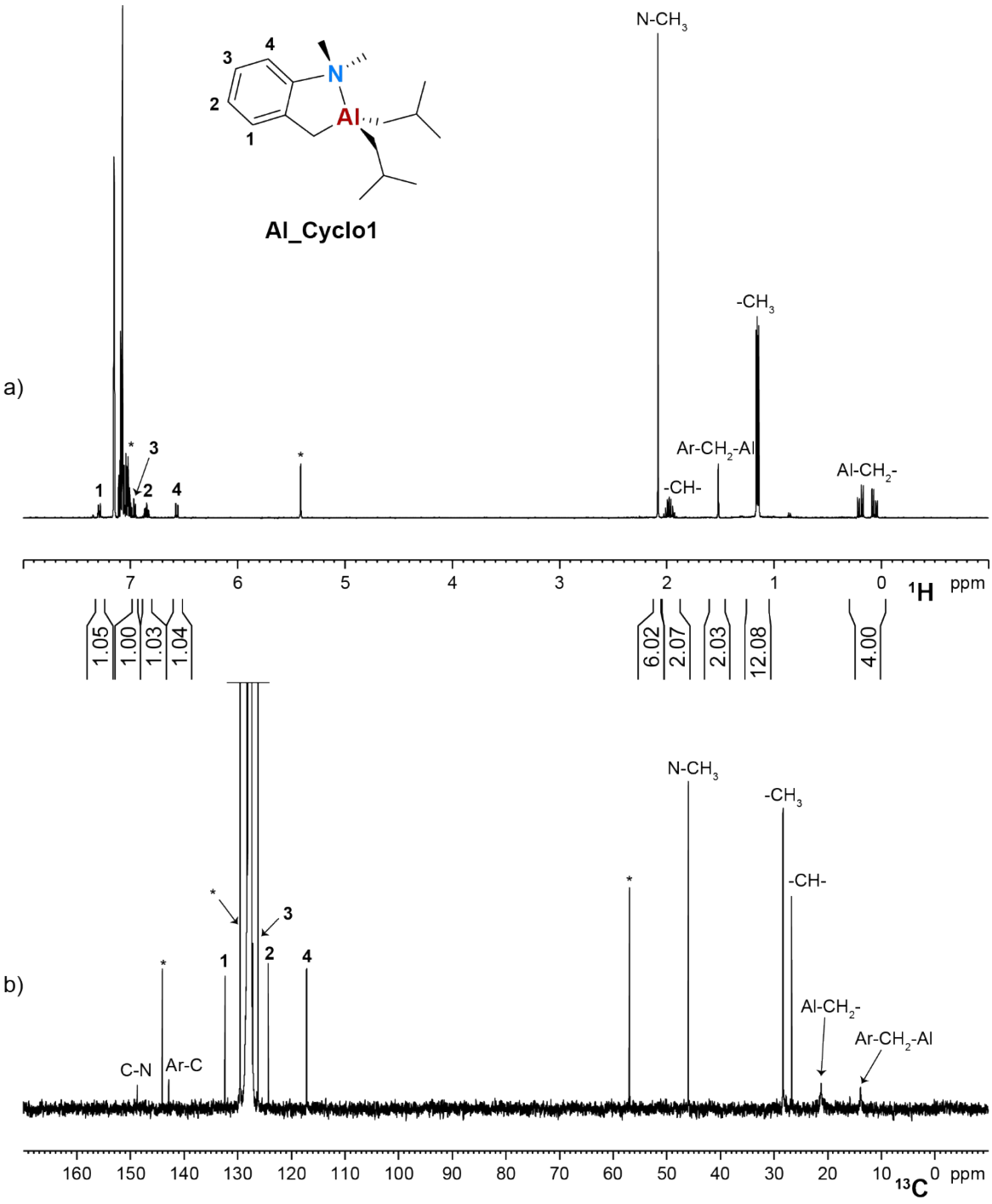


**Figure S24.** a) $^1$H and b) $^{13}$C NMR spectra (benzene-$d_6$, 298K) of **Al_Cyclo1**. * = residual $Ph_3CH$.

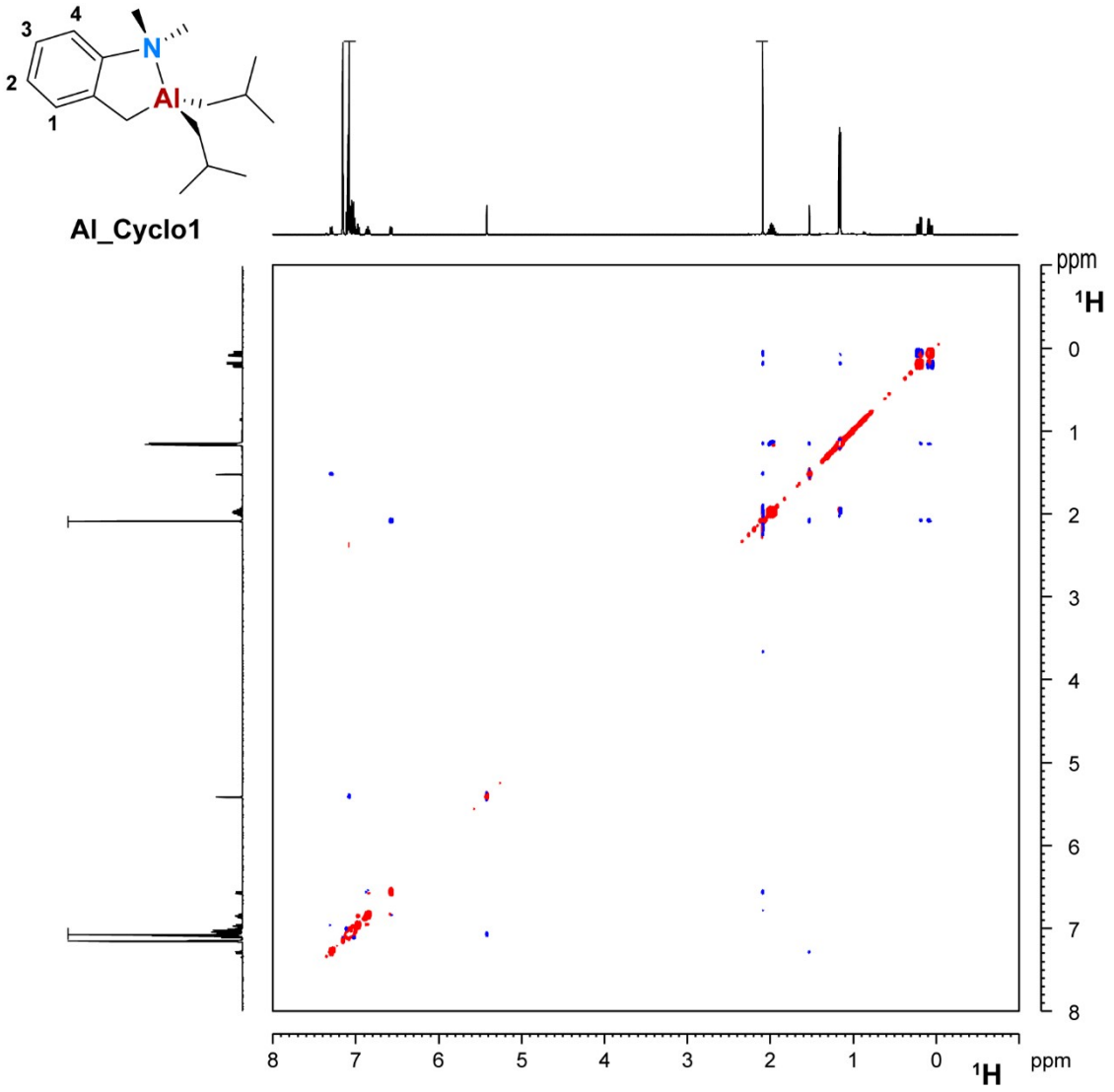


**Figure S25.** $^{1}$H NOESY NMR spectrum (benzene-$d_6$, 298K) of **Al_Cyclo1**.

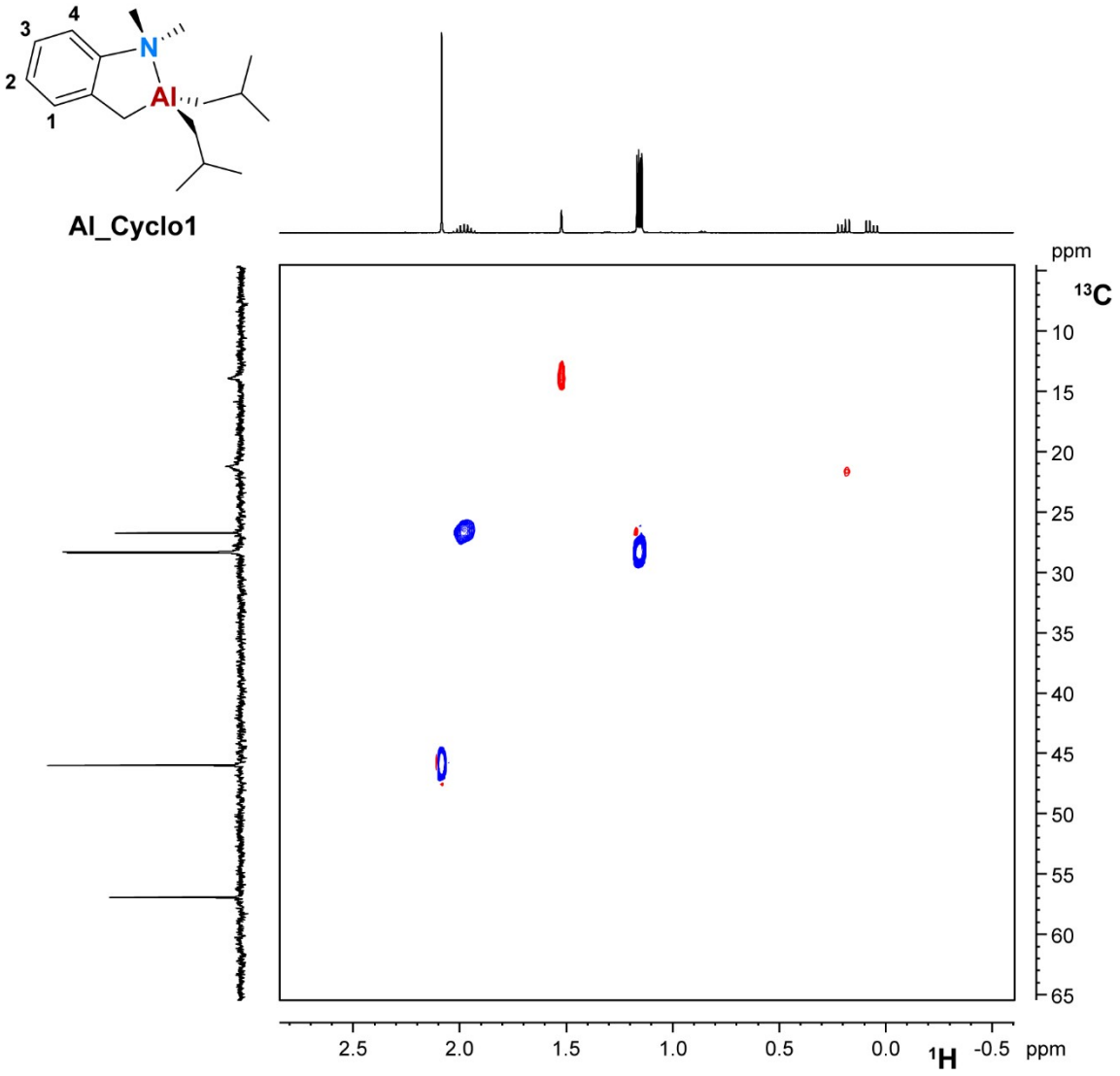


**Figure S26.** $^{1}H,^{13}C$ HSQC NMR spectra (benzene-$d_6$, 298K) of **Al_Cyclo1**.

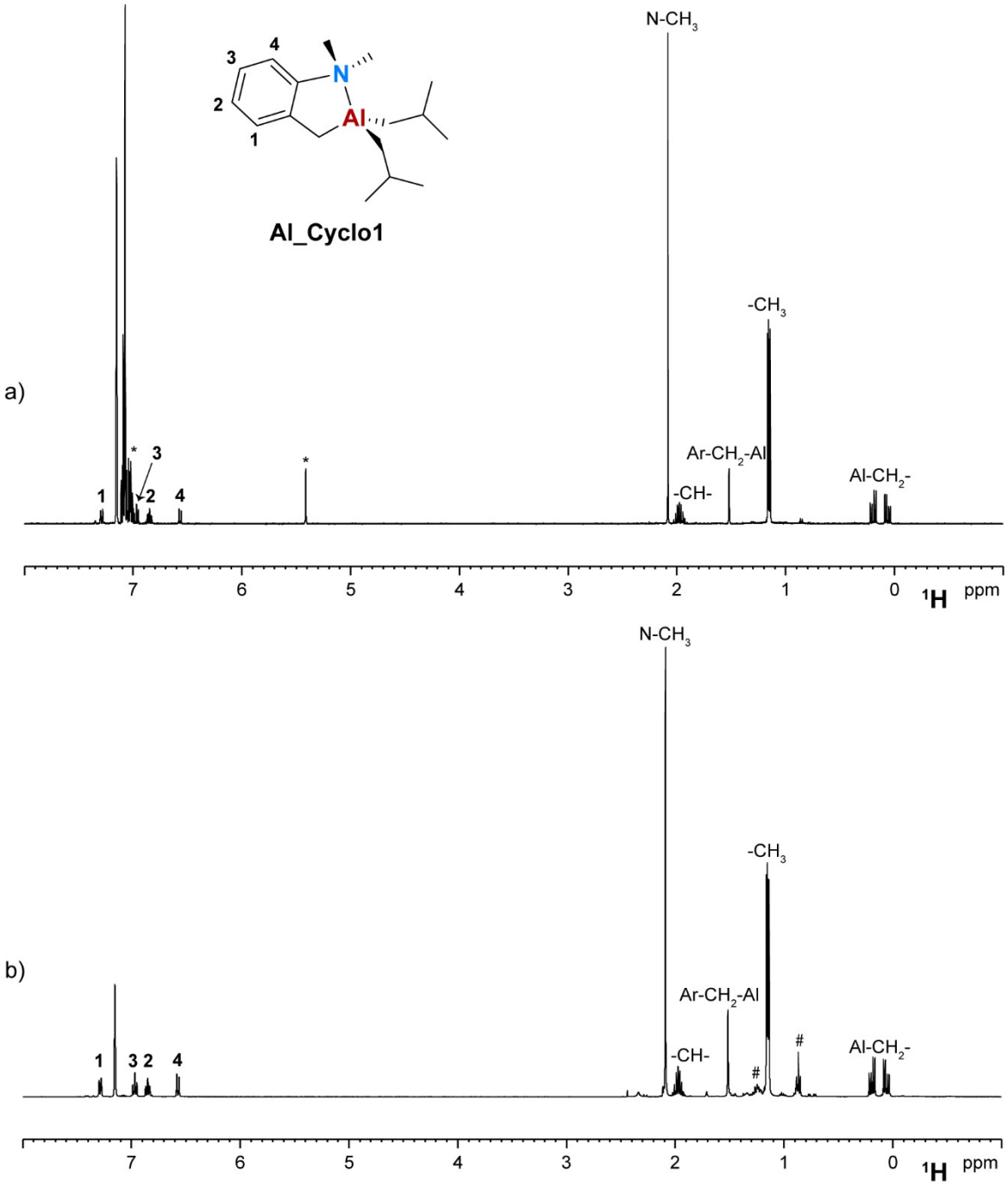


**Figure S27.** Comparison of $^{1}$H NMR spectra (benzene-$d_6$, 298 K) of **Al_Cyclo1** obtained from a) the self-decomposition of **Al_DMA-2-Me** and b) independently from the reaction of **DMA-2-Me** with BuLi and DIBAL-Cl. $^{\#}$ = residual heptane from synthesis

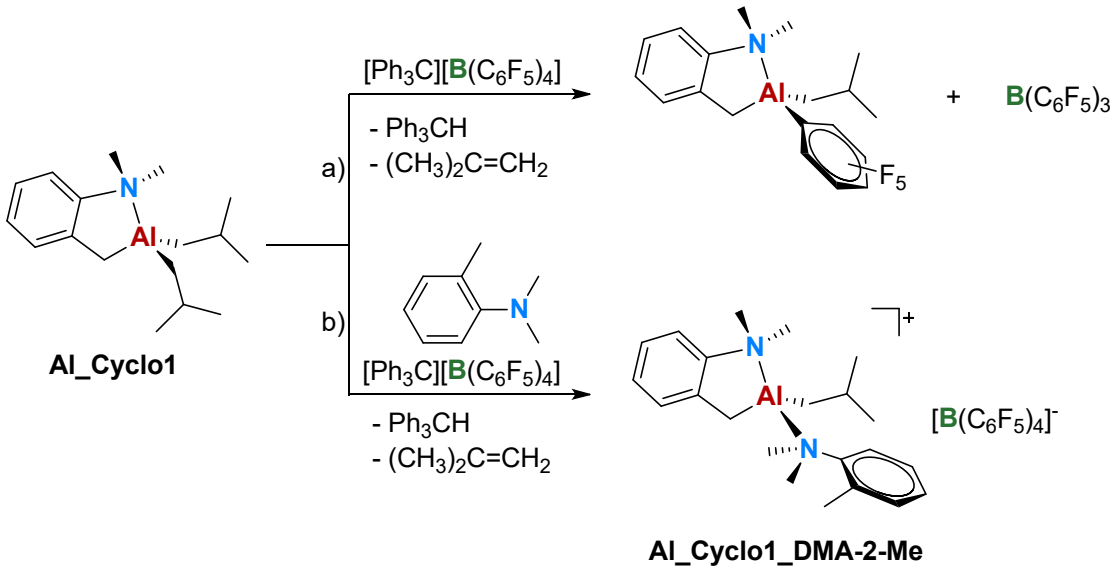


**Scheme S1.** Ionization of **Al_Cyclo1** in the a) absence and b) presence of an equivalent of **DMA-2-Me**.

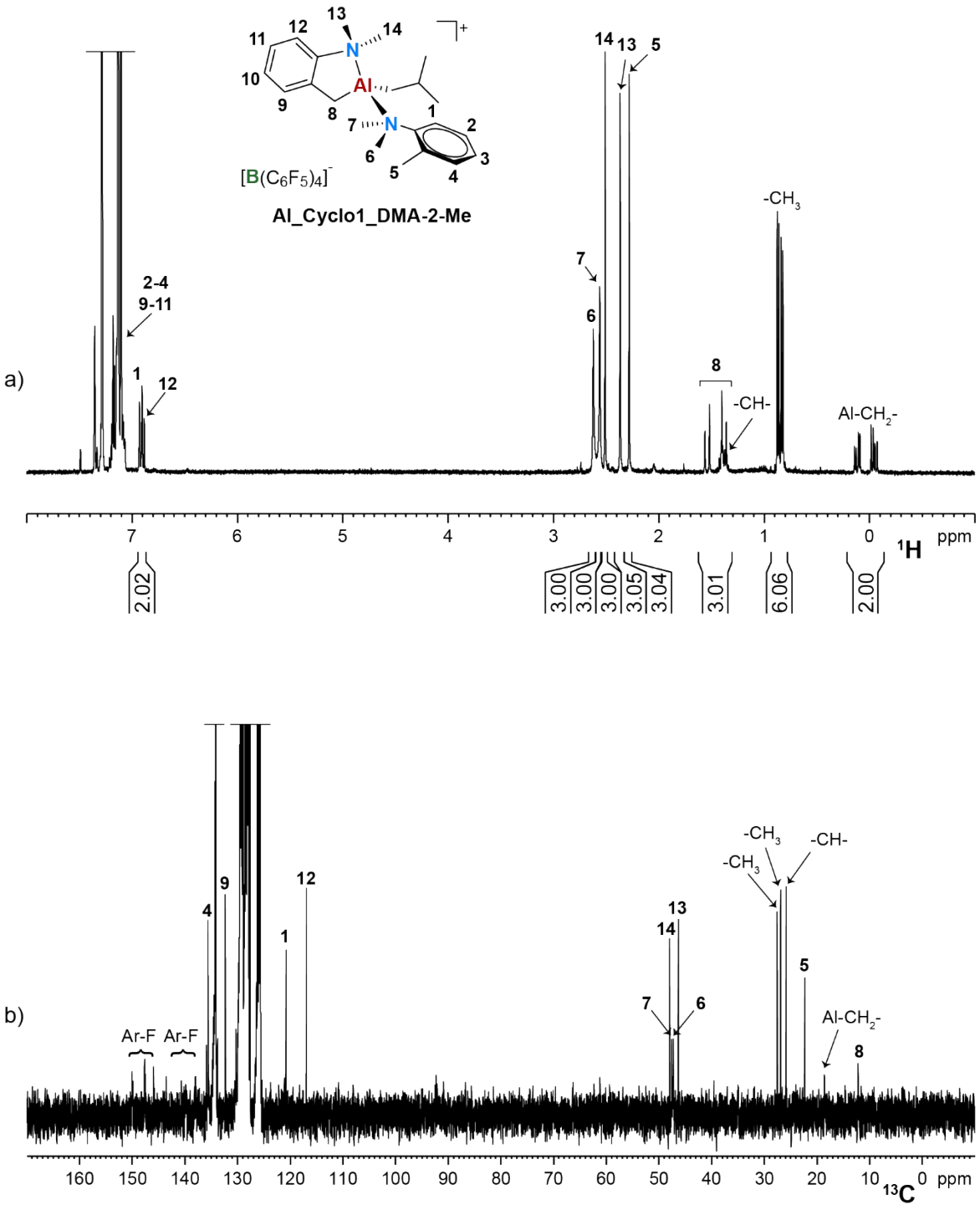


**Figure S28.** a) $^{1}$H and b) $^{13}$C NMR spectra (chlorobenzene-$d_5$, 298K) of **Al_Cyclo1_DMA-2-Me**.

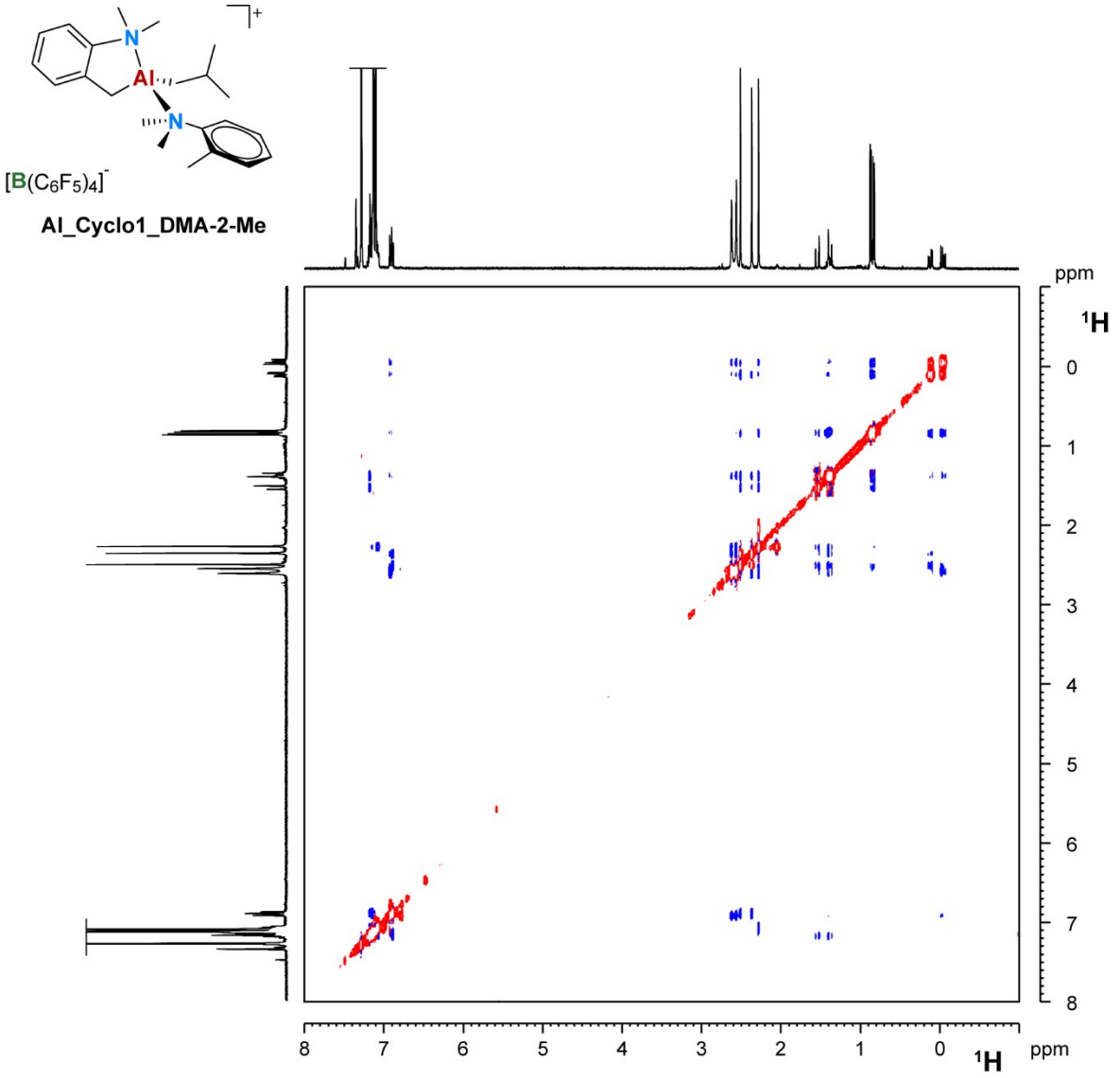


**Figure S29.** $^{1}$H NOESY NMR spectrum (chlorobenzene-$d_5$, 298K) of **Al_Cyclo1_DMA-2-Me**.

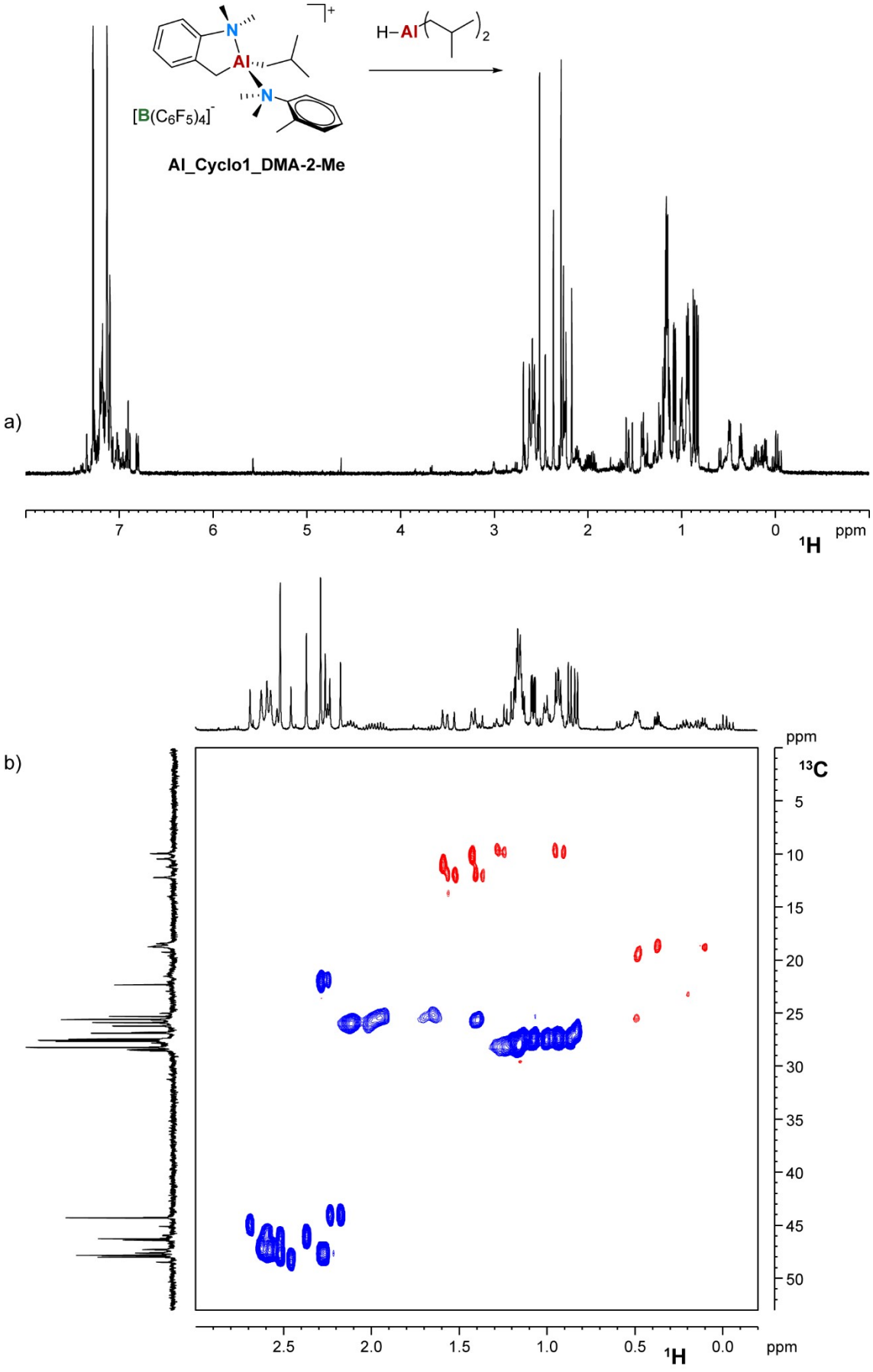


**Figure S30.** a) $^{1}$H and b) $^{1}$H,$^{13}$C HSQC NMR spectra (chlorobenzene-$d_5$, 298K) of the reaction mixture of **Al_Cyclo1_DMA-2-Me** and DIBAL-H.

### 1.3.2 Side reactions observed with DMA-2,4,6-Me

Upon reacting **DMA-2,4,6-Me** (2 equiv.) with TIBAL (1 equiv.) and TTB (0.9 equiv.; Scheme 2d) in benzene-$d_6$, a complex mixture of neutral and ionic products is formed. The neutral products remain in solution (Figure S31), while the ionic ones precipitate as a yellow-green oil. The latter were separated and dissolved in chlorobenzene-$d_5$ (Figure S32).

***Al_Cyclo2.*** $^1$H NMR (400 MHz, benzene-$d_6$): 7.03 (s, 1H, H1), 6.42 (bs, 1H, H3), 2.30 (s, 6H, N-$CH_3$), 2.06 (m, 1H, Al-$CH_2CH(CH_3)_2$), 2.04 (s, 3H, H2), 1.89 (s, 3H, H4), 1.57 (bs, 2H, Ar-$CH_2$-Al), 1.21 (d, 6H, $^3J$ = 6.6 Hz, Al-$CH_2CH(CH_3)_2$), 1.19 (d, 6H, $^3J$ = 6.6 Hz, Al-$CH_2CH(CH_3)_2$), 0.24 (dd, 1H, $^2J$ = 13.8 Hz, $^3J$ = 7.0 Hz, Al-$CH_2CH(CH_3)_2$), 0.13 (dd, 1H, $^2J$ = 13.8 Hz, $^3J$ = 7.0 Hz, Al-$CH_2CH(CH_3)_2$) ppm. $^{13}$C NMR (100 MHz, benzene-$d_6$): 143.7 (aromatic *C*-$CH_2$-), 143.1 (aromatic N-C), 136.5 (aromatic *C*-$CH_3$(2)), 131.3 (C1), 129.8 (C3), 129.6 (aromatic *C*-$CH_3$(4)), 45.1 (N-$CH_3$), 28.5 (Al-$CH_2CH(CH_3)_2$), 26.9 (Al-$CH_2CH(CH_3)_2$), 21.6 (Al-$CH_2CH(CH_3)_2$) ppm.

***Al_tri_DMA-2,4,6-Me.*** $^1$H NMR (400 MHz, chlorobenzene-$d_5$): 6.57 (bs, 2H, aromatic *m*-H), 2.59 (s, 6H, N-$CH_3$), 2.27 (bs, 6H, *o*-$CH_3$), 2.00 (s, 3H, *p*-$CH_3$), 1.71 (m, 2H, Al-$CH_2CH(CH_3)_2$), 0.85 (d, 12H, $^3J$ = 6.5 Hz, Al-$CH_2CH(CH_3)_2$), 0.22 (d, 4H, $^3J$ = 7.4 Hz, Al-$CH_2CH(CH_3)_2$) ppm. $^{13}$C NMR (100 MHz, chlorobenzene-$d_5$): 140.9 (aromatic *p*-C), 138.6 (aromatic C-N), 130.6 (aromatic *m*-C), 45.5 (N-$CH_3$), 27.4 (Al-$CH_2CH(CH_3)_2$), 20.0 (*p*-$CH_3$), 25.2 (Al-$CH_2CH(CH_3)_2$), 21.0 (Al-$CH_2CH(CH_3)_2$), 19.5 (*o*-$CH_3$) ppm.

***Protonated DMA-2,4,6-Me borate salt.*** $^1$H NMR (400 MHz, chlorobenzene-$d_5$): 6.52 (bs, 1H, aromatic *m*-H), 6.48 (bs, 1H, aromatic *m*-H), 2.52 (s, 6H, N-$CH_3$), 2.00 (s, 3H, *p*-$CH_3$), 1.86 (bs, 6H, *o*-$CH_3$) ppm. $^{13}$C NMR (100 MHz, chlorobenzene-$d_5$): 141.8 (aromatic *p*-C), 134.5 (aromatic N-C), 134.4 (aromatic *m*-C), 131.2 (aromatic *m*-C), 128.1 (aromatic *o*-C), 44.9 (N-$CH_3$), 20.0 (*p*-$CH_3$), 18.9 (*o*-$CH_3$) ppm.

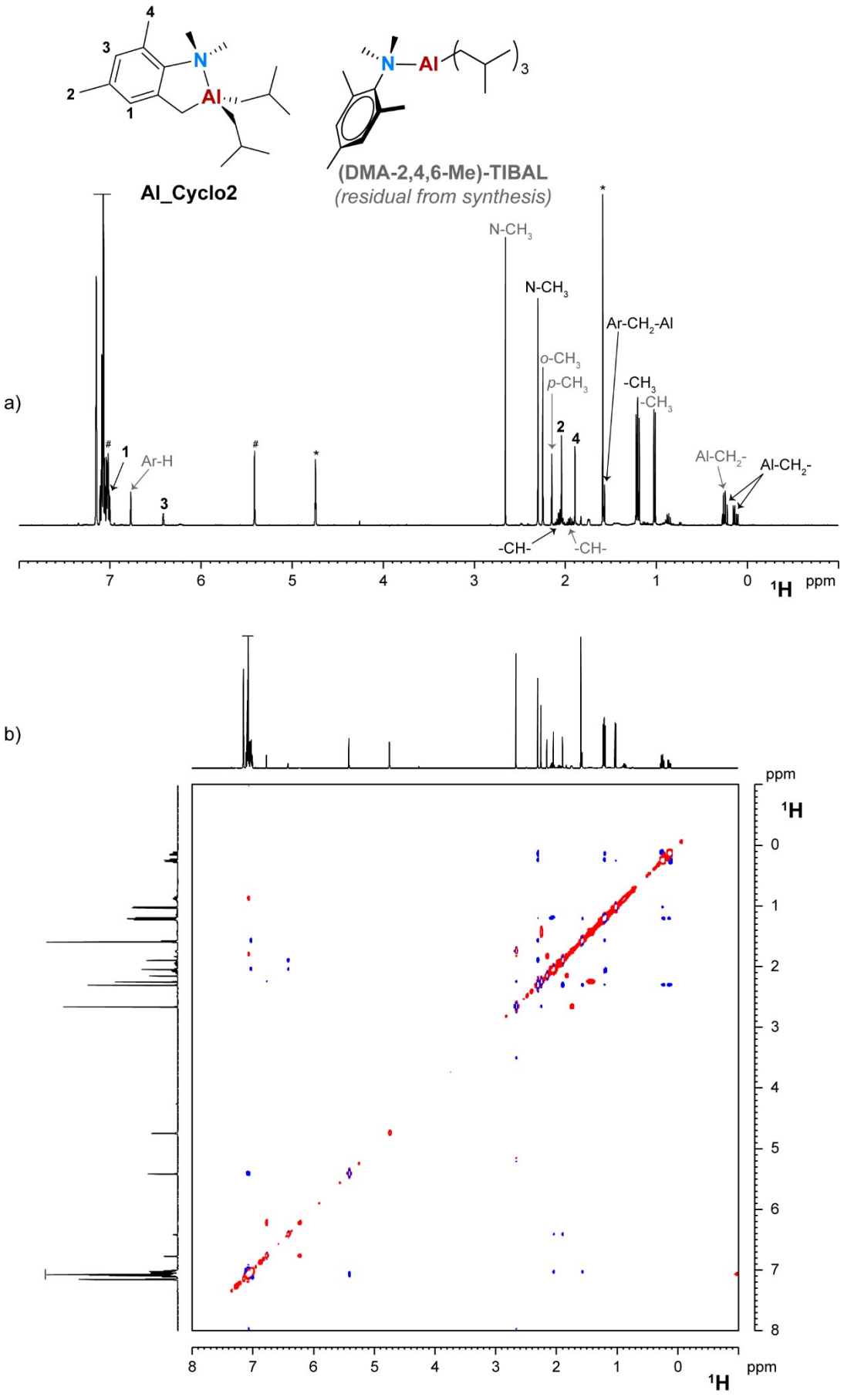


**Figure S31.** a) $^{1}$H and b) $^{1}$H NOESY NMR spectra (benzene-$d_5$, 298K) of the neutral products formed in the reaction of **DMA-2,4,6-Me** (2 equiv.) with TIBAL (1 equiv.) and TTB (0.9 equiv.). * = *iso*-butene; $^{\#}$ = $Ph_3CH$.

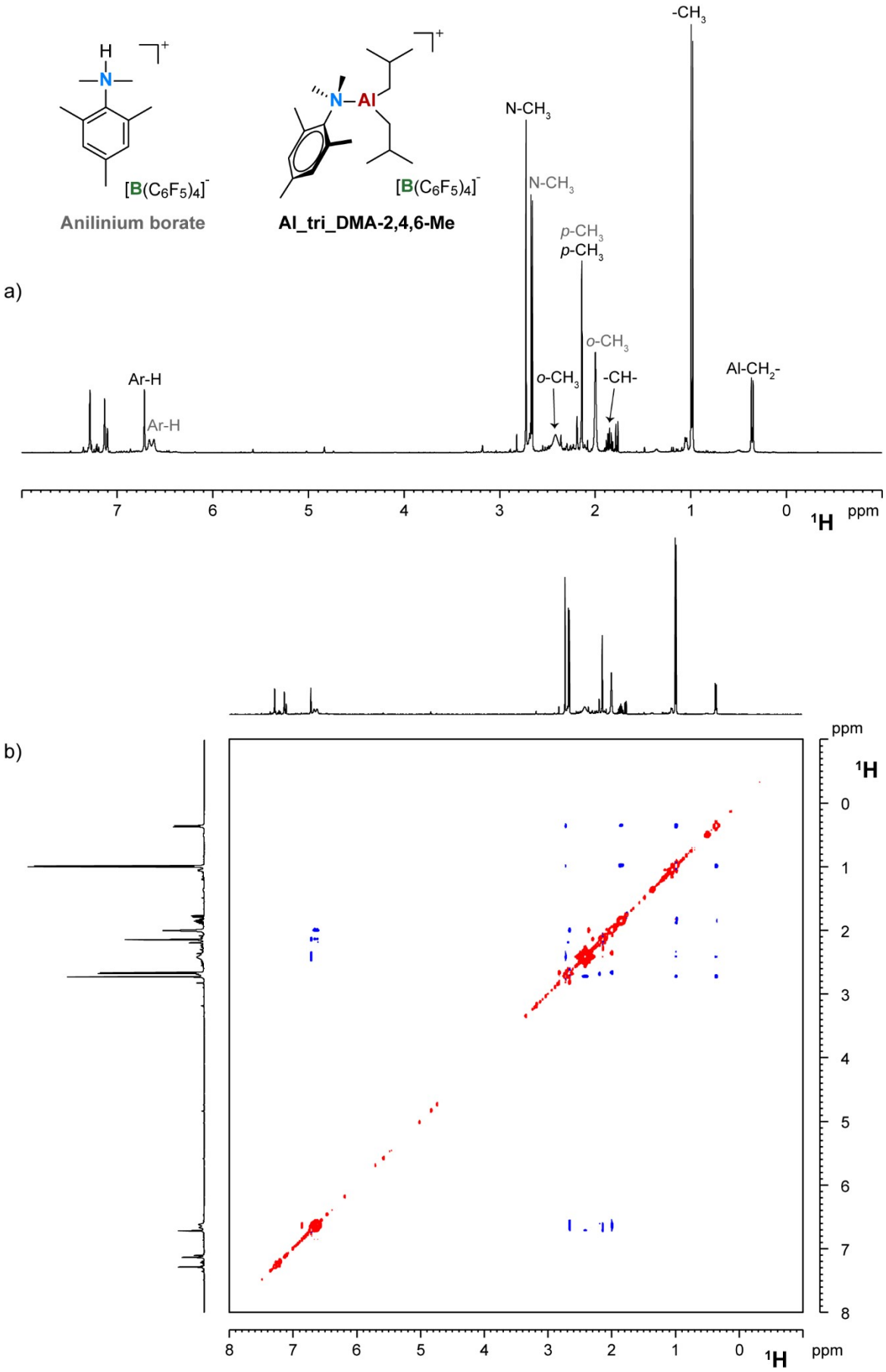


**Figure S31.** a) $^{1}$H and b) $^{1}$H NOESY NMR spectra (chlorobenzene-$d_5$, 298K) of the ionic products formed in the reaction of **DMA-2,4,6-Me** (2 equiv.) with TIBAL (1 equiv.) and TTB (0.9 equiv.).

### 1.3.3 Synthesis and reactivity of Al_tri_DEA

***Al_tri_DEA.*** Solid TTB (114 mg, 124 µmol) was added in small aliquots to a preformed and stirred solution of TIBAL (46.8 µL, 185 µmol) and **DEA** (39.7 µL, 247 µmol) in toluene (1.5 mL). The resulting mixture was vigorously stirred for a few minutes at room temperature. Upon stopping the stirring, a colorless oil precipitated. Pentane (6 mL) was added to facilitate precipitation of ionic products. The supernatant was then removed, and the oil further washed with pentane (2 x 6 mL). After the last washing, the residue was dried under vacuum to obtain **Al_tri_DEA** as a white solid (121 mg, 87% yield).

$^{1}$H NMR (400 MHz, chlorobenzene-$d_5$): 7.26 (m, 4H, aromatic *m*-H), 7.17 (m, 2H, aromatic *p*-H), 6.82 (m, 4H, aromatic *o*-H), 2.99 (bd, 4H, $^{3}J$ = 6.4 Hz, N-C$H_2$CH$_3$), 1.57 (m, 2H, Al-CH$_2$C$H$(CH$_3$)$_2$), 0.78 (bt, 6H, $^{3}J$ = 6.4 Hz, N-CH$_2$C$H_3$), 0.72 (d, 12H, $^{3}J$ = 6.5 Hz, Al-CH$_2$CH(C$H_3$)$_2$), 0.19 (d, 4H, $^{3}J$ = 7.3 Hz, Al-C$H_2$CH(CH$_3$)$_2$) ppm. $^{13}$C NMR (100 MHz, chlorobenzene-$d_5$): 138.0 (aromatic N-C), 133.3 (aromatic *m*-C), 130.8 (aromatic *p*-C), 119.4 (aromatic *o*-*C*), 46.6 (N-*C*H$_2$CH$_3$), 27.4 (Al-CH$_2$CH(*C*H$_3$)$_2$), 25.0 (Al-CH$_2$*C*H(CH$_3$)$_2$), 22.2 (Al-*C*H$_2$CH(CH$_3$)$_2$), 9.03 (N-CH$_2$*C*H$_3$) ppm.

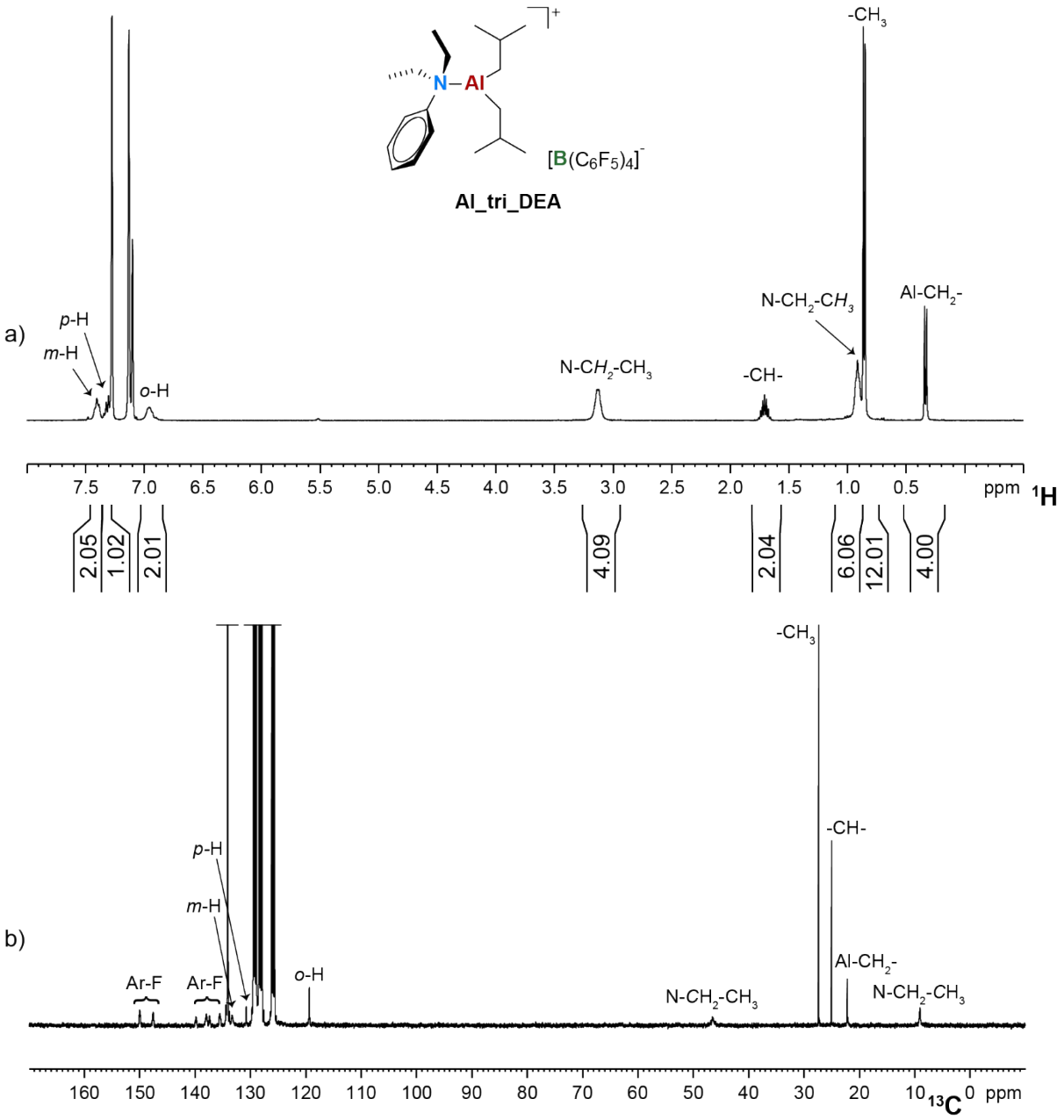


**Figure S32.** a) $^{1}$H and b) $^{13}$C NMR spectra (chlorobenzene-$d_5$, 298K) of **Al_tri_DEA**.

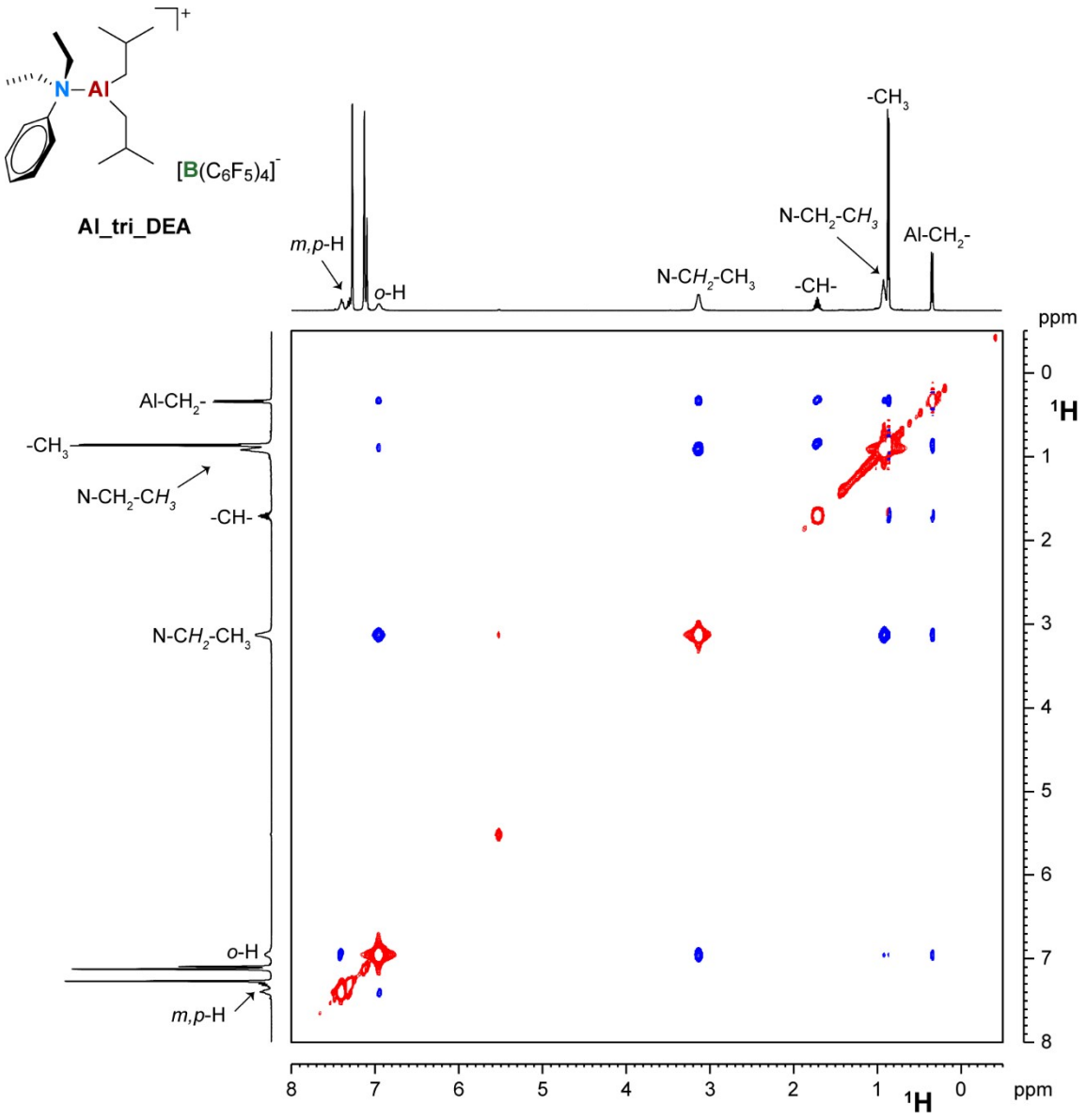


**Figure S33.** $^{1}$H NOESY NMR spectrum (chlorobenzene-$d_5$, 298K) of **Al_tri_DEA**.

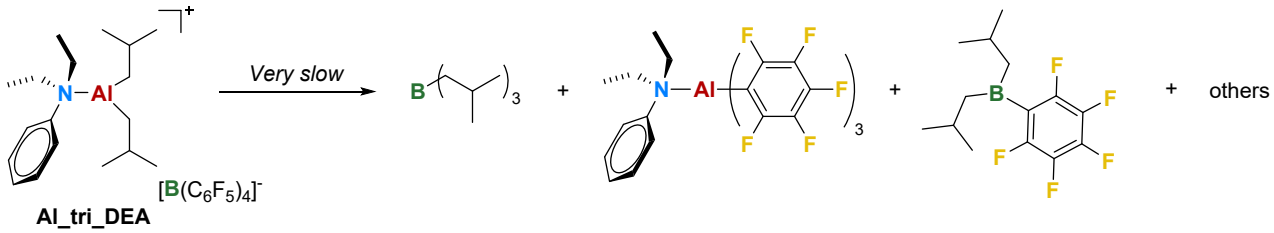


**Scheme S2.** Self-decomposition of **Al_tri_DEA** in solution.

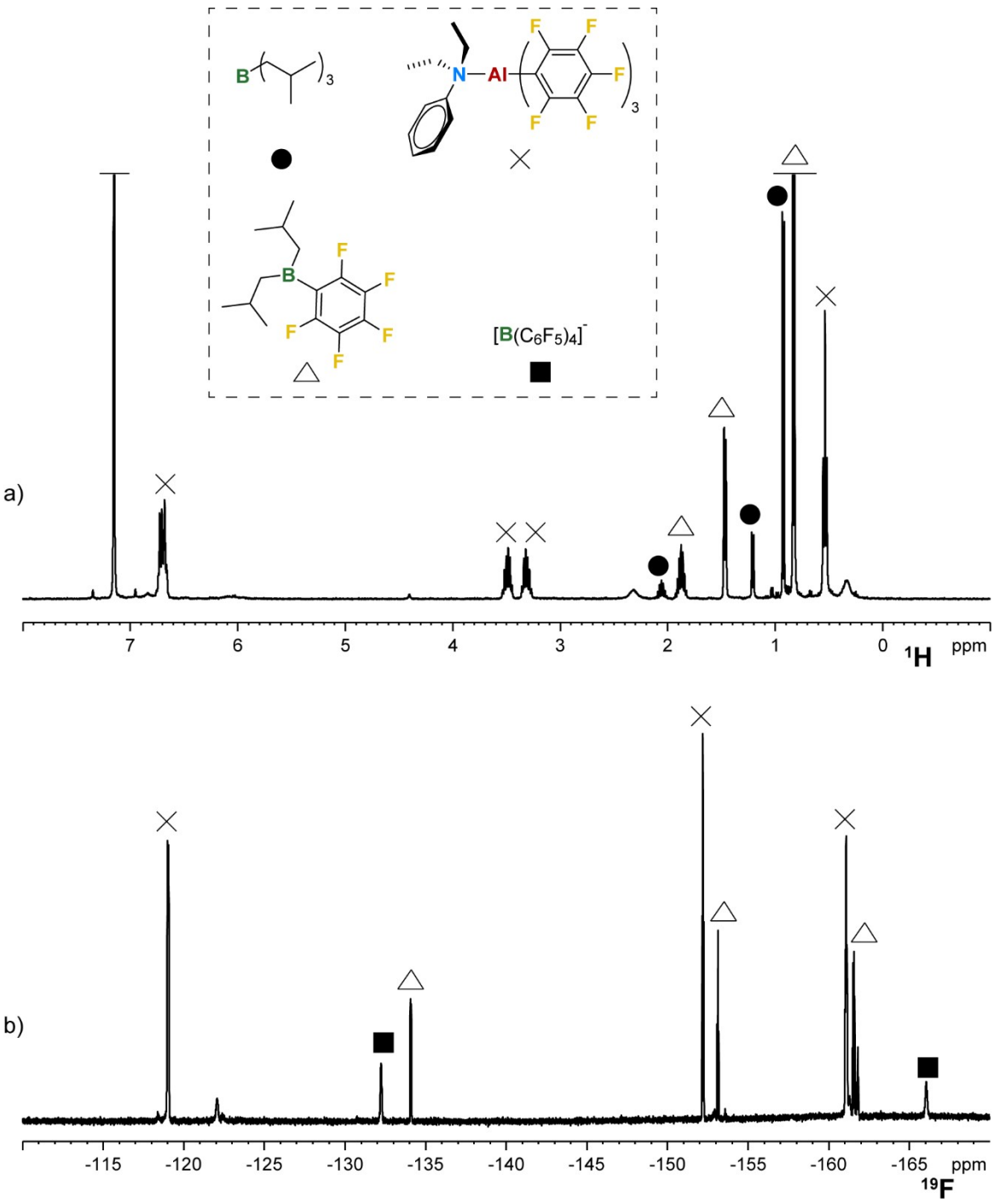


**Figure S34.** a) $^{1}$H and b) $^{19}$F NMR spectra (benzene-$d_6$, 298K) of **Al_tri_DEA** decomposition products (see also Scheme S2).

### 1.3.4 Side reactions observed with DIPA

Upon reacting **DIPA** (2 equiv.) with TIBAL (1 equiv.) and TTB (0.9 equiv.; Scheme 2d) in benzene-$d_6$, a complex mixture of neutral and ionic products is formed. The neutral products ($Ph_3CH$ and other minor species) remain in solution, while the ionic ones precipitate as a yellow-green oil. The latter were separated and dissolved in chlorobenzene-$d_5$ (Figure S35).

***Al_tri_DIPA.*** $^1$H NMR (400 MHz, chlorobenzene-$d_5$): 7.22 (bm, 3H, aromatic *m*,*p*-H), 6.69 (bm, 2H, aromatic *o*-H), 3.55 (h, 2H, $^3J$ = 6.8, N-C*H*$(CH_3)_2$), 1.70 (m, 2H, Al-$CH_2$C*H*$(CH_3)_2$), 0.93 (bm, 12H, N-CH(C*H*$_3)_2$), 0.82 (d, 12H, $^3J$ = 6.6 Hz, Al-$CH_2$CH(C*H*$_3)_2$), 0.25 (d, 4H, $^3J$ = 7.6 Hz, Al-C*H*$_2$CH$(CH_3)_2$) ppm.
*In another solvent.* $^1$H NMR (400 MHz, dichlorobenzene-$d_4$): 7.40 (m, 3H, aromatic *m*,*p*-H), 6.87 (d, 2H, $^3J$ = 8.0 Hz, aromatic *o*-H), 3.76 (bs, 2H, N-C*H*$(CH_3)_2$), 1.77 (m, 2H, Al-$CH_2$C*H*$(CH_3)_2$), 1.09 (d, 12H, $^3J$ = 6.2 Hz, N-CH(C*H*$_3)_2$), 0.85 (d, 12H, $^3J$ = 6.6 Hz, Al-$CH_2$CH(C*H*$_3)_2$), 0.36 (d, 4H, $^3J$ = 7.6 Hz, Al-C*H*$_2$CH$(CH_3)_2$) ppm. $^{13}$C NMR (100 MHz, dichlorobenzene-$d_4$): 131 (aromatic *m*,*p*-C), 122.0 (aromatic *o*-C), 56.2 (N-C*H*$(CH_3)_2$), 27.4 (Al-$CH_2$CH(*C*H$_3)_2$), 25.6 (Al-*C*H$_2$CH$(CH_3)_2$), 25.4 (Al-$CH_2$*C*H$(CH_3)_2$), 20.6 (N-CH(*C*H$_3)_2$) ppm.

***Protonated DIPA borate salt.*** $^1$H NMR (400 MHz, chlorobenzene-$d_5$): 7.21 (m, 3H, aromatic *m*,*p*-H), 6.49 (bd, 2H, $^3J$ = 7.0 Hz, aromatic *o*-H), 4.92 (bm, 1H, N-H$^+$), 3.33 (m, 2H, N-C*H*$(CH_3)_2$), 0.71 (d, 6H, $^3J$ = 6.4 Hz, N-CH(C*H*$_3)_2$), 0.60 (d, 6H, $^3J$ = 6.6 Hz, N-CH(C*H*$_3)_2$) ppm.
*In another solvent.* $^1$H NMR (400 MHz, dichlorobenzene-$d_4$): 7.25 (m, 3H, aromatic *m*,*p*-H), 6.70 (d, 2H, $^3J$ = 7.6 Hz, aromatic *o*-H), 3.61 (m, 2H, N-C*H*$(CH_3)_2$), 0.91 (d, 6H, $^3J$ = 6.4 Hz, N-CH(C*H*$_3)_2$), 0.82 (d, 6H, $^3J$ = 6.4 Hz, N-CH(C*H*$_3)_2$) ppm. $^{13}$C NMR (100 MHz, dichlorobenzene-$d_4$): 131.5 (aromatic N-C), 131 (aromatic m,*p*-*C*), 122.8 (aromatic *o*-C), 58.6 (N-C*H*$(CH_3)_2$), 19.0 (N-CH(C*H*$_3)_2$), 16.8 (N-CH(C*H*$_3)_2$) ppm.

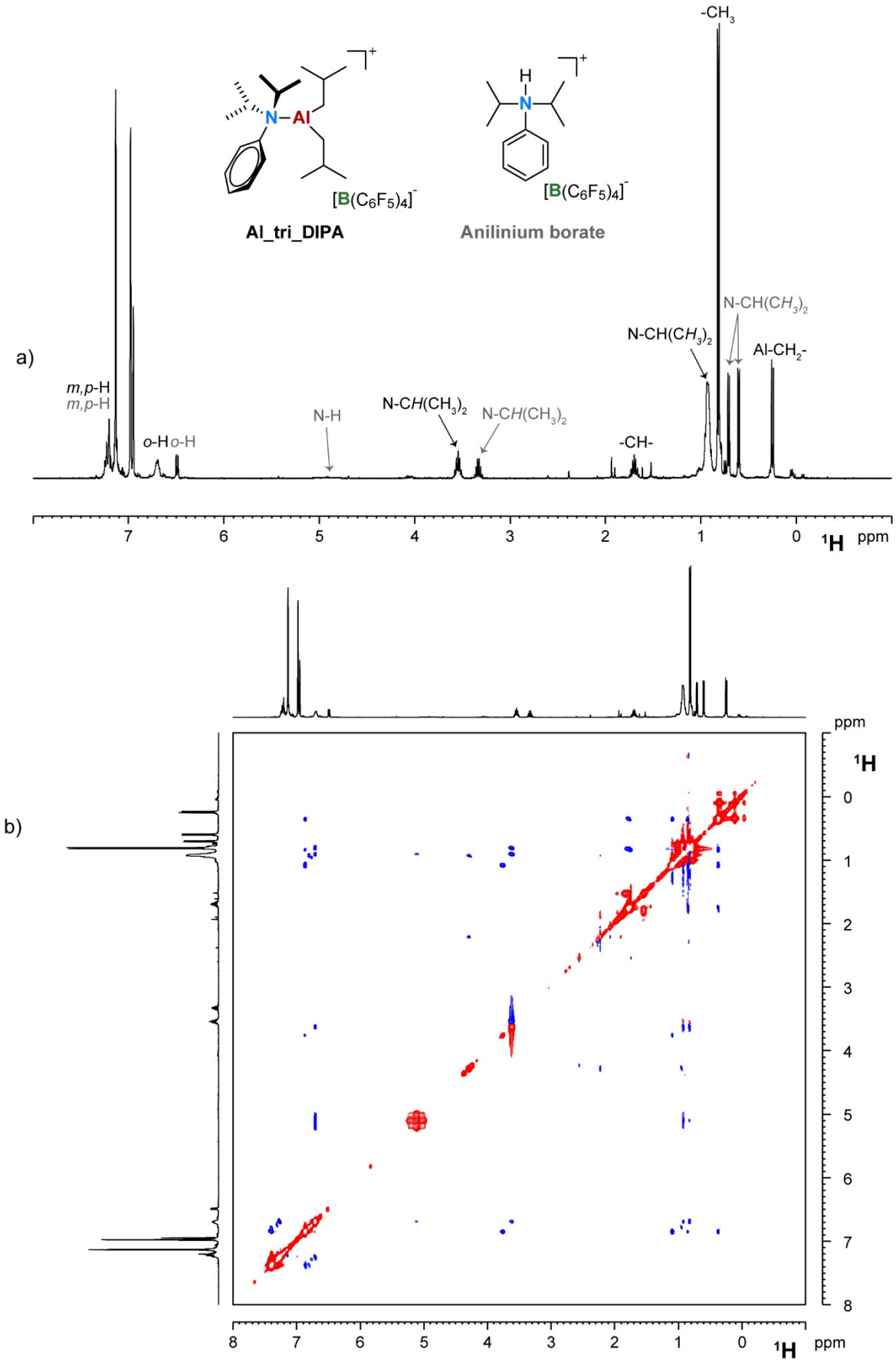


**Figure S35.** a) $^{1}$H and b) $^{1}$H NOESY NMR spectra (chlorobenzene-$d_5$, 298K) of the ionic products formed in the reaction of **DIPA** (2 equiv.) with TIBAL (1 equiv.) and TTB (0.9 equiv.).

### 1.3.5 Side reactions observed with TEA

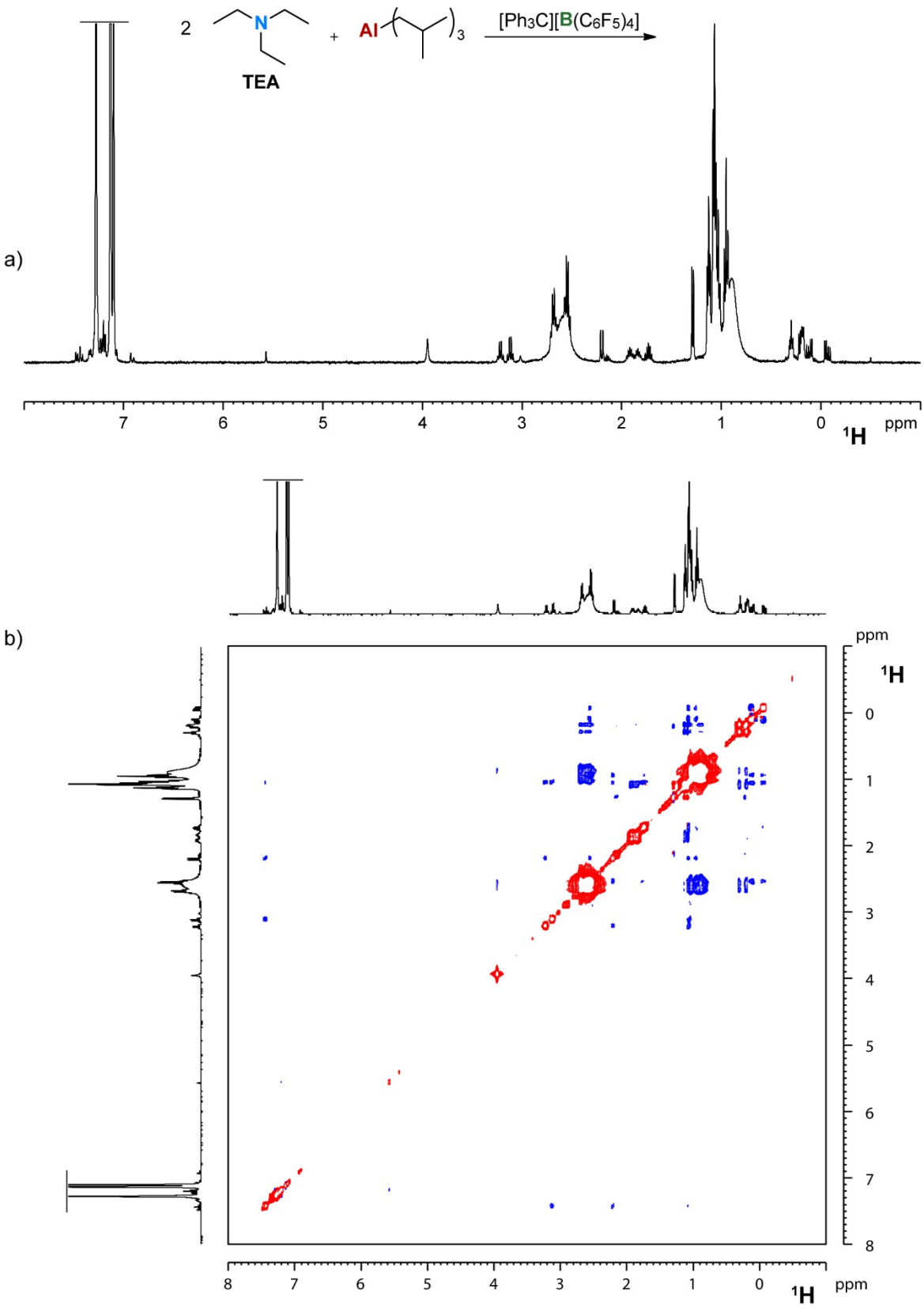


**Figure S36.** a) $^{1}$H and b) $^{1}$H NOESY NMR spectra (chlorobenzene-$d_5$, 298K) of the ionic products formed in the reaction of **TEA** (2 equiv.) with TIBAL (1 equiv.) and TTB (0.9 equiv.).

### 1.3.6 Synthesis and characterization of DMA-Ph

***DMA-Ph.*** Inspired by literature procedures,[3] methyliodide (1.18 mL, 19.0 mmol) was added dropwise to a stirred solution of $K_2CO_3$ (2.63 g, 19.0 mmol) and 4-aminobiphenyl (1.53 g, 9.0 mmol) in 25 mL of ethanol. The resulting mixture was vigorously stirred for 18h under reflux at 85°C. Subsequently, the mixture was cooled down to room temperature, filtered and extracted three times with $H_2O$. The organic layer was dried over sodium sulfate, filtered and concentrated under vacuum to obtain an orange solid, which was purified through column chromatography on silica gel using chloroform as eluent. The desired eluted fractions were combined and all the volatiles were removed under vacuum to afford the product as a pale orange solid (904 mg; 51% isolated yield).

$^1$H NMR (400 MHz, chloroform-*d*): 7.60 (dd, 2H, $^3J$ = 8.2 Hz, H3), 7.53 (d, 2H, $^3J$ = 8.8 Hz, H2), 7.42 (m, 2H, H4), 7.27 (t, 1H, $^3J$ = 7.2 Hz, H5), 6.82 (d, 2H, $^3J$ = 8.8 Hz, H1), 3.03 (s, 6H, N-$CH_3$) ppm. $^{13}$C NMR (100 MHz, chloroform-*d*): 150.1 (aromatic N-C), 141.1 (aromatic *C*-C), 128.7 (aromatic *C*-C), 128.6 (C4), 127.4 (C2), 126.0 (C3)), 125.8 (C5), 112.6 (C1), 40.4 (N-$CH_3$) ppm. See Figure S2 for nomenclature.

### 1.3.5 Addendum: comparison between $^{1}$H NMR spectra of AlHAl_DMA and AlHAl_DMA-Ph

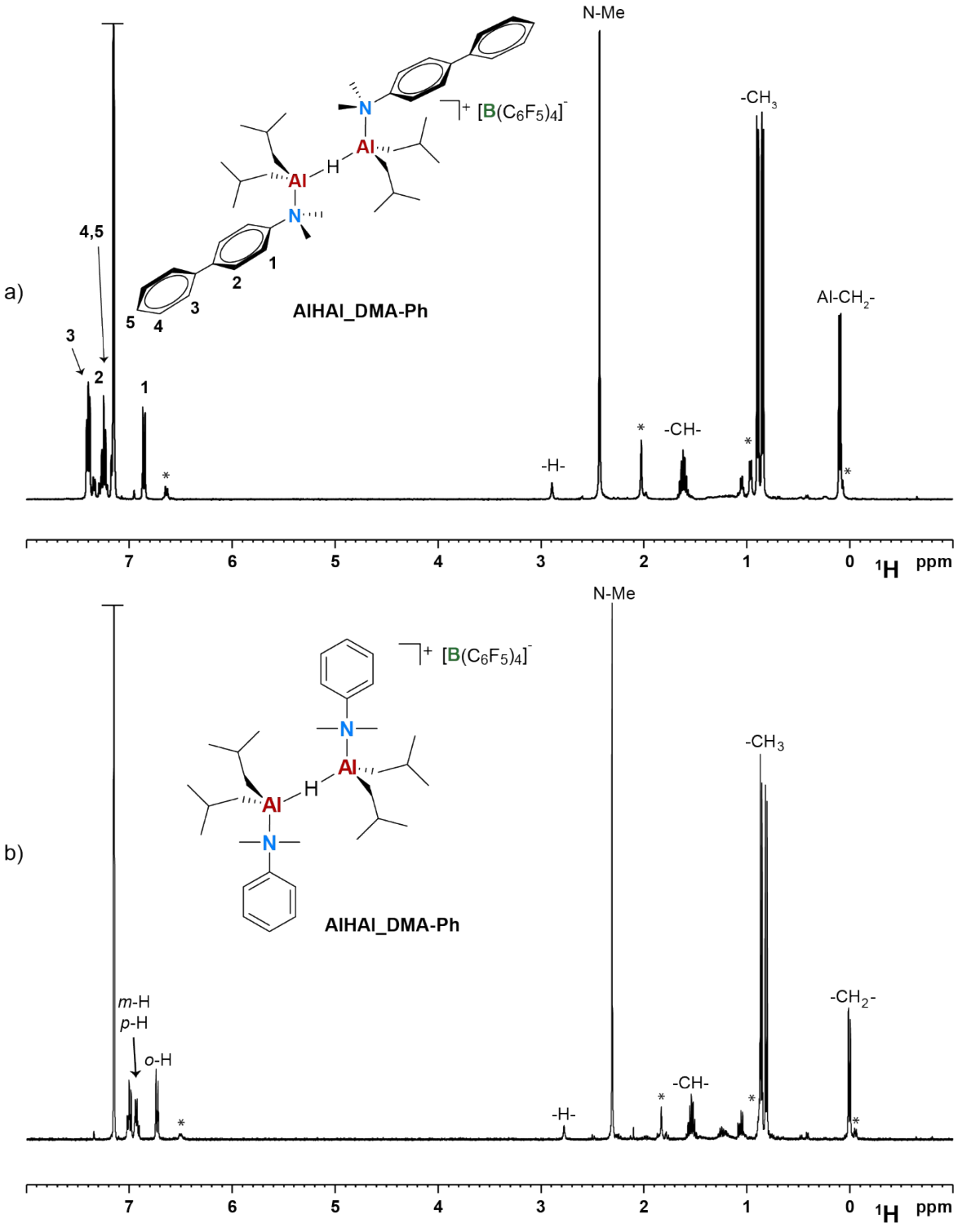


**Figure S37.** Comparison between $^{1}$NMR spectra (benzene-$d_6$, 298K) of a) **AlHAl_DMA** and b) **AlHAl_DMA-Ph**.

## 1.4 Crystallographic details

**Table S1.** Crystal data and structure refinement for **Al_DMA**.

| Complex | **Al_DMA** |
|---|---|
| CCDC n. | 2372889 |
| Elemental formula | $C_{48}$ $H_{40}$ Al B $F_{20}$ $N_2$ |
| Formula weight | 1062.61 |
| Crystal system | Triclinic |
| Space group | P-1 |
| Unit cell dimensions: | |
| a = (Å) | 12.6860(6) |
| b = | 12.8057(6) |
| c = | 16.3034(9) |
| α = (°) | 66.945(2) |
| β = | 69.445(2) |
| γ = | 85.521(2) |
| Volume ($Å^3$) | 2276.4(2) |
| Z, Calculated density ($g/cm^3$) | 2, 1.550 |
| F(000) | 1080 |
| Absorption coefficient ($mm^{-1}$) | 0.165 |
| Temperature (K) | 150.(2) |
| Crystal colour, shape | Clear colourless, prism |
| Crystal size (mm) | 0.200 x 0.100 x 0.080 |
| On the diffractometer: | |
| Theta range for data collection | 2.6067 to 28.2565 |
| Limiting indices | -16<=*h*<=16, -14<=*k*<=17, -21<=*l*<=21 |
| Completeness | 99.4% |
| Max. and min. transmission | 0.7457 and 0.6879 |
| Reflns collected (not incl. absences) | 40474 |
| No. of unique reflns, R(int) for equivs | 11256, 0.0375 |
| No. of 'observed' reflns ($I > 2\sigma_I$) | 8862 |
| Refinement: | |
| Data/restraints/parameters | 11256/0/667 |
| Goodness-of-fit on $F^2$ | 1.025 |
| Final R indices ('obsd' data) | 0.0395, 0.0874 |
| Final R indices (all data) | 0.0587, 0.0983 |
| Reflns weighted: 1/w = [a] | [\s^2^(Fo^2^)+(0.0357P)^2^+1.2327P] |
| Largest diff. peak and hole (e. $Å^{-3}$) | 0.484 and -0.332 |

[a]where P=(Fo^2^+2Fc^2^)/3

**Table S2.** Crystal data and structure refinement for **Al_DMA-Cl**.

| Complex | **Al_DMA-Cl** |
|---|---|
| CCDC n. | 2372892 |
| Elemental formula | $C_{51}$ $H_{38}$ Al B $Cl_2$ $F_{21}$ $N_2$ |
| Formula weight | 1186.52 |
| Crystal system | Monoclinic |
| Space group | P2(1)/n |
| Unit cell dimensions: | |
| a = (Å) | 15.1327(8) |
| b = | 19.0563(11) |
| c = | 20.0028(12) |
| α = (°) | 90 |
| β = | 110.397(2) |
| γ = | 90 |
| Volume ($Å^3$) | 5406.6(5) |
| Z, Calculated density ($g/cm^3$) | 4, 1.458 |
| F(000) | 2396 |
| Absorption coefficient ($mm^{-1}$) | 0.246 |
| Temperature (K) | 120.(2) |
| Crystal colour, shape | Clear colourless, plate |
| Crystal size (mm) | 0.400 x 0.140 x 0.140 |
| On the diffractometer: | |
| Theta range for data collection | 2.5752 to 28.0428 |
| Limiting indices | -20<=*h*<=17, -24<=*k*<=25, -26<=*l*<=25 |
| Completeness | 99.5% |
| Max. and min. transmission | 0.7457 and 0.6660 |
| Reflns collected (not incl. absences) | 42890 |
| No. of unique reflns, R(int) for equivs | 13416, 0.0344 |
| No. of 'observed' reflns ($I > 2\sigma_I$) | 9891 |
| Refinement: | |
| Data/restraints/parameters | 13416/450/820 |
| Goodness-of-fit on $F^2$ | 1.129 |
| Final R indices ('obsd' data) | 0.0706, 0.1870 |
| Final R indices (all data) | 0.0934, 0.1976 |
| Reflns weighted: 1/w = [a] | \s^2^(Fo^2^)+(0.0686P)^2^+9.5321P |
| Largest diff. peak and hole (e. $Å^{-3}$) | 0.768 and -0.437 |

[a]where P=(Fo^2^+2Fc^2^)/3

**Table S3.** Crystal data and structure refinement for **Al_tri_DEA**.

| Complex | **Al_tri_DEA** |
|---|---|
| CCDC n. | 2372891 |
| Elemental formula | $C_{42}$ $H_{33}$ Al B $F_{20}$ N |
| Formula weight | 969.48 |
| Crystal system | Monoclinic |
| Space group | P2(1)/c |
| Unit cell dimensions: | |
| a = (Å) | 13.9977(3) |
| b = | 18.7908(4) |
| c = | 17.0814(4) |
| α = (°) | 90 |
| β = | 112.5680(10) |
| γ = | 90 |
| Volume (Å$^3$) | 4148.84(16) |
| Z, Calculated density (g/cm$^3$) | 4, 1.552 |
| F(000) | 1960 |
| Absorption coefficient (mm$^{-1}$) | 0.172 |
| Temperature (K) | 150.(2) |
| Crystal colour, shape | Clear colourless, prism |
| Crystal size (mm) | 0.100 x 0.100 x 0.040 |
| On the diffractometer: | |
| Theta range for data collection | 2.4553 to 28.2669 |
| Limiting indices | -18<=*h*<=18, -24<=*k*<=25, -22<=*l*<=22 |
| Completeness | 99.2% |
| Max. and min. transmission | 0.7457 and 0.6609 |
| Reflns collected (not incl. absences) | 36584 |
| No. of unique reflns, R(int) for equivs | 10226, 0.0239 |
| No. of 'observed' reflns (I > 2$\sigma_I$) | 8322 |
| Refinement: | |
| Data/restraints/parameters | 10226/0/592 |
| Goodness-of-fit on $F^2$ | 1.031 |
| Final R indices ('obsd' data) | 0.0377, 0.0902 |
| Final R indices (all data) | 0.0492, 0.0975 |
| Reflns weighted: 1/w = [a] | \s^2^(Fo^2^)+(0.0367P)^2^+2.1017P |
| Largest diff. peak and hole (e. Å$^{-3}$) | 0.309 and -0.319 |

**Table S4.** Crystal data and structure refinement for **Al_Py-3,5-Me**.

| Complex | **Al_Py-3,5-Me** |
|---|---|
| CCDC n. | 2372890 |
| Elemental formula | $C_{52}$ $H_{41}$ Al B Cl $F_{20}$ $N_2$ |
| Formula weight | 1147.11 |
| Crystal system | Monoclinic |
| Space group | P2(1)/n |
| Unit cell dimensions: | |
| a = (Å) | 9.0723(9) |
| b = | 18.0700(18) |
| c = | 31.168(3) |
| α = (°) | 90 |
| β = | 96.700(3) |
| γ = | 90 |
| Volume (Å$^3$) | 5074.7(9) |
| Z, Calculated density (g/cm$^3$) | 4, 1.501 |
| F(000) | 2328 |
| Absorption coefficient (mm$^{-1}$) | 0.205 |
| Temperature (K) | 145.(2) |
| Crystal colour, shape | Clear intense grey, plate |
| Crystal size (mm) | 0.320 x 0.300 x 0.100 |
| On the diffractometer: | |
| Theta range for data collection | 2.4292 to 28.2355 |
| Limiting indices | -12<=*h*<=12, -24<=*k*<=22, -40<=*l*<=41 |
| Completeness | 99.8% |
| Max. and min. transmission | 0.98 and 0.91 |
| Reflns collected (not incl. absences) | 122848 |
| No. of unique reflns, R(int) for equivs | 12533, 0.0600 |
| No. of 'observed' reflns (I > 2$\sigma_I$) | 9512 |
| Refinement: | |
| Data/restraints/parameters | 12533/179/786 |
| Goodness-of-fit on $F^2$ | 1.093 |
| Final R indices ('obsd' data) | 0.0536, 0.1070 |
| Final R indices (all data) | 0.0797, 0.1238 |
| Reflns weighted: 1/w = [a] | [\s^2^(Fo^2^)+(0.0317P)^2^+5.4476P] |
| Largest diff. peak and hole (e. Å$^{-3}$) | 0.438 and -0.685 |

[a]where P=(Fo^2^+2Fc^2^)/3

**Table S5.** Crystal data and structure refinement for **Al_QUI**.

| Complex | **Al_QUI** |
|---|---|
| CCDC n. | 2372888 |
| Elemental formula | $C_{50}$ $H_{32}$ Al B $F_{20}$ $N_2$ |
| Formula weight | 1078.56 |
| Crystal system | Monoclinic |
| Space group | P2(1)/n |
| Unit cell dimensions: | |
| a = (Å) | 9.5866(16) |
| b = | 26.774(6) |
| c = | 18.128(5) |
| α = (°) | 90 |
| β = | 94.417(8) |
| γ = | 90 |
| Volume (Å$^3$) | 4639.1(17) |
| Z, Calculated density (g/cm$^3$) | 4, 1.544 |
| F(000) | 2176.0 |
| Absorption coefficient (mm$^{-1}$) | 0.164 |
| Temperature (K) | 150.(2) |
| Crystal colour, shape | Colourless, plate |
| Crystal size (mm) | 0.200 x 0.200 x 0.100 |
| On the diffractometer: | |
| Theta range for data collection | 2.7668 to 19.5483 |
| Limiting indices | -12<=*h*<=9, -35<=*k*<=35, -24<=*l*<=24 |
| Completeness | 99.4% |
| Max. and min. transmission | 0.98 and 0.92 |
| Reflns collected (not incl. absences) | 50221 |
| No. of unique reflns, R(int) for equivs | 11632, 0.0908 |
| No. of 'observed' reflns ($I > 2\sigma_I$) | 6286 |
| Refinement: | |
| Data/restraints/parameters | 11632/69/674 |
| Goodness-of-fit on $F^2$ | 1.036 |
| Final R indices ('obsd' data) | 0.0580, 0.1108 |
| Final R indices (all data) | 0.1310, 0.1426 |
| Reflns weighted: 1/w = [a] | [\s^2^(Fo^2^)+(0.0448P)^2^+3.3646P] |
| Largest diff. peak and hole (e. Å$^{-3}$) | 0.588 and -0.520 |

[a]where P=(Fo^2^+2Fc^2^)/3

## 1.5 Estimation of $K_{eq}$

The $K_{eq}$ for the reaction depicted in Eq. 1 (Manuscript) was estimated by quantitative $^1$H NMR spectroscopy, using a 50 mM external standard solution of 2,6-di-*tert*-butyl-4-methylphenol and the *intscl* routine of the Topspin 3.6 software suite. The diagnostic N-Me signals of **Al_L** and **AlHAl_L**, and Al-$CH_2$ signals of DIBAL-H dimer and trimer were used to estimate the concentration of reagents and products.

$$K_{eq} = \frac{[AlHAl\_L] \times \left[(AliBu_2H)_2\right]}{[Al\_L] \times \left[(AliBu_2H)_3\right]}$$

Concentrations are reported in Table S6, while $K_{eq}$ are reported in Table 1 (Manuscript).

**Table S6.** Concentrations of reactants and products of Eq. 1.[a]

| Entry | L | Solvent | [AlHAl-L] (mM) | [Al-L] (mM) | [(Al*i*Bu$_2$H)$_3$] (mM) | [(Al*i*Bu$_2$H)$_2$] (mM) |
|---|---|---|---|---|---|---|
| 1 | **DMA** | Toluene | | | (ref. 4) | |
| 2 | **DMA** | Chlorobenzene | 33 | 1.7 | 3.8 | 2.5 |
| 3 | **DMA-C$_{16}$** | Toluene | | | (ref. 5) | |
| 4 | **DMA-Ph** | Toluene | 2.5 | 0.4 | 0.2 | 0.4 |
| 5 | **DMA-Cl** | Chlorobenzene | 3.2 | 0.7 | 0.2 | 0.5 |
| 6 | **DMHA** | Toluene | 9.6 | 0.7 | 2.3 | 2.3 |

[a] estimated by quantitative $^1$H NMR at 298 K.

# 2. Additional details on polymerization experiments

## 2.1 Full polymerization procedure

Prior to the execution of a polymerization library, the PPR modules undergo 'bake-and-purge' cycles overnight (8 h at 90-140°C with intermittent dry $N_2$ flow), to remove any contaminants and left-overs from previous experiments. After cooling to glovebox temperature, the module stir tops are taken off, and the 48 cells are fitted with disposable 10 mL glass inserts (pre-weighed in a Mettler-Toledo Bohdan Balance Automator) and polyether ether ketone (PEEK) stir paddles. The stir tops are then set back in place, and $N_2$ in the reactors is replaced with ethene (ambient pressure).

The cells are then loaded with the appropriate amounts of toluene and 1-hexene (1.8 v/v%). The system is then thermostated at the reaction temperature and brought to 65 psi of pressure with ethene. At this point, the catalyst injection sequence is started; aliquots of (a) a toluene 'chaser', (b) a toluene solution of catalyst, (c) a toluene spacer, (d) a toluene solution of the proper activator, and (e) a toluene 'buffer', all separated by nitrogen gaps, are uploaded into the needle and subsequently injected into the cell of destination in reverse order, thus starting the reaction. This is left to proceed under stirring (800 rpm) at constant temperature and pressure with feed of ethene on demand for 10 minutes and quenched by over-pressurizing the cell with 50 psi (3.4 bar) of dry air (preferred over other possible catalyst quenchers because in case of cell or quench line leakage oxygen is promptly detected by the dedicated glove-box sensor). Conversion of 1-hexene was kept below 15% to ensure a constant comonomer concentration. All experiments were performed at least in duplicate.

Once all cells have been quenched, the modules are cooled down to glovebox temperature and vented, the stir-tops are removed, and the glass inserts containing the reaction phases are taken out and transferred to a centrifugal evaporator (Genevac EZ-2 Plus or Martin Christ RVC 2-33 CDplus), where all volatiles are removed, and the polymers are thoroughly dried overnight. Reaction yields are double-checked against on-line monomer conversion measurements by robotically weighing the dry polymers while still in the reaction vials, subtracting the pre-recorded tare. Polymer aliquots are then sent to the characterizations.

All polymers were characterized by means of high-temperature gel permeation chromatography (GPC) and $^{13}C$ NMR spectroscopy. GPC curves were recorded with a Freeslate Rapid GPC setup, equipped with a set of two mixed-bed Agilent PLgel 10 $\mu$m columns and a Polymer Char IR4 detector. Calibration was performed with the universal method, using 10 monodisperse polystyrene samples ($M_n$ between 1.3 and 3,700 kDa).

Quantitative $^{13}C$ NMR spectra were recorded using a Bruker Avance III 400 spectrometer equipped with a high-temperature cryoprobe for 5 mm OD tubes, on 45 mg $mL^{-1}$ polymer solutions in tetrachloroethane-$d_2$ (with BHT added as a stabilizer, [BHT] = 0.4 mg $mL^{-1}$). Acquisition conditions were: 45° pulse; acquisition time, 2.7 s; relaxation delay, 5.0 s; 2 K transients. Broad-band proton decoupling was achieved with a modified WALTZ16 sequence (BI_WALTZ16_32 by Bruker).

## 2.1 Additional polymerization results

**Table S7.** Preliminary screening of polymerization conditions with **AlHAl_DMA** and TIBA/AB.[a]

| Entry | $n_{Zr}$ (nmol) | Cocatalyst | $n_{AlHAl}$ (nmol) | B/Zr | Al/Zr | $R_p$ ($kg_{PE} \cdot mmol_{Cat}^{-1} \cdot h^{-1}$) | $M_n$ (kDa)[d] | $M_w$ (kDa)[d] | PDI[d] |
|---|---|---|---|---|---|---|---|---|---|
| 1 | 1.5 | TiBA/AB | - | 2 | 3333 | -[b] | - | - | - |
| 2 | 10 | TiBA/AB | - | 2 | 500 | 124 | 87 | 218 | 2.5 |
| 3 | 1.5 | **AlHAl_DMA** | 75 | 50 | 100 | 268 | 92 | 218 | 2.4 |
| 4 | 1.5 | **AlHAl_DMA** | 100 | 67 | 133 | 313 | 80 | 202 | 2.5 |
| 5 | 1.5 | **AlHAl_DMA** | 150 | 100 | 200 | 462 | 80 | 188 | 2.3 |
| 6 | 1.5 | **AlHAl_DMA** | 250 | 167 | 333 | 485 | 82 | 192 | 2.3 |
| 7 | 1.5 | **AlHAl_DMA** | 325 | 217 | 433 | 469 | 85 | 202 | 2.4 |
| 8 | 2.5 | **AlHAl_DMA** | 75 | 30 | 60 | >>0[c] | - | - | - |
| 9 | 2.5 | **AlHAl_DMA** | 250 | 100 | 200 | >>0[c] | - | - | - |

[a] Experimental conditions: ethylene/1-hexene copolymerization in toluene (6 mL), $T$ = 60°C, $p_{C2}$ = 4.5 bar (65 psi), $t$ = 10 min, $[H]_{feed}$ = 1.8 v/v%; [b] not active, $t$ = 120 min; [c] exceedingly active, uncontrolled kinetics; [d] determined by GPC. Results are average of at least triplicates.

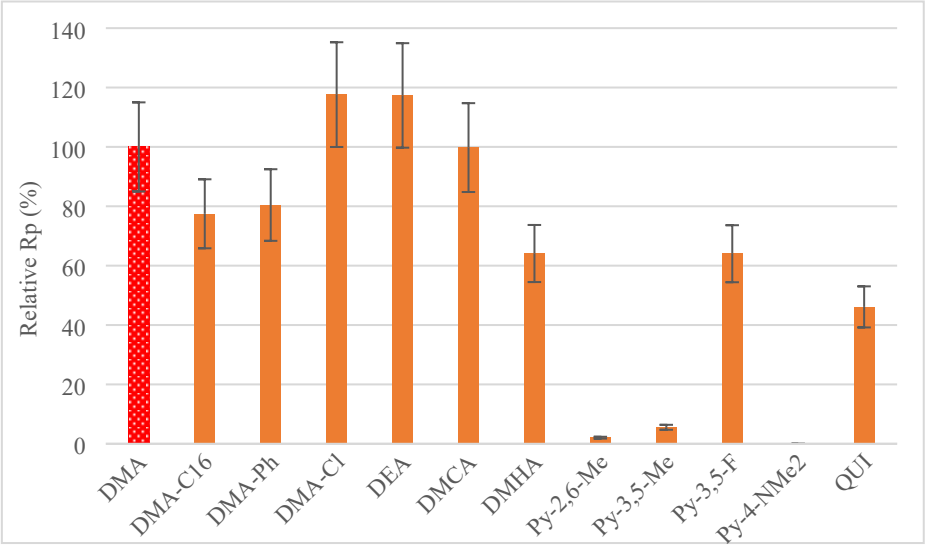


**Figure S38.** Relative productivities with respect to that with **AlHAl_DMA** obtained with **Cat-Zr** in combination with the various AAB cocatalysts at B/Zr = 167 (compare with Figure 5). 15% experimental uncertainty is assumed on $R_p$.

# 3. Additional details on computational study

## 3.1 Final Energies, Enthalpy and Entropy corrections

**Table S8.** Final Energies, Enthalpy and Entropy corrections in Hartree.

| Structure | TPSSh/DZ | | | | M06-2X(PCM)/TZ |
|---|---|---|---|---|---|
| | Energy | ZPECorr | EnthalpyCorr | GibbsCorr | Energy |
| **Al_DMA:** | -1290.58625 | 0.59293 | 0.62601 | 0.53039 | -1290.34613 |
| **Al_DMA-$C_3$** | -1526.51152 | 0.76095 | 0.80300 | 0.68511 | -1526.19735 |
| **Al_DMA-Ph** | -1752.78024 | 0.75351 | 0.79623 | 0.67689 | -1752.42678 |
| **Al_DMA-Cl** | -2209.81920 | 0.57366 | 0.60915 | 0.50712 | -2209.56069 |
| **Al_DEA** | -1447.85223 | 0.70627 | 0.74481 | 0.63836 | -1447.56767 |
| **Al_DMCA** | -1297.83266 | 0.73194 | 0.76757 | 0.66823 | -1297.57302 |
| **Al_DMPA** | -1064.32981 | 0.60042 | 0.63302 | 0.53923 | -1064.12737 |
| **Al_Py-2,6-Me** | -1212.01133 | 0.53279 | 0.56442 | 0.47107 | -1211.77953 |
| **Al_Py-3,5-Me** | -1212.03612 | 0.53166 | 0.56460 | 0.46366 | -1211.79169 |
| **Al_Py-3,5-F** | -1451.66682 | 0.38983 | 0.41864 | 0.32755 | -1451.50918 |
| **Al_Py-$NMe_2$** | -1322.74422 | 0.56834 | 0.60283 | 0.49937 | -1322.49096 |
| **Al_QUI** | -1362.07568 | 0.51652 | 0.54704 | 0.45420 | -1361.80773 |

## 3.2 QSAR model data

**Table S9.** Descriptor values determined from **Al_L** and free donor and single descriptor correlations.

| | | | | Descriptors | | | | | | | | | | | |
|---|---|---|---|---|---|---|---|---|---|---|---|---|---|---|---|
| | | | | determined from Al_L | | | | | | | | | | determined from free N-donor | |
| Activator | | $R_p$ | relative $R_p$ | CAlC | NAlN | e- (Al) | $V_{bur}$ | WBI Al-C (average) | WBI Al-C (lowest) | WBI Al-N (average) | WBI Al-N (lowest) | Al-N | q (N, e-) | EN-LPIBO | EHOMO |
| DEA | | 422 | 91 | 124.26 | 107.37 | 0.97006 | 57.4 | 0.83683 | 0.83664 | 0.42685 | 0.42672 | 2.17 | -0.20052 | -0.28052 | -0.17177 |
| DMA | | 462 | 100 | 127.2 | 105.37 | 0.96623 | 55.6 | 0.83825 | 0.83822 | 0.44042 | 0.44005 | 2.134 | -0.19138 | -0.28654 | -0.17586 |
| DMA-Cl | | 466 | 101 | 127.47 | 105.39 | 0.96662 | 55.5 | 0.83965 | 0.83954 | 0.43806 | 0.4379 | 2.137 | -0.18896 | -0.29466 | -0.18154 |
| Py35Me_corr | | 12 | 3 | 126.48 | 95.2 | 0.99596 | 41.4 | 0.82662 | 0.82658 | 0.48148 | 0.48135 | 2.045 | -0.27343 | -0.3397 | -0.22928 |
| Py26Me | | 3 | 1 | 125.31 | 102.38 | 0.92155 | 54.7 | 0.82407 | 0.81687 | 0.49593 | 0.49357 | 2.111 | -0.31802 | -0.33653 | -0.22863 |
| Py35F_corr | | 224 | 48 | 129.19 | 93.98 | 0.99743 | 41.0 | 0.83897 | 0.83884 | 0.45894 | 0.45886 | 2.068 | -0.2468 | -0.3672 | -0.2589 |
| QUI | | 95 | 21 | 129.04 | 106.17 | 0.97142 | 47.4 | 0.8172 | 0.81719 | 0.49243 | 0.49238 | 2.059 | -0.28378 | -0.35124 | -0.23784 |
| DMA-C16 (propyl) | | 401 | 87 | 126.81 | 105.30 | 0.96418 | 55.6 | 0.8367 | 0.8363 | 0.45517 | 0.45485 | 2.13 | -0.19322 | -0.28538 | -0.17158 |
| DMAPh | | 367 | 79 | 126.84 | 105.44 | 0.97087 | 55.6 | 0.83577 | 0.83569 | 0.44135 | 0.43977 | 2.13 | -0.18602 | -0.29143 | -0.17361 |
| Py4NMe2 | | 1 | 1 | 131.88 | 96.89 | 0.97895 | 41.4 | 0.81424 | 0.8113 | 0.5027 | 0.50059 | 2.023 | -0.31961 | -0.33265 | -0.22203 |
| DMHA (propyl) | | 267 | 58 | 129.51 | 107.20 | 0.96418 | 53.7 | 0.8367 | 0.8363 | 0.45517 | 0.45485 | 2.114 | -0.25463 | -0.27125 | -0.18376 |
| DMCA | | 533 | 116 | 119.72 | 106.69 | 0.93939 | 57.5 | 0.83498 | 0.83474 | 0.46404 | 0.46352 | 2.14 | -0.26228 | -0.27415 | -0.18368 |
| **Single Descriptor Correlations** | | | SDC (EXP) | 0.11 | 0.37 | 0 | 0.5 | 0.71 | 0.74 | 0.89 | 0.88 | 0.68 | 0.92 | 0.6 | 0.62 |
| | | | SDC (DFT) | 0.27 | 0.4 | 0.03 | 0.54 | 0.66 | 0.69 | 0.72 | 0.72 | 0.69 | 0.66 | 0.55 | 0.61 |

**Table S10.** QSAR model and regression statistics.

| Model (negative prections are set to zero) | | | | | | | | | | | | | |
|---|---|---|---|---|---|---|---|---|---|---|---|---|---|
| Activator | Rp | WBI Al-C (lowest) | $V_{bur}$ | Predicted | SUMMARY OUTPUT | | | | | | | | |
| DEA | 422 | 0.83664 | 57.4 | 424 | | | | | | | | | |
| DMA | 462 | 0.83822 | 55.6 | 420 | *gression Statistics* | | | ANOVA | | | | | |
| DMA-Cl | 466 | 0.83954 | 55.5 | 435 | Multiple R | 0.9173481 | | | *df* | *SS* | *MS* | *F* | *Significance F* |
| Py35Me_corr | 12 | 0.82658 | 41.4 | 88 | RSquare | 0.8415276 | | Regression | 2 | 367808.9 | 183904.5 | 23.89610743 | 0.000251068 |
| Py26Me | 3 | 0.81687 | 54.7 | 143 | Adjusted RSqu | 0.8063115 | | Residual | 9 | 69264 | 7696.001 | | |
| Py35F_corr | 224 | 0.83884 | 41.0 | 236 | Standard Error | 87.726852 | | Total | 11 | 437072.9 | | | |
| QUI | 95 | 0.81719 | 47.4 | 51 | Observations | 12 | | | | | | | |
| DMA-C16 (propyl) | 401 | 0.8363 | 55.6 | 396 | | | | | | | | | |
| DMAPh | 367 | 0.83569 | 55.6 | 389 | | | | | *Coefficients* | *Standard Erro* | *t Stat* | *P-value* | |
| Py4NMe2 | 1 | 0.8113 | 41.4 | 0 | | | | Intercept | -10738.8 | 2381.812 | -4.50864901 | 0.00147056 | |
| DMHA (propyl) | 267 | 0.8363 | 53.7 | 371 | | | | X Variable 1 | 12439.65 | 2988.248 | 4.16285733 | 0.002437341 | |
| DMCA | 533 | 0.83474 | 57.5 | 402 | | | | X Variable 2 | 13.15986 | 4.523246 | 2.909384305 | 0.017328607 | |

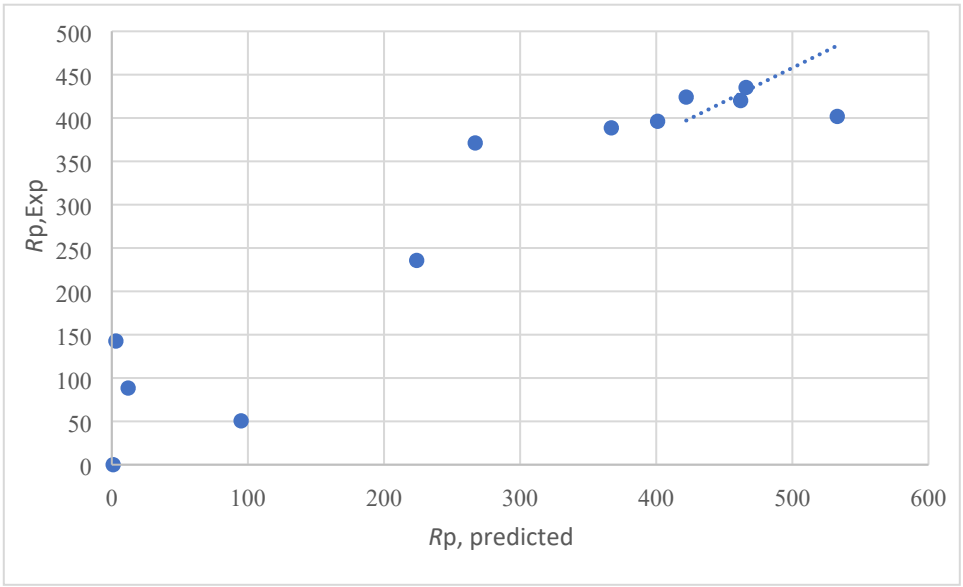


**Figure S39.** Experimental and predicted $R_p$ correlation.

**Table S11.** Descriptor cross-correlations.

| Important cross correlations | | | | | | | | | | | | |
|---|---|---|---|---|---|---|---|---|---|---|---|---|
| | CAIC | NAIN | e-(Al) | $V_{bur}$ | WBI Al-C (average) | WBI Al-C (lowest) | WBI Al-N (average) | WBI Al-N (lowest) | Al-N | e-(N) | EN-LPIBO | EHOMO |
| CAIC | - | 0.16 | 0.29 | 0.36 | 0.12 | 0.1 | 0.08 | 0.08 | 0.39 | 0.03 | 0.19 | 0.15 |
| NAIN | | - | 0.32 | 0.79 | 0.1 | 0.1 | 0.23 | 0.23 | 0.59 | 0.21 | 0.59 | 0.57 |
| e-(Al) | | | - | 0.48 | 0 | 0.02 | 0.01 | 0.01 | 0.24 | 0.03 | 0.14 | 0.09 |
| $V_{bur}$ | | | | - | 0.28 | **0.22** | 0.38 | 0.37 | 0.88 | 0.31 | 0.68 | 0.69 |
| WBI Al-C (average) | | | | | - | 0.97 | 0.8 | 0.8 | 0.55 | 0.66 | 0.33 | 0.31 |
| WBI Al-C (lowest) | | | | | | - | 0.84 | 0.83 | 0.47 | 0.72 | 0.32 | 0.31 |
| WBI Al-N (average) | | | | | | | - | 0.9991 | 0.64 | 0.86 | 0.44 | 0.51 |
| WBI Al-N (lowest) | | | | | | | | - | 0.65 | 0.86 | 0.45 | 0.52 |
| Al-N | | | | | | | | | - | 0.49 | 0.63 | 0.65 |
| e-(N) | | | | | | | | | | - | 0.35 | 0.51 |
| EN-LPIBO | | | | | | | | | | | - | 0.93 |
| EHOMO | | | | | | | | | | | | - |

**Table S12.** Descriptor contributions to the QSAR model.

| Model Contributions | | | | | | |
|---|---|---|---|---|---|---|
| | | | | | Contributions | |
| Activator | Rp | WBI Al-C (lowest) | $V_{bur}$ | Predicted | WBI Al-C (lowest) | $V_{bur}$ |
| DEA | 422 | 0.83664 | 57.4 | 424 | -331.245 | 755.3759853 |
| DMA | 462 | 0.83822 | 55.6 | 420 | -311.59 | 731.6882366 |
| DMA-Cl | 466 | 0.83954 | 55.5 | 435 | -295.17 | 730.3722505 |
| Py35Me_corr | 12 | 0.82658 | 41.4 | 88 | -456.388 | 544.8182193 |
| Py26Me | 3 | 0.81687 | 54.7 | 143 | -577.177 | 719.8443623 |
| Py35F_corr | 224 | 0.83884 | 41.0 | 236 | -303.878 | 539.5542752 |
| QUI | 95 | 0.81719 | 47.4 | 51 | -573.196 | 623.7773816 |
| DMA-C16 (propyl) | 401 | 0.8363 | 55.6 | 396 | -335.474 | 731.6882366 |
| DMAPh | 367 | 0.83569 | 55.6 | 389 | -343.063 | 731.6882366 |
| Py4NMe2 | 1 | 0.8113 | 41.4 | -102 | -646.466 | 544.8182193 |
| DMHA (propyl) | 267 | 0.8363 | 53.7 | 371 | -335.474 | 706.6845019 |
| DMCA | 533 | 0.83474 | 57.5 | 402 | -354.88 | 756.6919713 |
| | | | | | | |
| | | | | MIN | -646.466 | 539.5542752 |
| | | | | MAX | -295.17 | 756.6919713 |
| | | | | Span | 351.2958 | 217.1376961 |
| | | | | **weight** | **0.62** | **0.38** |

**Al-iBu bond WBI as a reflection of electron donation ability of the N-donor**

There is a relative good correlation (R2 = 0.72) between the WBI for the bond and the IBO charge on the free donor. Unlike a descriptor determined from the free donor, the WBI determined from the Al_L structure also reflects steric contraints present in the Al_L structure. Al-C bonds are intrisincally highly covalend (WBI Al-C in AliBu2H 0.84, Pauling EN C 2.55, Al 1.61) and even more so in aluminum cations (AliBu2+ Al-C WBI 0.90). A reduction of the WBI shows increased ionic contributions. Electron donation to aluminum stabilizes the contributing Al-dication.

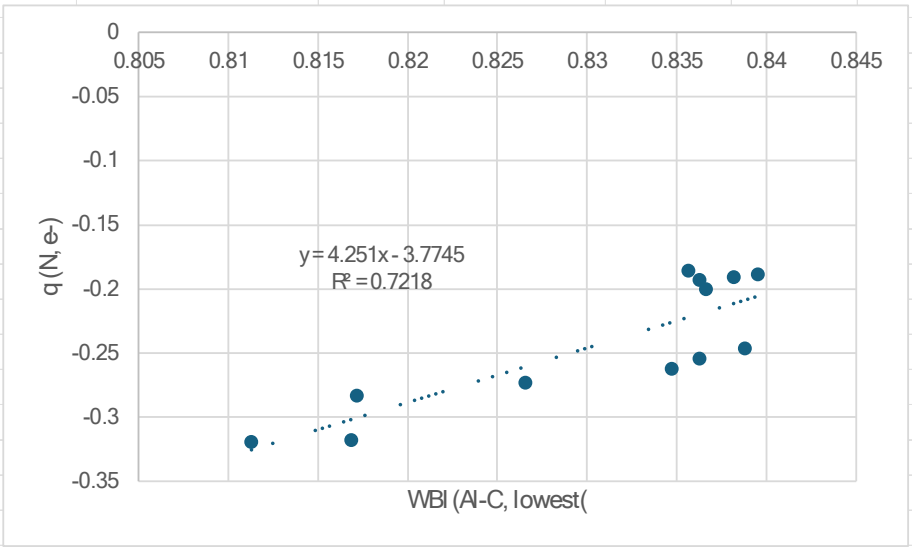


**Figure S40.** Wiberg bond index for the Al-C bond. Electronic and steric origins.

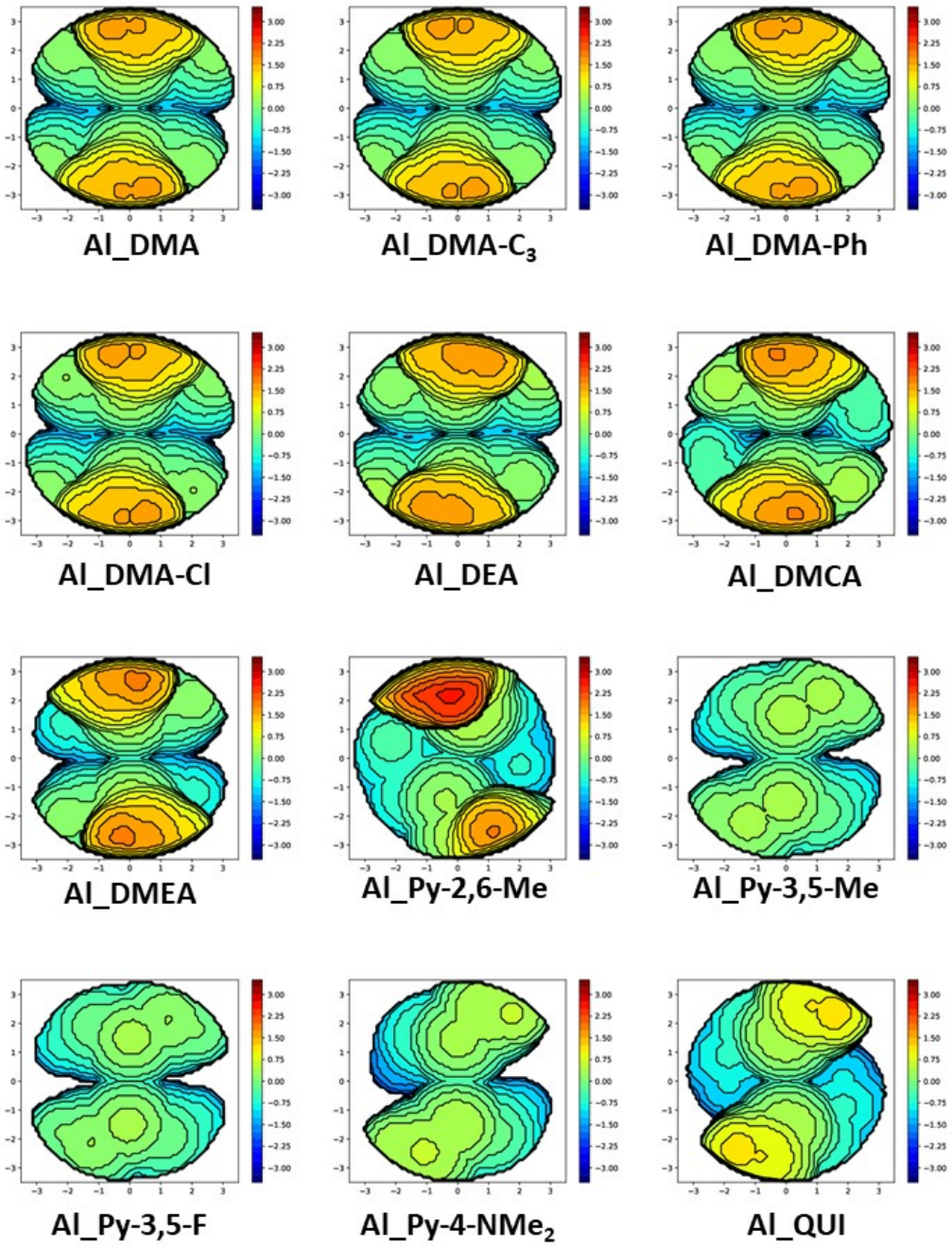


**Figure S41.** Topographic steric maps of donor steric bulk around **Al_L**.

# 4. References


1 H. T. Al-Masri, *J. Organomet. Chem.*, 2020, **905**, 121021.

2 J. T. B. H. Jastrzebski, G. Van Koten, M. F. Lappert, P. C. Blake and D. R. Hankey, in *Inorganic Syntheses*, 1989, pp. 150–155.

3 K. Kinashi, K.-P. Lee, S. Matsumoto, K. Ishida and Y. Ueda, *Dye. Pigment.*, 2012, **92**, 783–788.

4 F. Zaccaria, C. Zuccaccia, R. Cipullo, P. H. M. Budzelaar, A. Vittoria, A. Macchioni, V. Busico and C. Ehm, *ACS Catal.*, 2021, **11**, 4464–4475.

5 G. Urciuoli, F. Zaccaria, C. Zuccaccia, R. Cipullo, P. H. M. Budzelaar, A. Vittoria, C. Ehm, A. Macchioni and V. Busico, *Polymers*, 2023, **15**, 1378.